Ultradian- and stress-induced glucocorticoid pulsatility and its role in the kinetics of immune- and transcriptional responses

Dissertation zur Erlangung der naturwissenschaftlichen Doktorwürde
durch den Fachbereich I – Psychobiologie der Universität Trier

vorgelegt von M.Sc Slavena T. Trifonova

Gutachter:
Prof. Dr. C. P. Muller
Prof. Dr. J Meyer

Luxembourg, December 2012

Dissertationsort: Trier

This doctoral thesis has been performed at the Institute of Immunology, National Public Health Laboratory, Luxembourg

under the guidance of

Prof. Dr. Claude P. Muller, Institute of Immunology, National Public Health Laboratory, Luxembourg; Department of Immunology, University of Trier, Germany

and

Prof. Dr. Jobst Meyer, Department of Neurobehavioral Genetics, University of Trier, Germany

"Science knows no country, because knowledge belongs to humanity, and is the torch which illuminates the world. Science is the highest personification of the nation because that nation will remain the first which carries the furthest the works of thought and intelligence.''

Louis Pasteur (1822-1895)

"The biologist . . . knows that life as a whole is a ceaseless change, that the accomplishments even of natural evolution far surpasses any other type of progress that he could have imagined possible, and that there is no sign of a physical limit yet.''

Hermann Joseph Muller (1890-1967)
Scientist, Nobel Prize 1946

Acknowledgements

I thank my promoter Prof. Dr. Claude P. Muller, Institute of Immunology, National Public Health Laboratory and the Public Research Centre for Health (CRP-Santé), Luxembourg, for allowing me to be part of his team and for his support and scientific guidance over the last years.

I thank my supervisor Dr. Jonathan D. Turner, Institute of Immunology, National Public Health Laboratory and the Public Research Centre for Health (CRP-Santé), Luxembourg for his most valuable expertise, in both my theoretical and practical scientific education, for all the fruitful discussions and suggestions.

I also want to thank Prof. Dr. Jobst Meyer, Department of Neurobehavioral Genetics, University of Trier, for his support and precious guidance. I thank Prof. Dr. Hartmut Schächinger, Institute of Psychobiology, University of Trier, for his initiatives within the International Research Training Group, Trier-Leiden.

I also acknowledge the collaboration of the Flow Cytometry unit and the Clinical and Epidemiological Investigation Center, CRP-Santé, Luxembourg, especially to Jerome Graas, and Telma Velez who helped me with the organization and the conduction of my clinical study. I would like to thank also to Patricia Borde from the National Laboratory of Health, Luxembourg.

I would like to thank my colleagues from the Institute of Immunology who were part of my daily life the last four years. To all members of the Psychoneuroimmunology research group: Lei, Sara, Sophie Mériaux, Stephanie and Carlos; as well as the other current and former members of the laboratory:

Anja, Wim, Sebastien, Aurelie, Emilie, Patrick, Konstantin, Sophie Farinelle, Stéphanie. I also wish to thank Ulla Muller and Carole Weis for their assistance in administrative tasks.

For their financial support, I would like to thank the Fonds National de Recherche, the Centre de Recherche Public-Santé, and the Ministère de la Culture, de L'Enseignement Superérieur et de la Recherche from Luxembourg and the International Research Training Group,Trier-Leiden.

I would like to thank my parents, my sister and all my friends for their love, affection and support. I thank them for their encouragement, tolerance and philosophical discussions during the frustrating time.

Table of Contents

Acknowledgements **IV**

Table of Contents **VI**

Index of Abbreviations **IX**

Index of Tables **XI**

Index of Figures **XII**

General Abstract **XVI**

Chapter 1: General Introduction **1**

1.1 Adjustment of internal homeostasis to major changes 2

1.2 The HPA axis 3

1.2.1 Circadian an ultradian secretion of GCs 4

1.2.2 Stress induced secretion of GCs 6

1.3 Physiological and pathological variability in GCs pulsatility 8

1.4. GCs in therapy and research 9

1.4.1 Free vs. bound cortisol 10

1.4.2 Saliva vs. plasma sampling 12

1.4.3 Methods for studying GC pulsatility 12

1.5. Structure of GR gene 17

1.6 GR protein isoforms 19

1.7 GR and MR actions 20

1.7.1 Cytosolic GR-mediated genomic effects 21

1.7.2 Intracellular GR dynamic 22

1.7.3 GR-mediated rapid non-genomic effects 24

1.8 Glucocorticoid circadian rhythms and the immune system 26

1.9 Research objectives 30

1.10 Outline of the thesis 32

Chapter 2: The use of saliva for assessment of cortisol pulsatile secretion by deconvolution analysis **33**

2.1 Abstract 34

2.2 Introduction 36

2.3 Materials and Methods 39
2.3.1 Subjects and experimental design 39
2.3.2 Hormone assays 40
2.3.3 Deconvolution analysis 41
2.3.4 Concordance of secretion events 41
2.3.5 Statistical analysis 42
2.4 Results 42
2.4.1 Plasma and saliva cortisol concentration profiles 42
2.4.2 Deconvolution analysis of pulsatile cortisol secretion 48
2.4.3 Concordance 50
2.5 Discussion 56

Chapter 3: Diurnal redistribution of human lymphocytes and their temporal associations with salivary cortisol profiles 63

3.1Abstract 64
3.2 Introduction 66
3.3 Materials and Methods 68
3.3.1 Subjects and experimental design 68
3.3.2 Cortisol ELISA 69
3.3.3 Cellular immune parameters 69
3.3.4 Data analysis 70
3.4 Results 71
3.4.1 Ultradian salivary cortisol 71
3.4.2 Ultradian variations of T and B lymphocytes 72
3.4.3 Ultradian variations of NK lymphocytes 73
3.4.4 Redistribution of CD8 and KIR expressing NK cells 76
3.4.5 Correlations between lymphocyte ultradian variations and cortisol levels 77
3.5 Discussion 83

Chapter 4: Gene responses to Trier Social Stress Test (TSST) in healthy males and females 87

4.1 Abstract 88
4.2 Introduction 90
4.3 Materials and Methods 93
4.3.1 Subjects 93
4.3.2 Study protocol 93
4.3.3 Saliva and blood sampling 94
4.3.4 Biochemical analysis 95
4.3.5 Gene expression analysis 95
4.3.6 Statistical analysis and data reduction 96
4.4 Results 98
4.4.1 TSST induced hormone profiles 98
4.4.2 Gene expression profiles 100
4.4.3 Gene expression trajectories 103
4.4.3.1 Anticipation effects 103
4.4.3.2 TSST related effects 113
4.5 Discussion 109

Chapter 5 115
5.1 General Discussion 116
5.2 Future perspectives 129

References 132

Annexes 152

Index of Abbreviations

ACTH	Adrenocorticotrophic hormone
AIC	Akaike information criterion
APC	Allophycocyanin
APC Cy7	Allophycocyanin-cyanin 7
ATP	Adenosine triphosphate
AVP	arginin vasopressin
AUC	Area under the curve
BMI	Body mass index
CBG	Corticosteroid-binding globulin
CDK	Cyclin-dependent kinase
cDNA	Complementary DNA
CNER	National research ethics comittee
CNS	Central nervous system
CpG	Cytosine-phosphate-guanine
CRH	Corticotrophin-releasing hormone
CXCR 4	C-X-C chemokine receptor type 4
DBD	DNA-binding domain
DC	Dendritic cells
DEX	Dexamethasone
DNA	Deoxyribonucleic acid
DNTPs	Deoxyribonucleotides (dATP, dCTP, dGTP and dTTP)
EDTA	Ethylene diamine tetraacetic acid
ELISA	Enzyme-linked immunosorbent assay
FACS	Fluorescence activated cell sorting
FITC	Fluorescein isothiocyanate
FKBP	FK 506 binding protein
FSH	Follicule stimulating hormone
FYN	Proto-oncogene tyrosine-protein kinase
Fwd	Forward
GAPDH	Glyceraldehyde 3-phosphate dehydrogenase
GC	Glucocorticoid
gDNA	Genomic DNA
GH	Growth hormone
GILZ	Glucocorticoid-induced leucine zipper
GLM	General linear model
GnRH	Gonadotropin-releasing hormone
GR	Glucocorticoid receptor
GRE	Glucocorticoid responsive element
GSK3	glycogen synthase kinase-3
HSD	Hydroxysteroid dexidrogenase
HLA	Human leukocyte antigen
HPA	Hypothalamic-pituitary-adrenal
ICAM	Immunoglobulin cell adhesion molecule; soluble ICAM (sICAM)
IFN	Interferon
Ig	Immunoglobulin
IGF-1	Insuline-like growth factor 1
IL	Interleukin
IPI	Interpeak interval

JNK	c-Jun N-terminal kinase
KIR	Killer immunoglobulin-like receptor
LBD	Ligand binding domain
LC	Locus coeruleus
LH	Lutheinizing hormone
LPS	Lipopolysaccharide
MAPK	Mitogen-activated protein kinase
MDD	Major depressive disorder
MDL	Minimal detectable limit
mGR	Membrane glucocorticoid receptor
MHC	Major histocompatibility complex
MR	Mineralocorticoid receptor
NE	Norepinephrine
NF- κ B	Nuclear factor κ B
NKCA	Natural killer cell activity
PBMCs	Peripheral blood mononuclear cells
PCR	Polymerase chain reaction
PE	Phycoerythrin
PE-Cy7	Phycoerythrin-cyanine 7
PerCP	Peridinin-chlorophyll-protein complex
POMC	Pro-opiomelanocortin
PVN	Paraventricular nucleus
RNA	Ribonucleic acid; messenger RNA (mRNA)
Rev	Reverse
RT	Reverse transcription
sAA	Sympathetic alpha-amylase
SAM axis	Sympathetic-adrenal medullary axis
SCN	Suprachiasmatic nucleus
SEM	Standard error of the mean
SNP	Single nucleotide polymorphism
STAT `	signal transducer and activator of transcription
TNF	Tumor necrosis factor
TSST	Trier social stress test
UTR	Untranslated region
VCAM-1	Vascular cell adhesion molecule-1; soluble VCAM-1 (sVCAM-1)
VEGF	Vascular endothelial growth factor

Index of Tables

Table 1. Quantitative features of episodic cortisol secretion resolved by multi-parameter deconvolution analysis. 52
Table 2. Average percentages of KIR/CD8 populations within CD56/16 NK subsets. 77
Table 3. Primers and PCR conditions. 96

Index of Figures

Figure 1. Schematic representation of the hypothalamo-pituitary adrenal (HPA) axis. 4
Figure 2. The 24-h circadian ultradian rhythms of ACTH and cortisol in human. 5
Figure 3A. Major differences in both glucocorticoid frequency and amplitude between male and female rodents. 8
Figure 3B. Animal genetic background determines the pulsatile profile of glucocorticoid release. 8
Figure 4. A hypothetical secretory bust of symmetric form that can be modeled as a Gaussian event. 16
Figure 5. Structure of the GR (NR3C1) gene. 18
Figure 6. Models of glucocorticoid receptor transcriptional modulation. 23
Figure 7. A schematic representation of cyclic GR interactions with response elements leading to a pulsatile release of a nascent RNA. 25
Figure 8-10. Plasma and saliva cortisol concentrations analysed by deconvolution analysis for three representative donors. Initial concentration profiles for plasma (A) and saliva (B) we used to generate model-independent secretory profiles (C and D), and subsequently deconvoluted using the Autodecon algorithm to give the underlying cortisol pulsatile structure (E and F). The pulsatile patterns were convoluted to give the theoretical concentration profiles (G and H) that were not statistically different from the initial concentration profiles (A and B). 45-47
Figure 11. Pearson correlations between the midday peak AUC and the amplitudes in plasma (A) and in saliva (B). AUC is expressed in nmol/l and amplitude is expressed in nmol/l/min. Each dot represents one donor. 48
Figure 12. Pearson correlations between plasma and saliva cortisol concentrations in individual donors with the highest (A) and the lowest (B) correlation and for all donors (C) throughout the complete observation period. Insert to panel (C) represents the mean plasma and salivary cortisol concentration for all donors. Pearson correlations between the AUC of the complete observation period in plasma and saliva (D), midday peak AUC (E) and midday peaks amplitudes (F) of all donors. Insert to panel (D) is mean plasma and salivary cortisol AUC of all donors. 49
Figure 13. Pearson correlations between the corresponding number (A), AUC (B) and amplitudes (C) of plasma and saliva peaks of all donors. Insert to panel (A) represents the

mean number of corresponding peaks/8h in plasma and saliva of all donors. Insert to panel (B) is the mean peak AUC in plasma and saliva of all donors. Insert to panel (C) is the mean peak amplitude in plasma and saliva of all donors. Pearson correlations between model estimated and cortisol half-life calculated from the steepest negative slope from the concentration curve (D), between cortisol half-life (E) and interpeak interval (F) in plasma and saliva peaks of all donors. Insert to panel (E) is the mean cortisol half-life in plasma and saliva of all donors. Insert to panel (F) is the mean interpeak interval in plasma and saliva of all donors. 51

Figure 14. Correlations between total plasma AUC and sum of peak AUC (A) and between total saliva AUC and sum of peak AUC (B). AUC is expressed in nmol/l. 53

Figure 15. Concordance of saliva and plasma cortisol pulses. The percentage of salivary pulses for a total number of plasma pulses was assessed using a fixed time window (A), a donor-specific variable window (C) and during the morning hours with a variable time window (E). The number of salivary pulses for a total number of plasma pulses was assessed using a fixed time window (B), a donor-specific variable window (D) and during the morning hours with a variable time window (F). Each dot represents one donor. 55

Figure 16. The relationship between the number of plasma cortisol pulses and the percentage of coincident salivary cortisol pulses using the fixed (A) and variable (B) time window. Each dot represents one donor. 56

Figure 17. Ultradian salivary cortisol rhythm of three representative donors (A-C) and mean ±SEM of 19 healthy male donors (D). Clock time runs from 0700 to 1700 h. 72

Figure 18. Dot plot from a representative donor of CD3/CD19 gating (A) and CD3/CD8 gating (B). Daily changes of total CD3+(C), CD3+CD8+ (D), CD3+CD8– (E), CD19+ (F) counts as percentage of total lymphocyte counts. Clock time runs from from 0700 to 1700 h. 74

Figure 19**.** Dot plot from a representative subject of CD56/CD16 gating (A). Daily changes of total NK (B), CD56+16+ (C), CD56+16– (D), CD56–CD16+ cells (E) counts as percentage of total lymphocyte counts. Clock time runs from 0700 to 1700 h. 75

Figure 20. Dot plot from a representative donor of KIR/CD8 gating of CD56-16+ (A), CD56+16-(B), CD56+16+ (C) Daily distribution of KIR/CD8 counts as percentage of the counts of CD56+16+ NK subset (D), CD56–16+ NK subset (E) and CD56+16– NK subset (F). Clock time runs from 0700 to 1700 h. 79

Figure 21. Average Pearson correlation profiles of CD3+ (A) CD3+CD8– (B) and total NK (C) cell counts as percentage of total lymphocyte counts with salivary cortisol

concentration. Open circles indicate time points with significant correlation ($p<0.05$). Arrows correspond to the time points of maximal significant correlation and data for these points are included as inserted dot plots. 80

Figure 22. Average Pearson correlation profiles of CD56+16+ (A), CD56–16+ (B), CD56+16– (C) cell counts as percentage of total lymphocyte counts with salivary cortisol concentration. Open circles indicate time points with significant correlation ($p<0.05$). Arrows correspond to the time points of maximal significant correlation and data for these points are included as inserted dot plots. 82

Figure 23. Average Pearson correlation profiles of total KIR+ (A), KIR– (B) cell counts as percentage of total lymphocyte counts with salivary cortisol concentration. Open circles indicate time points with significant correlation ($p<0.05$). Arrows correspond to the time points of maximal significant correlation and data for these points are included as inserted dot plots. 83

Figure 24. Mean (±SEM) ACTH (A) and cortisol (B) responses (nmol/l) for all donors. C. Mean (±SEM) ACTH (C) and cortisol (D) responses in male and female donors. The shaded area indicates the period of stress exposure. *$p<0.05$, **$p<0.01$, ***$p<0.001$, indicate significant differences between the individual time points (RM-ANOVA). 99

Figure 25. Mean (±SEM) ACTH (A) and cortisol (B) stress responses. Correlation between ACTH and cortisol net increases (C). Mean (±SEM) cortisol (D) anticipatory responses, ACTH (E) and cortisol (F) meal induced responses in responders and non-responders male and female donors. 102

Figure 26. Mean (±SEM) fold changes for FKBP5, GILZ and SDPR in male (A, C, E) and female donors (B, D, F). *$p<0.05$, **$p<0.01$, ***$p<0.001$, indicate significant differences between the individual time points (RM-ANOVA). 104

Figure 27. Cortisol responses and their respective GILZ and FKBP expression profiles from three representative donors: stress responder (A, B), stress anticipator (C, D), and stress anticipator and responder (E, F). 105

Figure 28. Log-transformed GILZ (A) and FKBP5 (B) expression trajectories for high (mean +1SD; dashed line) and low (mean-1SD; solid line) increases of cortisol in anticipation of the TSST; grey lines show individual observed gene expression trajectories. 107

Figure 29. Log-transformed GILZ (A) and FKBP5 (B) expression trajectories for high (mean +1SD; dashed line) and low (mean-1SD; solid line) increases of cortisol during the TSST; grey lines show individual observed gene expression. 108

General Abstract

Hormone secretion is highly organized temporally, achieving optimal biological functioning and health. The master clock located in the suprachiasmatic nucleus (SCN) of the hypothalamus coordinates the timing of circadian rhythms, including daily control of hormone secretion. The hypothalamo-pituitary-adrenal (HPA) axis is one of the body's major neuroendocrine axes, responsible for maintaining homeostasis and adaptation during challenges. Its end mediator cortisol is primarily affecting energy intake, storage, and expenditure, but also guides fundamental processes such as cellular differentiation, growth and development, functions of the nervous and immune systems and is indispensable for maintaining the homeostasis under stress. Cortisol exhibits pronounced ultradian and circadian rhythm and disturbances in its characteristic temporal secretory pattern have often been described in stress-related pathology. However, the significance of glucocorticoids' (GCs) secretory patterns for physiology, stress responsiveness and nuclear receptor signalling remains largely unexplored. The overall objective of this thesis was therefore to dissect the underlying structure of glucocorticoid pulsatility and to develop tools to investigate the physiological effects of this pulsatility on immune cell trafficking and the responsiveness of the neuroendocrine system and GC target genes to stress.

Deconvolution modeling was successfully set up as a tool for investigation of the pulsatile secretion underlying the ultradian cortisol rhythm. The results showed that the pulsatile cortisol rhythm is maintained in saliva and suggested saliva sampling as a stress free alternative to plasma for studying the cortisol pulsatility in future psychobiological research. This further allowed us to investigate the role of these single endogenous cortisol pulses in the redistributional changes within the immune system.

We found that the major players of innate and adaptive immunity exhibit diurnal fluctuations, with an inverse bimodal redistribution, that were significantly correlated with cortisol diurnal levels. Moreover, we studied the role of induced endogenous cortisol pulses on the kinetics of expression of primary GR target genes. The perturbation of the HPA axis resulted in additional cortisol pulses superimposed on the natural diurnal rhythm which were subsequently translated in pulsatile gene expression confirming data from animal models and suggesting that the gene pulsing is a common phenomenon occurring within the HPA axis in basal as well as perturbed conditions.

The results shown here have given better understanding of the pulsatile GC release and the resultant glucocorticoid receptor (GR)-mediated gene expression as well as the redistributional effects within the immune system under natural and stress conditions. The development of these three tools enable us to induce, dissect and analyse the role of single pulses in different biological phenomena and would allow us to induce and investigate the role of single endogenous as well as exogenous cortisol pulses for health and disease in future.

Keywords: HPA axis, cortisol, pulsatility, immunity, lymphocytes, stress, gene expression

Chapter 1

General Introduction

Section 1.5 from this chapter has been published in:

Jonathan D. Turner, Simone R. Alt, Lei Cao-Lei, Sara Vernocchi, **Slavena Trifonova,** Nadia Battello and Claude P. Muller

Transcriptional control of the glucocorticoid receptor: CpG islands, epigenetics and more

Biochemical Pharmacology (2010) Dec 15;80(12):1860-8

1.1 Adjustment of internal homeostasis to major changes

All organisms live under the influence of the 24 h day/night cycles created by the Earth rotation. The organisms adapt to these external changes and synchronize their physical activities, such as behavior, food intake, energy metabolism, sleep, reproductive activity and immune function with circadian cycles (Takahashi et al, 2008). During the evolution, a highly conserved ubiquitous molecular ‘‘clock’’, named the CLOCK system, have been developed. It creates internal circadian rhythm under the influence of the 24 h day/night cycle (Ko & Takahashi, 2006). This CLOCK system has efferent connections to numerous organs and tissues, transferring information from a centrally created circadian rhythm (Hastings et al, 2007). The circadian rhythm (from the Latin *circa*, meaning “around”, and *diem*, meaning “day”), is a 24 h cycle in any biological process (i.e. biochemical, physiological, endocrine or behavioural) in all organisms including plants, animals, fungi and cyanobacteria (Kalsbeek et al, 2006; Panda et al, 2002). These rhythms allow organisms to anticipate and prepare for precise environmental changes (i.e. light/dark cycle, seasonal changes), thereby increasing the efficiency in metabolic demand. In addition to adaptation to the day/night changes, organisms face unforeseen environmental changes with external (e.g. extreme heat or cold, food deprivation, trauma and pathogen invasion) or internal (e.g. hurtful memories, injuries, neoplasias) origin called ‘‘stressors’’(Chrousos, 2009). The adaptation towards these stressful stimuli is mediated by another regulatory system, called the Stress system. It receives information about environmental changes through various sensory organs, processes them in the central nervous system (CNS) and adjusts the CNS and peripheral organ activities to improve chances for survival (Chrousos, 2009). The system consists of the HPA axis and its end-effectors GCs (Chrousos, 2009), as well as the sympathetic-adrenal medullary (SAM) axis and its end-effectors, norepinephrine and epinephrine. Its main function is to

restore the internal homeostasis by regulation of many biological functions, such as CNS, intermediary metabolism, immunity and reproduction (Chrousos, 2009; Chrousos & Kino, 2007). In addition to the benefical effects, the stress system can also exert adverse effects when its response is not properly tailored to the stressful stimulus. The CLOCK and Stress systems are both essential for survival, and interact with one another at multiple levels to adjust numerous physiological activities. Dysregulation in either of these systems can lead to similar pathological conditions.

1.2. The HPA axis

The HPA axis is one of the body's major neuroendocrine axes, characterized with circadian activity as well as mediating the adaptive response to stressors (De Kloet et al, 1998). Corticotrophin releasing hormone (CRH) and the arginine vasopressin (AVP) are released from the paraventricular nucleus (PVN) in response to a variety of stressors under the regulation originating from hippocampus, amygdala and locus coeruleus (LC). CRH and AVP release leads to adrenocorticotrophic hormone (ACTH) secretion by the cleavage of pro-opiomelanocortin (POMC) from the corticotropic cells of the anterior pituitary gland. ACTH released into the peripheral circulation stimulates both production and secretion of GCs (cortisol in humans and corticosterone in rodents) from the adrenal cortex. Secreted GCs in turn suppress higher regulatory centers, the PVN and the pituitary gland, forming a closed negative feedback loop that resets the activated HPA axis and restores homeostasis (Figure 1) The negative feedback occurs via the type I Glucocorticoid receptor (GR) and type II Mineralcorticoid receptor (MR). Both receptors are ligand activated transcription factors, transmitting information from the circulating steroids into transcriptional responses in target cells. Due to its 10 fold higher affinity for

cortisol, MR is thought to remain activated throughout the ultradian cycle, whilst the GR becomes activated during ultradian, circadian or stress induced peak cortisol levels. Despite the classical glucocorticoid feedback hypothesis suggesting that MR plays a predominantly regulatory role during the circadian nadir (Conway-Campbell et al, 2007; Pascual-Le Tallec & Lombes, 2005) and GR during the circadian hormonal peak (de Kloet et al, 2005), Young et al. suggested a prolonged effect of both MR and GR, with both receptors mediating the GC negative feedback during the peak diurnal secretion as well as at nadir levels (Young et al, 2004).

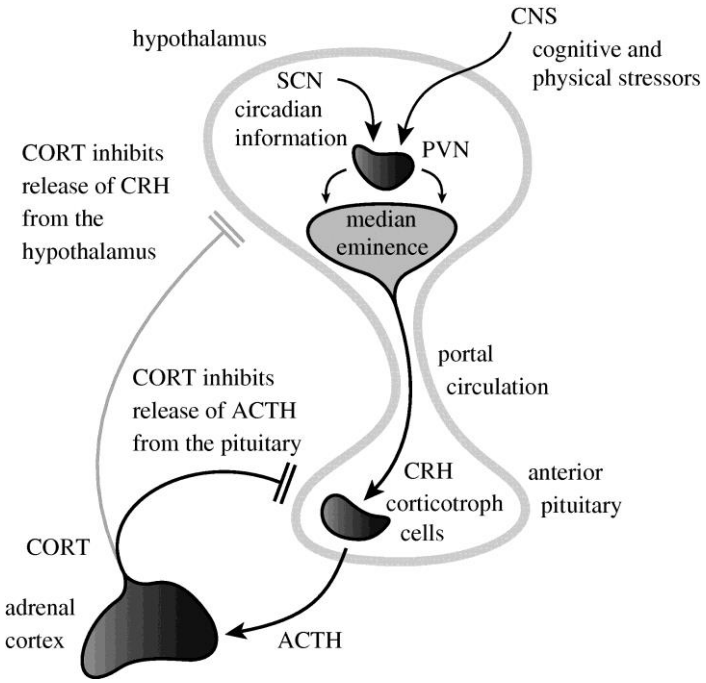

Figure 1. Schematic representation of the HPA axis. Adapted and modified from (Walker et al, 2010).

1.2.1 Circadian and ultradian secretion of GCs

The HPA axis has a unique pattern of activity, with a classical circadian rhythm, with cortisol levels in humans peaking at the end of the resting period in preparation of the

increased metabolic demands of the active phase, subsequently decreasing to low levels in the late afternoon (Lightman et al, 2002; Weitzman et al, 1971). Highest cortisol levels, measured in the morning, reach 10^{-6} M dropping in the evening between 10^{-7} M and 10^{-8} M (Haller et al, 2008). Nocturnal animals such as rodents, peak in corticosterone levels towards the end of the afternoon when the dark cycle begins. These diurnal fluctuations arise from signaling between the hypothalamic SCN and the adrenal gland, and consist of both the autonomic nervous system and hormonal regulation of the HPA axis (Walker et al, 2010). The development of high frequency (automated) sampling paradigms, intra-tissue microdialysis in non-stressed conditions and statistical algorithms led to the discovery that circadian release of GCs in fact consists of more frequently released hormone bursts reflected in blood as a distinct ultradian rhythm (< 24 h), previously regarded as "experimental noise" (Henley et al, 2009). Ultradian GC pulses are released with a periodicity of approximately 60 min in blood and have been described in numerous species including rat (Jasper & Engeland, 1991), rhesus monkey (Tapp et al, 1984), Syrian hamster (Cook, 2001; Loudon et al, 1994), sheep (Cook, 2001) and humans (Henley et al, 2009; Lewis et al, 2005; Weitzman et al, 1971) (Figure 2).

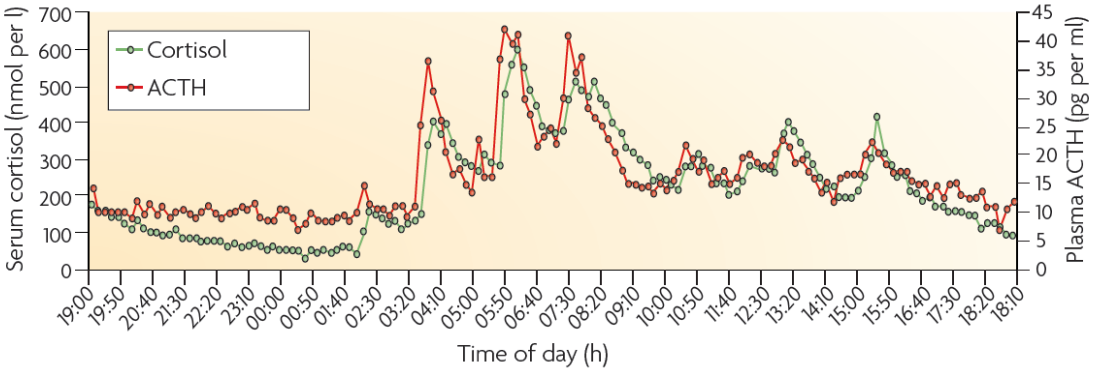

Figure 2. The 24-h circadian ultradian rhythms of ACTH and cortisol in human. Adapted and modified from (Lightman & Conway-Campbell, 2010).

The secretory pattern of GCs is also maintained across the blood-brain barrier in the extracellular fluid suggesting that target tissues are exposed to rapidly fluctuating steroid levels (Cook, 2001; Droste et al, 2008). In fact the circadian profile of hormone release is made up by changes in pulse amplitude and to lesser extent frequency (Iranmanesh et al, 1989; Liu et al, 1987; Veldhuis et al, 1990; Veldhuis et al, 1989b) (Figure 2). The morning rise in cortisol, called the cortisol awakening response (CAR) is a distinct component of the diurnal pattern of cortisol and is considered to be a marker of the HPA axis integrity. It is supposed to represent the capacity of the adrenal cortex to produce cortisol and is characterized with a mean cortisol increase by 50-100 %, peaking about 30 min after awakening (Pruessner et al, 1997; Wust et al, 2000). In addition to the diurnal variation, psychological and physiological stressors can activate the HPA axis, preparing the body for a "fight or flight" response. Within minutes blood GCs increase up to 10^{-5} M, resulting in catabolic processes to provide free energy sources such as glucose, amino acids and lipids.

1.2.2 Stress induced secretion of GCs

Generally stressful events are thought to contribute to many diseases, including not only cardiovascular, infection, autoimmune and mood disorders, but also substance use disorders and relapse to drug abuse (Desai & Jann, 2000; Godbout & Glaser, 2006; Jorm et al, 1987; Reagan et al, 2008). One of the classical characteristics of the human stress response is the wide inter-individual variation, which is likely to contribute to risk for these stress-linked disorders. There is evidence that men and women vary in response to acute stress (Kudielka et al, 2004; Kudielka & Kirschbaum, 2005), and they also differ in the prevalence of stress-linked disorders (Carter-Snell & Hegadoren, 2003). Functional

interactions between GC pulsatility and the stress response have been known for more than a decade. It is evident that the onset of a stressor in relation to the phase of an ultradian pulse can determine the physiological response to stress. Another study in rats assessed their stress-responsiveness during different phases of their ultradian corticosterone secretory profile (Windle et al, 1998b). The rats showed greater HPA axis response when a noise stress was applied during the ascending phase of an ultradian pulse, suggesting a facilitated stress response during the ascending phase and/or an inhibitory effect during the descending phase. Additionally, pulse amplitude and frequency were shown to be major determinants in the stress response (Haller et al, 2000). Others reported reduced corticosterone responses with increased pulse amplitude and frequency (Atkinson et al, 2006; Windle et al, 2001). These observations show that acute HPA axis reactivity strongly depends on the individual pulse characteristics that make up the ultradian pattern. Endocrine stress response modulates gene expression ensuring dynamic adaptation to stress and as already mentioned represent important factor contributing to vulnerability for psychopathology. A genome wide and targeted gene expression studies have conducted to investigate the complex psychological stress-associated gene response in humans and animal models (Le-Niculescu et al; Morita et al, 2005; Murata et al, 2005; Nater et al, 2009; Pajer et al). This allowed them to identify potential gene markers of psychological stress and further correlate them with pathological responses in stress-related disorders. However, these studies have measured gene expression pattern using one (Macedo et al, 2008; Murata et al, 2005; Pajer et al, 2012) or limited number (Morsink et al, 2006; Nater et al, 2009) of measurement points post GC exposure, thus allowing only the identification of potential stress-responsive genes. Studies on the kinetics of stress induced gene expression are warranted, after

recent findings of a pulsatile pattern of GR-target gene expression after GCs stimulation in adrenalectomized animals (Stavreva et al, 2009).

1.3 Physiological and pathological variability in GCs pulsatility

The secretory corticosteroid pattern is remarkably plastic with high variability between and within individuals, as well as depending on the physiological and pathophysiological state of the individuals. Major differences in GC pulse frequency and amplitude have been seen between male and female rodents (Figure 3A). These sexual differences are mainly due to the gonadal steroids, as it is reversed by oophorectomy or orchidectomy (Seale et al, 2004a; Seale et al, 2004b).

A.

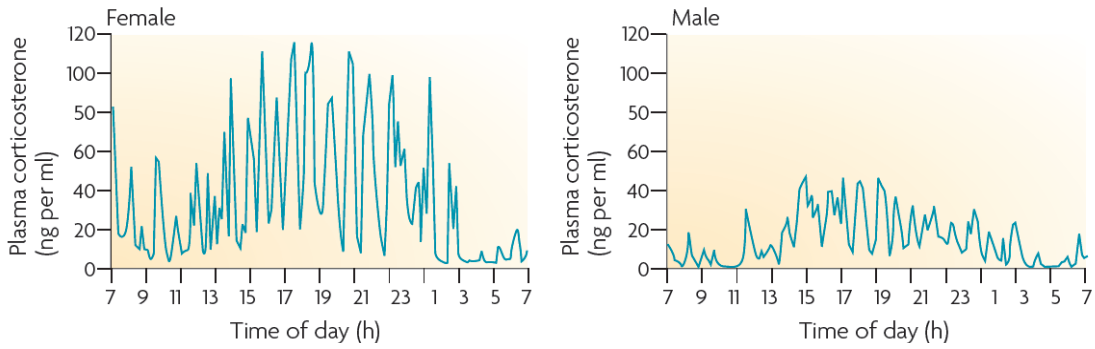

B.

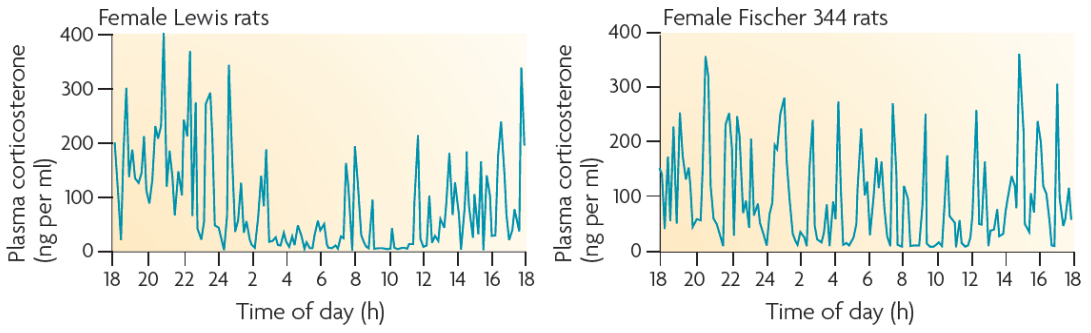

Figure 3A. Major differences in both glucocorticoid frequency and amplitude between male and female rodents. **3B.** Animal genetic background determines the pulsatile profile of glucocorticoid release. Adapted and modified from (Lightman & Conway-Campbell, 2010).

The physiological state can also modify the pattern of HPA axis activity. For instance in rodents, lactation increases pulse amplitude while during ageing the hourly pattern becomes disorganised (Lightman, 1992; Lightman, 2008; Young et al, 2004). The animals' genetic background was also shown to determine the pulsatile profile of GC release. Lightman et al. have demonstrated differences in the GC secretory profile in different but histocompatible strains of rat (Fisher and Lewis), with differences in stress responsiveness (hyper- and hyporesponsive to stress) and susceptibility to autoimmune disease (Windle et al, 1998a) (Figure 3B).

Various pathopysiological conditions are associated with altered GC secretory patterns. For instance chronic inflammation in an animal model of inflammatory arthritis resulted in an increase in the pulse frequency (Windle et al, 2001). A number of psychiatric, neurological and immune diseases are associated with changes in GC ultradian pusaltility. For instance, increased pulse frequency together with hypercortisolemina has been reported in major depressive disorder (MDD) patients (Deuschle et al, 1997; Holsboer, 2000). In Cushing's syndrome, the normal variation of cortisol is flattened or totally abolished due to elevations in cortisol levels in the quiescent period (Boyar et al, 1979). Flattened cortisol secretion curves were reported in Parkinson disorder cohort in addition to elevated cortisol production (Hartmann et al, 1997). Other disorders such as Huntington's disease is also characterised by changes in pulse characteristics (Aziz et al, 2009). However, it remains unknown whether the disorganisation in pulsatile patterns is causal to the disorder or vice versa. Taking into account the fundamental role of GC concentrations for maintenance of physiology and the overall well being, it may be hypothesized that alterations from the optimal ultradian pattern could precipitate disease (Dallman et al, 2003; de Kloet et al, 2005; Young et al, 2004). The functional role of

ultradian GC pulses for HPA axis activity, stress responsiveness and the consequences of changes in pulse characteristics for physiology still remain largely unknown.

1.4. GCs in therapy and research

Together with the fundamental physiological role outlined above, GCs have been found to be exceptionally useful in the treatment of pathophysiological conditions. For more than 50 yrs, GCs are one of the most commonly prescribed drugs worldwide in treatment of inflammatory diseases (Lowenberg et al, 2008) such as rheumatoid arthritis, asthma, chronic obstructive pulmonary disease, dermatitis and systemic lupus erythematosus (Lowenberg et al, 2008). The GC immunosuppresive activity is also used to prevent graft rejection and in cancer therapy (Rhen & Cidlowski, 2005; Styczynski et al, 2005). At hyperphysiological concentrations GCs induce apoptosis and thereby are the main components in the treatment of lymphoproliferative diseases such as childhood acute lymphoblastic leukemia, multiple myeloma, chronic lymphocytic leukemia and non-Hodgkin's diseases (Greenstein et al, 2002; Haarman et al, 2003; Rajkumar et al, 2002; Rhen & Cidlowski, 2005). GCs causes also numerous side effects more pronounced in long term applications. Therefore, selective GR agonists that dissociate transactivation and transrepression mechanisms have been developed such as prednisone, dexamethasone and betamethasone to prevent from such adverse actions (Lowenberg et al, 2008).

1.4.1 Free vs. bound cortisol

Approximately 95 % of secreted cortisol is bound to carrier proteins; 80–90 % to corticosteroid-binding globulin (CBG) (Siiteri et al, 1982) and 10–15 % to albumin (Lewis et al, 2005). According to the traditional "free hormone hypothesis" (Mendel,

1992) steroid hormones bound to carrier proteins are considered biologically inactive and provide a reservoir of inactive circulating hormone, and regulate the amount of free hormone available for diffusion into tissues. The remaining 5 % of cortisol is thus unbound and free to diffuse across cell membranes and bind to intracellular GR and MR, leading to a broad spectrum of physiological effects. Cortisol is a small (MW 362), highly lipophilic molecule that rapidly diffuses in saliva through the cell membranes via passive diffusion. Several research groups have shown that salivary flow rate does not influence cortisol concentration in saliva (Hiramatsu, 1981; Kirschbaum & Hellhammer, 2000; Walker et al, 1978). As cortisol in saliva represents the fraction of circulating cortisol that is unbound to carrier proteins, saliva, as a sampling medium has been used for a considerable time for steroid analysis. Since the earliest reports, there is evidence that saliva free cortisol levels reflect the free cortisol concentrations in plasma (Umeda et al, 1981; Vining et al, 1983). Most of these studies have compared the levels of salivary free cortisol measured by radioimmunoassay and the levels of serum unbound cortisol determined by the method of equilibrium dialysis in paired saliva and serum samples in a large number of subjects. A linear relationship between the levels of saliva cortisol and serum unbound cortisol is seen over the whole range of serum free cortisol concentrations with most investigators reporting a correlation coefficient of r=0.9 (Cook et al, 1986; Hiramatsu, 1981; Vining et al, 1983). Moreover, Umeda et al. showed that salivary cortisol concentrations parallel these of free cortisol in plasma after CRH stimulation and cortisol injection as well as in the diurnal rhythm (Umeda et al, 1981). Typically lower correlation coefficients are reported if total plasma cortisol levels are compared to salivary free cortisol levels. The reason for this discrepancy is the the presence of CBG in plasma, which is largely saturated above cortisol concentrations of 500-600 nmol/l of cortisol (Vining et al, 1983). The data of Vining et al. showed that there is a biphasic

response in salivary cortisol when plotted against plasma total cortisol concentrations depending on CBG levels and saturation. Once the CBG binding capacity is exceeded, salivary cortisol concentrations increase more rapidly with increasing total cortisol concentrations, reflecting a disproportionate increase in plasma free cortisol. It might be also that under various conditions (chronic stress, contraceptives) CBG and/or albumin levels are altered with concurrent elevated levels of total cortisol but no apparent change of the amount of the free hormone fraction (Coolens et al, 1987).

1.4.2 Saliva vs. plasma sampling

For specific investigations, particularly in psychiatry, stress research, and pharmacokinetics, saliva analysis may deliver equivalent or even better results than blood analysis (Aardal-Eriksson et al, 1998; Lo et al, 1992; Vining et al, 1983). The predominant advantage of salivary hormone analysis is the noninvasiveness of collection procedures, enabling samples to be obtained from patients afraid of venipuncture, especially children and phobic patients, without an unwanted adrenal stress response. This make salivary GC values, more reliable compared to serum values in stress research, pediatric applications, and the diagnosis of Cushing syndrome (Wood, 2009). The convenience of rapid short-term interval sampling and the availability of non-protein-bound hormones are the other advantages of salivary analysis. However standardization of both collection and analysis are required in order saliva use to achieve broader acceptance by clinicians.

1.4.3 Methods for studying GCs pulsatility

It has been long recognized that signaling within many endocrine systems is pulsatile. Pioneers in this field are Knobil et al. who showed that the pulsatile release pattern of gonadotropin-releasing hormone (GnRH) is crucial to the effectiveness of this hormone (Knobil et al, 1980). GnRH is synthesized and released by the hypothalamic neurons in a pulsatile manner and stimulates the pulsatile release of the gonadotropins lutheinizing hormone (LH) and follicle-stimulating hormone (FSH) from cells within the anterior pituitary gland. From a physiologic perspective their work in rhesus monkey showed that GnRH needs to be administered in a pulsatile fashion to effect the secretion of LH and FSH by gonadotropes within the pituitary gland. Marshal et al. have demonstrated a role for GnRH pulse frequency in controlling gene expression of both LH and FSH (Marshall et al, 1993; Yen et al, 1972). These studies have demonstrated that the pulsatile nature of GnRH and gonadotropin release is vital to reproduction. Because of the physiological importance of episodic hormone release, considerable efforts have been put forward in order to define and characterize these pulses within the concentration time series by endocrine investigators. Examples of some initial efforts included defining pulses as an increase followed by a decrease of an arbitrary number of units e.g 5 mIU for LH (Yen et al, 1972), or an increase in the serum concentration of a hormone of at least 20 % over the proceeding nadir (Santen & Bardin, 1973). A decade passed before the development of computer-assisted algorithms for the identification and characterization of pulsatile hormone secretion. The early attempts in mid-1980's include the development of computerized pulse analysis techniques, each subserved by quite different mathematical constructs. The latter included Ultra (Van Cauter et al, 1981), Pulsar (Merriam & Wachter, 1982) and Cycle detector (Clifton & Steiner, 1983). The use of sampling protocols differing in sampling frequency and interval and analysis of the resultant hormonal concentration-time series with computer-assisted algorithms based on non-

uniform mathematical and statistical approaches resulted in quite diverse estimates of pulsatile hormone secretion, in many cases under theoretically similar physiological conditions. Such divergent results stimulated the further development of pulse detection algorithms. The second generation computer assisted algorithms included Detect (Oerter et al, 1986) and Cluster (Veldhuis & Johnson, 1986) with both programs being rigorously statistically based. However, it was soon recognized that such methods identify perturbations in concentration-times series rather than describing the actual underlying secretory events. The notion that a hormone pulse is comprised of both a secretory event and factors which affect clearance of the hormone such as distribution, binding to proteins, metabolism and excretion stimulated the search for methods that can separate the hormone pulse into constituent secretory burst and clearance components. Turner, Rebar and MacIntosh were among the first to employ deconvolution procedures to achieve this objective (McIntosh & McIntosh, 1985; Rebar et al, 1973; Turner et al, 1971). Their algorithms still suffered from a number of limitations such as the need of information about the hormone half-life. Recognizing the need of an approach that would not be constrained by the requirement for a priori information about the half-life (t½) Veldhuis, Carlson and Johnson developed a deconvolution procedure which allows for simultaneous assessment of both the hormone secretory burst characteristics and provided an estimate of the hormone half-life (Veldhuis et al, 1987). Their multi-parameter deconvolution method known as Deconv differed from earlier procedures in that it describes secretion as a variable number of Gaussian shaped secretion events which are convolved with a one or two component exponential elimination and then fit directly to the concentration-time series. Among the advantages of Deconv over the previous algorithms is the identification of the secretory bursts directly by the fitting process. It also provides information about the secretory burst mass (AUC), height (amplitude), burst

half-duration and hormone half-life estimates. However these latter methods also had significant limitations including the subjective nature of identification of the secretory bursts, the lack of robust statistical verification of resolved secretory bursts, and the user-unfriendly interface of the programs. To address these concerns, the latest generation deconvolution procedure, AutoDecon, has recently been developed and validated for LH and growth hormone (GH) (Johnson et al, 2008; Johnson et al, 2009). AutoDecon implements a rigorous statistical test for the existence of secretion events. In addition, the subjective nature defining earlier deconvolution procedures is eliminated by the ability of the program to automatically insert and subsequently test the significance of presumed secretion events. No user intervention is required subsequent to the initialization of the algorithm. This automatic algorithm combines three modules: a parameter *fitting* module, a new *insertion* module that automatically adds presumed secretion events, and a new *triage* module that automatically removes secretion events, which are recognized to be statistically non significant. It functions by developing a mathematical model for the time course of the hormone concentration and then fitting this mathematical model to bf experimentally observed time-series data with a weighted nonlinear least-squares algorithm. Specifically, this mathematical model (Johnson et al, 2004) is:

$$C(t)=\int_0^t S(\tau)E(t-\tau)d\tau+C(0)E(t)$$

where C(t) is the hormone concentration as a function of time t, S(t) is the secretion into the blood as a function of time, and E(t − z) is elimination from the serum as a function of

time. The resultant secretory waveform is assumed to have Gaussian or skewed distribution of release rates over time (Figure 4).

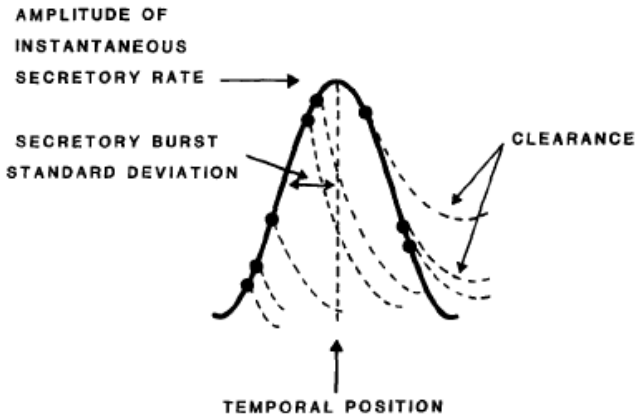

Figure 4. A hypothetical secretory bust of symmetric form that can be modeled as a Gaussian event. Adapted and modified from (Johnson et al, 2009).

The elimination fraction, E (t-z) can be approximated in many biological circumstances as a mono-, bi-, or pluriexponential decay function:

$$E(t - z) = A\,e^{-k_1(t-z)} + B\,e^{-k_2(t-z)} + C\,e^{-k_3(t-z)}$$

The rate constants k1, k2, and k3 are eliminaion constants in inverse time units, and they are related to the half-life as $t_{1/2}$=ln2/k.

When applied to synthetic GH concentration time series, AutoDecon performs substantially better than a number of alternative pulse detection algorithms in terms of optimizing the detection of true-positive secretory events, while at the same time minimizing the detection of false-positive and false-negative events. Although AutoDecon will require validation with regard to application to other hormonal systems,

it seems to hold substantial promise as a biomathematical tool with which to identify and characterize a variety of pulsatile hormonal signals.

1.5 Structure of GR gene

All human glucocorticoid receptor hGR isoforms are encoded by the NR3C1 gene located on chromosome 5q31-q326 (Hollenberg et al, 1985). It contains 8 translated exons (2-9) and 9 untranslated alternative first exons. We and others have shown that GR levels are under the transcriptional control of a complex 5' structure of the gene, containing the untranslated first exons important for differential expression of the GR. All of the alternative first exons identified are located in one of the two promoter regions: the proximal or the distal promoter region**,** located approximately 5 kb and 30 kb upstream of the translation start site, respectively (Barrett et al, 1996; Breslin et al, 2001; Breslin & Vedeckis, 1998; Geng & Vedeckis, 2004; Nunez & Vedeckis, 2002; Wei & Vedeckis, 1997). Alternative first exons 1A, and 1I are under the control of promoters in the distal promoter region, whereas the promoters of exons 1D, 1J**,** 1E, 1B, 1F, 1C (1C1-3), 1H (Figure 5) are located in the proximal promoter region (Presul et al, 2007; Turner & Muller, 2005). Exons 1D to 1H are found in an upstream CpG island with a high sequence homology between rats and humans. The region- or tissue-specific usage of alternative first exons leading to different GR mRNA transcripts (Presul et al, 2007; Turner & Muller, 2005) provides a mechanism for the local fine-tuning of GR levels. Since the ATG start codon lies only in the common exon 2, this 5'mRNA heterogeneity remains untranslated, but is important for translational regulation (Pickering & Willis, 2005). Alternative mRNA transcript variants are generated by splicing of these alternative first exons to a common acceptor site in the second exon of the GR. Exon 2 contains an in frame stop codon immediately upstream of the ATG start codon to ensure that this 5'

heterogeneity remains untranslated, and that the sequence and structure 1 of the GR is not affected. The GR also has a variable 3' region. Unlike the 5' region, the 3' variability encodes splice variants with different functions. The 3 main 3' splice variants of the GR are GRα, GRβ, and GR-P. GRα and GRβ are generated by two alternatively spliced 3' exons, 9α and 9β. GR-P lacks both exons 8 and 9 and is translated into a protein with a truncated ligand binding domain (LBD) which is thought to enhance GRα activity. GRα is by far the most active form of the receptor, GRβ is thought to be a dominant negative regulator of the receptor, and little is known about the function of GR-P

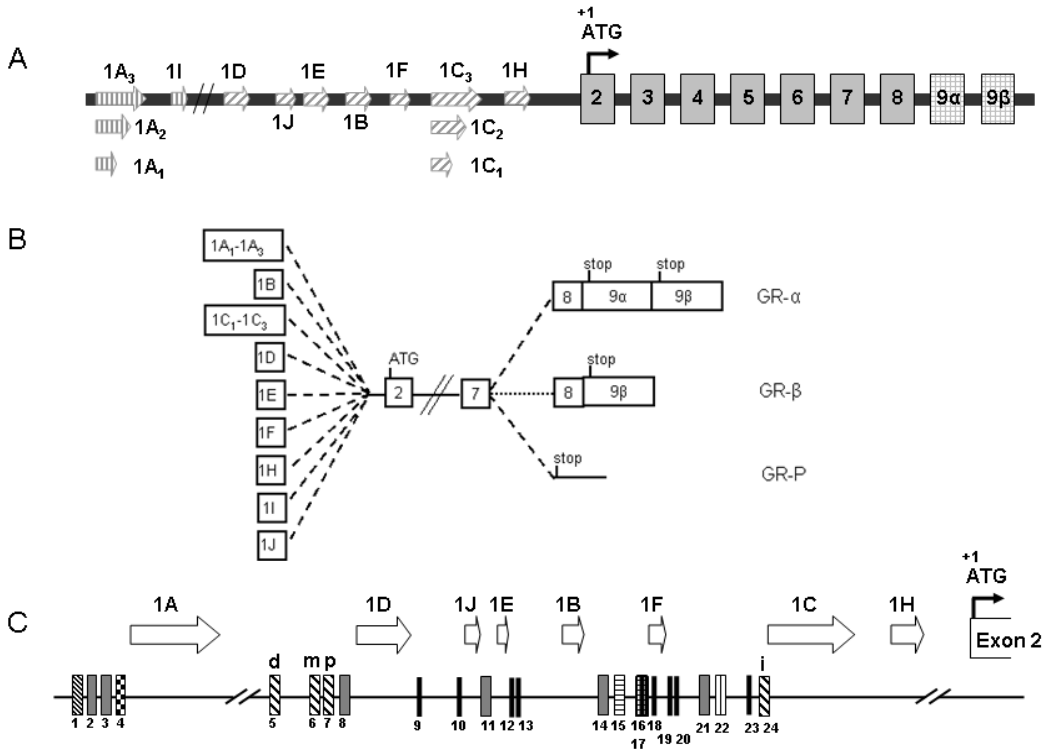

Figure 5. Structure of the GR gene (NR3C1; OMIM + 138040; NR3C1; 5q31-q32), the potential mRNA transcripts and the binding sites within the CpG island.

Panel A The genomic structure of the GR. ▥ 5' untranslated distal exons; ◪ 5'untranslated CpG island exons; ■ Common exons; ⊞ 3' alternatively spliced exons. Panel B shows the potential mRNA transcripts encoding the three GR isoforms: GRα GRβ and GR-P. Panel B shows the location of the known transcription factor binding sites. ▨ IRF 1 and IRF2 (position 1); ⚄ c-Myb, c-Ets ½ and PU1 (position 4); ⬔ Ying Yand 1 (positions 5,6,7 and 25); ■ Glucocorticoid response elements (GRE, positions 2, 3, 8, 21, and 22); ■ Sp1 binding sites (positions 9, 10, 12, 13, 16, 19, 20, 21, and 24); □ NGFIA binding site (position 17); ⊞ Glucocorticoid response factor-1 (GRF1, position 18); ⊟ Ap-1 (position 15); and ◫ Ap-2 (position 23). Adapted and modified from (Turner et al, 2009).

1.6 GR protein isoforms

GRα, the classical and most abundant GR splice variant, is ubiquitously expressed, with differences in expression levels between tissues and mediates genomic GC effects via different mechanisms (Kalinyak et al, 1987). As a member of the steroid receptor family GRα consists of three major domains: N-terminal domain, called immunogenic domain, which in hGRα is encoded by the first 420 amino acids and is necessary for transactivation. Amino acids 421-488 form the long zinc finger motif DNA-binding domain (DBD), important for GR dimerization, DNA-binding specificity and interactions with cofactors, and a C-terminal ligand-binding domain consisting amino acids 527-777, which is also involved in protein-protein interactions with chaperones and co-regulators depending on the presence of the ligand (Zhou & Cidlowski, 2005).

It has been shown that alternative translation initiation results in eight different N-terminal isoforms (A, B, C1, C2, C3 and D1, D2, D3) of GRα. These different GRα isoforms may homodimerize, heterodimerize or compete for coregulators, but also preferentially interact with different transcription factors and glucocorticoid response elements (GREs) (Lu & Cidlowski, 2005).

GRβ protein consists of 742 amino acids with 15 distinct amino acids at its carboxy end (Gross & Cidlowski, 2008). GRβ is not only shorter than GRα, but also varies due to its unique C-terminal ligand-binding domain (Gross & Cidlowski, 2008; Stahn et al, 2007).

Although GRβ forms homodimers that bind DNA, it does not bind any ligand examined so far, and thus fails to activate transcription. The relative levels of GRα and β in a cell influence cell's sensitivity to GCs with higher levels of GRβ resulting in GC resistance (Pujols et al, 2001). A third isoform, termed GR-P is encoded by exons 2-7 and part of intron 7. This truncated GR is missing a large portion of the ligand binding domain and

like GRβ encodes a unique carboxy terminal tail as a result of the inclusion of an intron fragment in the mRNA. GR-P is thought to enhance GRα mediated gene expression (Yudt & Cidlowski, 2002). GR-A lacks exons 5, 6 and 7, and together with GR-P have been associated with GC resistant phenotypes (Zhou & Cidlowski, 2005). GRγ has a single amino acid (arginine) insertion between exons 3 and 4, shown to halve the transactivation potential. Furthermore, GRγ expression levels were shown to correlate with childhood acute lymphoblastic leukemia (Zhou & Cidlowski, 2005).

The post-translational modifications of the GR include phosphorylations, ubiquitinations and sumoylations (Ismaili & Garabedian, 2004; Le Drean et al, 2002; Wallace & Cidlowski, 2001). The GR is constitutively phosphorylated under physiological conditions, but undergoes agonist and cell cycle induced hyperphosphorylation.

The five serine residues are phosphorylated selectively under different conditions by cyclin-dependent kinases (CDK), mitogen-activated protein kinases (MAPK), glycogen synthase kinase-3 (GSK3) and c-Jun N-terminal kinases (JNK). The phosphorylation of several of the serines is dependent on the binding of ligands, whilst others are phosphorylated in a ligand-independent manner. Kinases and phosphatases are essential for proper GR function and nucleocytoplasmic shuttling of the receptor (Zhou & Cidlowski, 2005). Another important modification of the GR induced by GC binding is the covalent attachment of ubiquitin to the receptor, thus marking it for proteasome degradation (Wallace & Cidlowski, 2001). Furthermore, sumoylation (the attachment of small, ubiquitin-related modifiers) of the GR potentiates its transcriptional activity (Le Drean et al, 2002).

1.7 GR and MR actions

GC effects are mediated either by the MR which has higher affinity for naturally occurring GCs, such as cortisol, and the GR which has 10 times lower affinity (de Kloet et al, 2008). Both receptors belong to the superfamily of nuclear receptors. The GR shows a widespread tissue distribution, whilst the MR has a more restricted expression. In certain brain areas including the hippocampus, both receptors are coexpressed, where they control neurotransmission and plasticity. In their inactive state the receptors reside mostly in the cytoplasm, as part of a large heteromeric compex with other several proteins such as hsp70, hsp90, FKBP51, FKBP52 and Cyp40 (Picard, 2006; Wochnik et al, 2005). The lipophilic nature of GCs allowed them to easily pass through plasma membranes by passive diffusion and bind the cGR and cMR. Upon ligation both receptors undergo conformational changes resulting in dissociation from their multiprotein complexes and the exposure of their nuclear localization signals and in the case of the GR, phosphorilation at five phosphorilation sites. Subsequently the ligand-bound receptors dimerize and translocate to the nucleus using the microtubule network as a guiding scaffold (Gross & Cidlowski, 2008). Here, the receptors function as ligand-activated transcription factors modulating genomic events (DeRijk et al, 2002). In addition to the classical nuclear receptors, anatomical and electrophysiological data have described membrane-bound variants of both the MR and GR (Di et al, 2003; Karst et al, 2005; Orchinik et al, 1991) that have been suggested to mediate rapid non-genomic effects via second messenger pathways. It is important that these genomic and non-genomic actions should not be seen as separate, but more as interacting and complementary mechanisms.

1.7.1 Cytosolic GR-mediated genomic effects

In the nucleus, the cGR modulates gene expression by several different modes of action. Firstly, GR binds as homodimer to specific GREs in the promoter region of target genes, and regulates the expression of target genes. The GR binding to highly conserved affinity GREs located within the promoter regions of GR target genes, results in the the recruitment of the basal transcriptional machinery and cofactors and in gene transcription (Gross & Cidlowski, 2008). GR binding to low affinity negative and less conserved negative GREs (nGREs) leads to transcriptional suppression. A number of genes harboring nGREs were identified such as human osteocalcin, type 1 vasoactive intestinal polypeptide receptor, human corticotrophin releasing hormone and neuronal serotonin receptor (Zhou & Cidlowski, 2005). The exact mechanism by which nGREs induce inhibition of gene expression is unknown, but it might result from interactions with the transcriptional machinery and/or GR inactivation due to interaction-mediated conformational changes (Gross & Cidlowski, 2008) (Figure 6). Secondly, the receptor can modulate gene expression, by interacting with other transcription factors such as AP-1, NFκB and members of STAT family (Kumar & Thompson, 2005).

1.7.2 Intracellular GR dynamics

While most studies have looked at gene regulation after long term stimulation by GCs, recently it was shown that ultradian hormone stimulation induces cyclic GR mediated transcriptional regulation, or gene pulsing (*PER1*, *GILZ*), both in cultured cells and in animal models (Conway-Campbell et al, 2010; Stavreva et al, 2009).

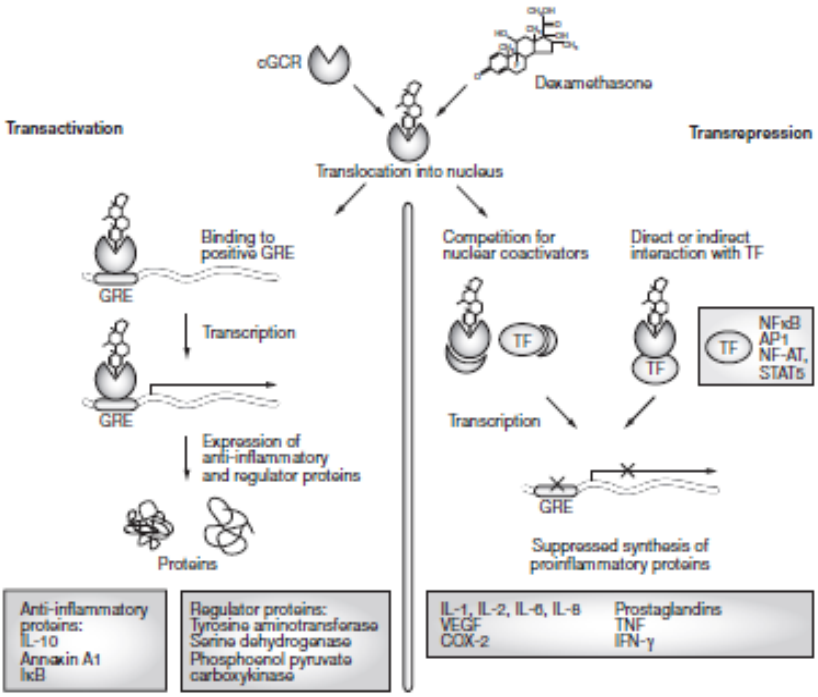

Figure 6. Models of glucocorticoid receptor transcriptional modulation. Adapted and modified from (Stahn & Buttgereit, 2008).

Recent studies have shown that the nuclear receptor mechanism is highly dynamic, rather than static process as previously considered. However, these studies have been performed in cell culture and adrenalectomized rats and translational studies in humans are warranted. Intra-tissue microdialysis demonstrated that GC target tissues are exposed to rapidly fluctuating hormone levels (Cook, 2001; Droste et al, 2008). It was first discovered that GR rapidly exchanges at promoters in the genome in a ligand and adenosine triphosphate (ATP)-dependent manner (Stavreva et al, 2004). Moreover, GR responds in an ultradian manner only to natural GCs and not to synthetic ligands such as DEX. This results in subsequent ultradian waves of GR nuclear translocation and GREs occupancy (Stavreva et al, 2009) (Figure 7). Moreover, the dynamic promoter occupancy of GR target genes coincides with oscillations in the "chaperone protein cycle", as well as RNA Polymerase II loading and exchange, which fluctuate according to the changes in

the extracellular hormone concentrations. Consequently, this results in "gene-pulsing" of transcriptional patterns of nascent RNA (Stavreva et al, 2009) (Figure 7).

Little information is available about the physiological relevance of this pulsatile GC release. For instance, episodic release of GnRH and GH prevent receptor desensitisation and maintain target tissue responsiveness. It was suggested that gene pulsing in the GR system is necessary for correct transcriptional programming (Lightman et al, 2008; Stavreva et al, 2009). Importantly, constant hormone treatment with synthetic GCs lead to constant gene expression and inappropriate protein expression resulting in altered body physiology (Belchetz et al, 1978; Wildt et al, 1981). At diagnostic level, an understanding of the role of the endogenous ultradian rhythm for normal function of GC responsive genes should result in new approaches to the diagnosis and treatment of abnormalities in HPA axis activity. Attention must be paid to the kinetics of therapy in patients with GCs' responsive diseases. The kinetics of the orally administered drugs results in a non-pulsatile increase in levels of plasma cortisol over the day, which will result in abnormal regulation of many GC-responsive genes. Therefore, as our knowledge of the effects of pulsatile endogenous GC release increases, pulsatile therapy must be investigated as an alternative to the old treatment regiments in order to maximize the therapeutic response and decrease GCs' side effects.

1.7.3 GR-mediated rapid non-genomic effects

GCs exert some of their immunosuppressive, anti-inflammatory and anti-allergic GC effects via nongenomic mechanisms (Buttgereit & Scheffold, 2002). Some of these effects occur within seconds and minutes and thus are too fast to be explained by classical nuclear signaling (Lowenberg et al, 2008).

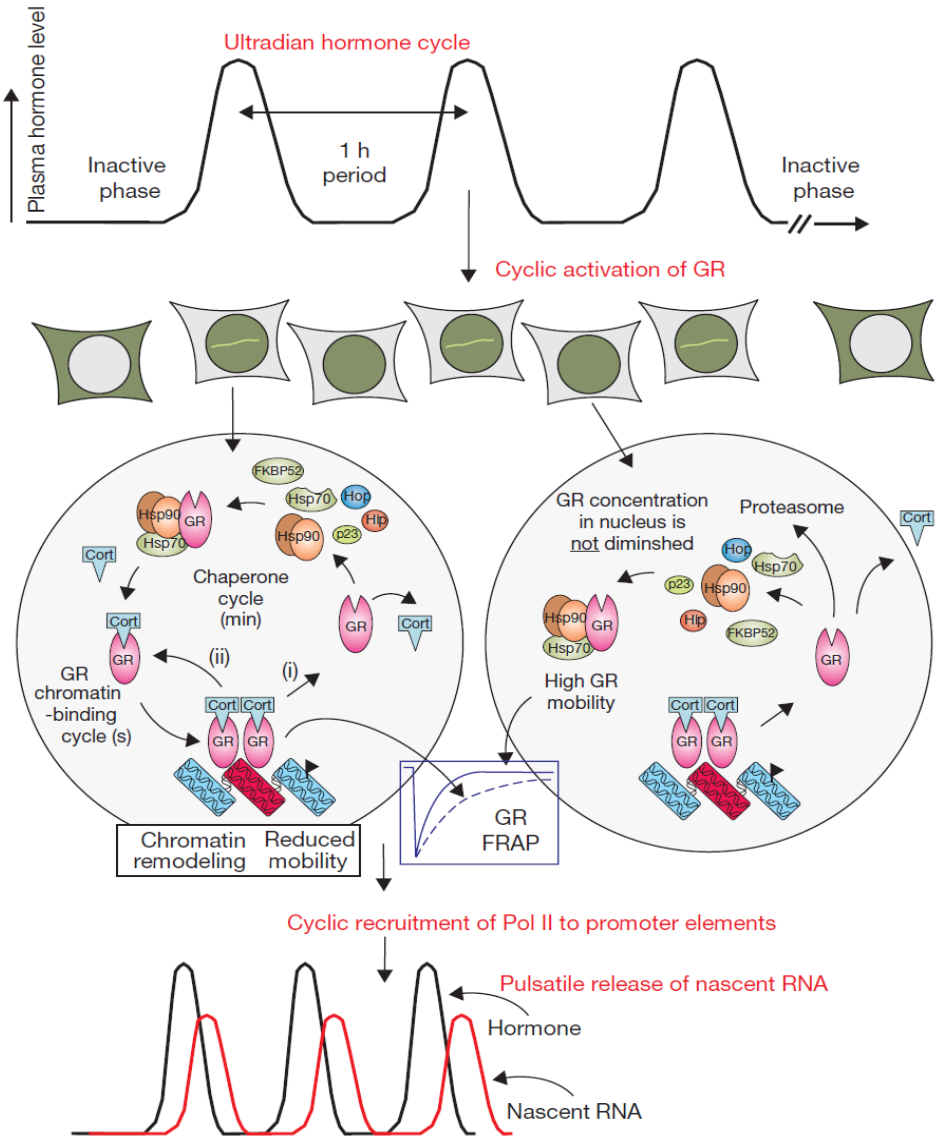

Figure 7. A schematic representation of cyclic GR interactions with response elements leading to a pulsatile release of a nascent RNA. Adapted and modified from (Stavreva et al, 2009).

Non-genomic effect do not directly influence gene expression, but may be mediated by the activation of signaling cascades. However, non-genomic effects may lead to subsequent genomic actions. Buttgereit et al. have given the following classification of the rapid non-genomic effects of GCs: nonspecific interactions of GCs with cellular membranes; nongenomic effects mediated by cGR; and specific interactions with

membrane GR (mGR) (Buttgereit & Scheffold, 2002). Recent findings suggest additional mechanism by cGR translocation to mitochondria (Boldizsar et al, 2010; Sionov et al, 2006). A high concentration of GCs (above 30 mg per day) can change the physicochemical properties of plasma and mitochondrial membranes. GCs are thought to intercalate into these membranes and change the function of membrane-associated proteins, thereby influencing membrane permeability and lipid peroxidation. The interaction of GCs with immune cells membrane leads to rapid immunosuppression and subsequent reduction of the inflammatory response through a decrease of calcium and sodium fluxes across plasma membranes. GCs also reduce ATP synthesis in the mitochondria (Buttgereit & Scheffold, 2002), which may also contribute to the antiinflamatory and immunosuppressive effects of high doses of GCs. Non-genomic effects can also be mediated by the proteins that dissociate from the cGR complex, following binding of GCs to the cGR. Released proteins such as Src, induce lipocortin activation and subsequent rapid inhibition of arachidonic acid release. This pathway has been considered as responsible for the rapid immunosuppressive effects of GCs (Croxtall et al, 2000). The third mechanism involves a membrane bound GR. It existence has been reported in amphibian neuronal membranes and in rodent lymphoma cells (Evans et al, 2000; Gametchu et al, 1999) and was further confirmed in human peripheral blood mononuclear cells. Lowenberg et al. have revealed the existence of mGR also in human T cells. They found that DEX inhibit T cell receptor signaling through inhibition of the enzymatic activities of components of the mGR-multiprotein complex, tyrosine kinase and FYN that have key role in initiatition of T cell signaling and subsequent cytokine synthesis, cell proliferation or migration (Lowenberg et al, 2006).

1.8 Glucocorticoid circadian rhythms and the immune system

Interactions between the nervous system, the HPA axis and components of the innate and adaptive immune system play a key role in the regulation of inflammation and immunity. Many of the studies carried out during the past 50 yrs have showed the wide spectrum of GC actions on the immune response with opposite effects on the innate and adaptive components of the immune system. In general, GCs assist the innate immunity and suppress the adaptive immunity. They act on the immune system by both suppressing and stimulating a large number of pro-inflammatory or anti-inflammatory mediators. In many ways, GCs lead to termination of inflammation by enhancing the clearance of foreign antigens by stimulating opsonization and macrophage phagocytotic ability and antigen uptake. GC stimulates the clearance of microorganisms by stimulation of expression of the manose receptor or the scavenger receptor CD163. GCs strongly downregulate a large number of cytokines (such as Il-1β, TNFα, IL-6, IL-12 and IL-18) and chemokines (including IL-8, Mip-1β, Mip-3β, Mcp-2, Mcp-3, Mcp-4 and eotaxin). Although GCs were shown to downregulate pro-inflammatory cytokines in vitro and in vivo, GCs enhance the receptor of some of these cytokines and chemokines such as IL-1RI, IL-8R, IFNαR, CSFRI, CSFRII, IFNγRI, IFNγRII, TNFR, CCR1 and complement factors C3a, C4a and C5a (Galon et al, 2002). GCs are shown to inhibit arachidonic acid metabolites, free oxygen radicals, and nitric oxide, explaining their potent anti-inflammatory properties. Antigen-presenting cells, such as macrophages and dendritic cells (DC), bridge innate and adaptive immunity. After exposure to GCs, the mature DC have a decreased ability to present antigens via the downregulation of MHC class II and co-stimulatory molecules and elicit a T cell response. The differentiation of CD4+ T cells into the mediators of cellular immunity T helper Th_1 lymphocytes, or into mediators of humoral immunity Th_2 lymphocytes, depends on the type of antigen encountered and the type of produced cytokines during antigen presentation. GCs inhibit Th_1 immune

response via inhibiton of IL-12 secretion from DC and monocytes. On the other hand they promote Th_2 immune response via enhancement of IL-10 secretion by macrophages. GCs also influence the cell viability by prevention or induction of apoptosis. The differentiation as well as the activation stage determines the T cell survival. Developing T lymphocytes, are highly susceptible to GC-mediated apoptosis, whilst mature T cells are more resistant and need pharmacological doses or prolonged GC treatment to undergo GC mediated apoptosis. GCs also suppress the humoral immunity, causing B cells to express smaller amounts of IL-2 and IL-2 receptors. This diminishes both B cell clone expansion and antibody synthesis.

Circadian rhythms are evident in both enumerative and functional immune measures (Knapp & Pownall, 1984). Peripheral counts of B cells and T cells peak nocturnally, while NK cells and macrophages peak diurnally (Ritchie et al, 1983). Plasma concentrations of cortisol and catecholamines exhibit most distinct circadian variations and their possible regulatory role in the circadian redistribution of the circulating immune cells have been extensively studied. Adrenalectomized mice were shown to loose their circadian leucocyte rhythm suggesting that immune cell redistribution is regulated by the adrenal hormones (Maisel et al, 1990). A clear negative correlation exists between T cell counts and plasma cortisol throughout the 24 h period suggesting a mechanistic link (Abo et al, 1981; Ritchie et al, 1983). Time-lagged cross correlation analysis revealed a negative correlation between T cells and plasma cortisol and a positive correlation between NK cells and plasma cortisol with a lag time of 2 h, whilst the correlations with epinephrine rhythm were non significant (Kronfol et al, 1997).

These redistributional changes are also associated with circadian variations in immune function (Fernandes et al, 1976; Knapp et al, 1979; Ratte et al, 1973). For instance the susceptibility of rats to reject skin and renal allografts, a measure of cell-mediated

immunity, depends on the circadian timing of transplantation (Ratte et al, 1973). In humans, the majority of renal allograft rejection episodes occur during the night, when GC levels are the lowest (Knapp et al, 1979). Similarly, specific antibody titers were higher in animals immunized during daylight when murine steroid concentrations are lowest than in those injected during the night (Fernandes et al, 1976). A circadian rhythm of natural killer cell cytotoxic activity (NKCA) in humans has been documented by substantial number of studies, most of which recorded increases of NKCA in the blood during the morning and early afternoon (Angeli, 1992; Kronfol et al, 1997). In rats maximal and minimal levels of activity were located in the early dark and the early light period respectively (Arjona et al, 2004). Other innate immune functions such as cytokine secretion by macrophages and NK cells undergoes similar time-of-day variation with high levels occurring after the onset of the dark phase and low levels during the light phase in mice (Keller et al, 2009).

1.9 Research Objectives

The main goal of this thesis was to investigate several facets of the complex temporal relationship between the central nervous, endocrine and immune systems. As outlined in this chapter cortisol, a key stress mediator in humans, exerts profound effects on a wide range of physiological and developmental processes that are crucial for the maintenance of homeostasis and adaptation to stress. Cortisol exhibits a circadian rhythm with peak levels in the early morning hours followed by a late afternoon nadir. Underlying the circadian pattern is an ultradian rhythm of cortisol secretory pulses. Detailed analysis of hormone pulsatility is necessary for understanding hormone signaling under both normal and pathophysiological conditions. So far this analysis was performed only in blood samples where higher cortisol levels may occur due to the invasiveness of the venipuncture procedure. Therefore, the first aim of this thesis was to investigate the utility of saliva as an alternative sampling medium for future psychobiology studies on cortisol pulsatile secretion.

Circadian rhythms of the HPA axis and of cortisol have been implicated in circadian redistribution of circulating lymphocytes and granulocytes reflected also in circadian changes in their immune function. However, information regarding the diurnal redistribution of immune cells and their temporal correlations with cortisol is scarce. Therefore the second aim of this thesis was to investigate the diurnal redistribution of T, B and NK cell subsets in relation to the endogenous cortisol rhythm.

Superimosed on these natural circadian rhythms is the central nervous system-mediated glucocorticoid response to stressor. Psychosocial stress is involved in the ethiology and pathogenesis of many neurodegenerative and immune diseases and the inter-individual variation in responses to stress are suggested to play a key role in the different prevalence of stress-related disorders. Together with SAM axis, HPA axis activation and CG-GR

mediated slow genomic effects play a central role in the complex stress response. Therefore our third aim was to investigate the effects of a psychosocial stressor on the levels and kinetics of expression of primary GR target genes, previously associated with stress-related disorders in both male and female subjects.

1.10 Outline of the thesis

The thesis is organized in five main chapters. **Chapter 1** gives an overall introduction into the subject of the thesis. **Chapter 2** is focused on comparing the natural GC rhythm in saliva and in plasma samples in healthy male donors and aimed to investigate saliva as an alternative sampling medium for studing the pulsatile cortisol secretion by deconvolution analysis for future psychobiological research. **Chapter 3** is focused on interplay between the non perturbed neuro-endocrine and the immune systems. Circadian cortisol rhythm has been suggested as a possible regulator of the circadian redistribution of the circulating immune cells. Focusing on an 8 h observation period throughout the day we investigated the diurnal redistribution of human lymphocytes and their temporal associations with salivary cortisol profiles. In **Chapter 4,** we focused on the GR-mediated genomic effects in a perturbed HPA axis. We investigated the kinetics of GR-mediated gene expression in response to a laboratory psychosocial stress in a cohort of healthy males and females.

The key findings of this thesis as well as suggestions for future research are discussed in **Chapter 5**.

Chapter 2

The use of saliva for assessment of cortisol pulsatile secretion by deconvolution analysis

Slavena T. Trifonova [a,b], Manon Gantenbein [c], Jonathan D. Turner [a,b], Claude P. Muller [a,b]

[a] Institute of Immunology, CRP-Sante / National Public Health Laboratory, 20A rue Auguste Lumière, L-1950 Luxembourg, Grand Duchy of Luxembourg

[b] Department of Immunology, Research Institute of Psychobiology, University of Trier, D-54290 Trier, Germany

[c] Clinical and Epidemiological Investigation Center, CRP-Santé, 1A rue Thomas Edison, L-1445, Luxembourg, Grand Duchy of Luxembourg.

This study has been published in *Psychoneuroendocrinology* (2013) Jul; 38(7):1090-101

2.1 Abstract

Cortisol is the key effector molecule of the HPA axis and is secreted in a pulsatile manner in all species studied. In order to understand cortisol signalling in health and disease, detailed analysis of hormone pulsatility is necessary. To dissect cortisol pulsatility in plasma deconvolution techniques have been applied. Blood sampling is a labour-intensive, expensive and invasive technique that causes stress and alters HPA axis activity. Therefore saliva has been extensively investigated as an alternative sample to measure cortisol. Here we use state of the art deconvolution algorithms to investigate cortisol pulsatility in saliva. Blood and saliva samples were obtained at 15 min intervals over an eight hour period in 18 healthy men to analyse their diurnal cortisol levels. A multiparameter deconvolution technique was used to generate statistically significant models of cortisol secretion and elimination in plasma and saliva. The models consisted of estimates of the number, amplitude, duration and frequency of secretory bursts as well as the elimination t½ in a subject specific manner. No significant differences were noted between plasma and saliva with regard to the observed secretory bursts (7.8± 1.5 vs. 7.0 ±1.4) and the interpeak interval (59.6±10.5 min vs. 61.0±11.5 min). Moreover a strong positive correlation between the numbers of peaks in both fluids were observed ($r=0.83$, $p<0.0001$). Monte Carlo simulations revealed an 84 % temporal concordance between plasma and saliva peaks in all donors ($p<0.005$) with a mean of 1.3±0.8 plasma peaks unmatched in saliva. The percentage concordance increased to 90 % when concording only the morning cortisol peaks in plasma and saliva up to 1100 h. The deconvolution of the most distinct component of cortisol diurnal rhythm-CAR, revealed an average 2.5±1.1 peaks based on the individual time for cortisol to return to baseline levels. In conclusion, deconvolution analysis of plasma and salivary cortisol concentration time series showed a close correlation and similar pulsatile characteristics between saliva and plasma cortisol.

Similarly, Monte Carlo simulations revealed a high concordance between the peaks in these coupled time series suggesting that saliva is a suitable medium for subsequent deconvolution analysis yielding accurate and reliable models of cortisol secretion in particular during the morning hours.

Keywords: cortisol, secretion, half-life, saliva, Deconvolution, modelling, Monte Carlo simulations, concordance

2.2 Introduction

Cortisol, exerts profound effects on a wide range of physiological and developmental processes that are crucial for the maintenance of homeostasis and adaptation to stress. Secretion of cortisol, the final product of the HPA axis is regulated by a hormonal cascade initiated by the PVN of the hypothalamus. The PVN receives circadian pulses from the SCN of the hypothalamus, and integrates information from cognitive processes and emotional and physical stress reactions (Reppert & Weaver, 2002; Ulrich-Lai & Herman, 2009). Circadian oscillations in cortisol concentrations peak in the early morning hours and reach their nadir by the first half of the night. Underlying the circadian pattern is an ultradian rhythm of cortisol secretion pulses. These secretory episodes occur at a constant frequency of approximately one hour in both rats and humans. These secretory episodes occur at a fairly stable frequency in both rats and humans, but have variable amplitudes responsible for the typical circadian rhythm (Lightman et al, 2000; 2002; 2008; Lightman, 2006; Stavreva et al, 2009; Young et al, 2004) although variations in the interpeak interval (IPI) between the active and quiescent phases have also been reported (Veldhuis et al, 1989b). The pulsatility model of Walker et al. (Walker et al, 2010) suggests that activation alternating with inhibition of the HPA axis regulates cortisol pulses. During the secretory phase of a pulse, rapidly rising corticosteroid levels induce a rapid feedback signal, inhibiting secretion. The circulating hormone is metabolised and cleared. After a more or less constant interval the next pulse is triggered.

Detailed analysis of hormone pulsatility is necessary for understanding hormone signalling under both normal and pathophysiological conditions. A number of psychiatric and neurological diseases have been associated with changes in glucocorticoid pulsatility. For example, Deuschle et al. showed an increased HPA activity in MDD with a higher pulse frequency (Deuschle et al, 1997). Conversely, Halbreich et al. reported a reduced

pulse frequency in patients with endogenous depression (Halbreich et al, 1985). An approximate doubling of cortisol pulse frequency was observed in an animal model of chronic inflammation (Windle et al, 2001). Thus, monitoring cortisol secretion patterns may help to elucidate mechanisms underlying some of these neuroendocrine disorders.

Serial measurements of hormone concentrations provide limited information about hormone pulsatility. Initially computer-based modeling techniques were used to identify and characterize perturbations in hormone concentration time series rather than describing actual underlying secretory events (Clifton & Steiner, 1983; Merriam & Wachter, 1982; Oerter et al, 1986). Deconvolution analyses, commonly used in physics correspond to mathematical dissection of concentration profiles into underlying release and elimination steps. This was later adapted to characterize hormonal secretion and clearance, revealing the underlying ultradian pulses in plasma (Johnson et al, 2004; McIntosh & McIntosh, 1985; Rebar et al, 1973; Veldhuis et al, 1987). However these earlier deconvolution procedures had several limitations including subjective identification of secretory bursts, the necessity of a priori knowledge of the t½, the lack of robust statistical verification and user-unfriendly interface (Clifton & Steiner, 1983; Merriam & Wachter, 1982; Oerter et al, 1986; Veldhuis & Johnson, 1986). These disadvantages have recently been corrected by a fully automated and statistically-based deconvolution procedure, AutoDecon, developed by Johnson et al. (Johnson et al, 2008; Johnson et al, 2010). It provides both an objective approach to initial secretory burst selection with no user intervention required and a statistically based verification of candidate secretory bursts. It was shown that analysis with Autodecon resulted in substantially higher true-positive rates of identification of hormone secretory events than earlier deconvolution algorithms (Johnson et al, 2010). The application of deconvolution analyses to study the normal HPA physiology in humans has however advanced the understanding of amplitude modulation

and changes in frequency, which are characteristic of the circadian hormonal secretion (Veldhuis et al, 1990; Veldhuis et al, 1989b).

Cortisol pulsatile patterns have so far been investigated exclusively in plasma samples (Henley et al, 2009; Kerrigan et al, 1993; Metzger et al, 1993; Veldhuis et al, 1989b). An important prerequisite of any investigation of the HPA axis requires a stress-free sampling method, especially in psychobiological research. Several studies have shown that venipuncture represents a stress that can significantly enhance cortisol levels in infants (Mantagos et al, 1991), healthy adults and patients with Cushing` syndrome (Stahl & Dorner, 1982). Moreover it was shown that this response to sampling may result in a state of low reactivity of the whole HPA axis, potentially masking the effect of experimental stimuli (Follenius & Brandenberger, 1986). This may be overcome by measuring salivary cortisol levels.

Measurement of salivary cortisol has proven to be a valuable research tool, to monitor circadian rhythm, ACTH stimulation, dexamethasone suppression in normal subjects and patients with neuroendocrine disorders (Laudat et al, 1988; Peters et al, 1982; Umeda et al, 1981; Walker et al, 1978). Salivary cortisol levels are thought to reflect the free fraction in plasma. A high concordance between the two free cortisol fractions has been reported and can be explained with the fact that cortisol enters the oral cavity mainly by passive diffusion. It is therefore independent of transport mechanisms, saliva flow rates and volumes. The correlation itself between free cortisol levels in both plasma and saliva are independent of CBG levels, even if CBG influences the level of free cortisol (Laudat et al, 1988; Peters et al, 1982; Umeda et al, 1981; Vining et al, 1983; Walker et al, 1978). Nevertheless circadian fluctuations of CBG and lower cortisol levels during the afternoon hours, reduce free cortisol fractions in both plasma and saliva. Thus salivary cortisol has several additional advantages over venipuncture in psychobiological research.

In this study, we analysed ultradian salivary and plasma cortisol profiles between 0800 h and 1600 h by mathematical deconvolution and compared the deconvoluted models with each other. Deconvolution permitted us to resolve the cortisol secretory bursts in both plasma and saliva generating individual deconvolution models and to study the underlying pulsatile structure of the major component of cortisol diurnal rhythm-CAR. We obtained similar deconvolution models and high concordance between secretory events in both fluids. Therefore because of its non-invasive nature and limited effect on the HPA axis saliva sampling suggesting that saliva may be the preferred sampling procedure for cortisol in psychobiological studies. This study investigates the utility of salivary cortisol during the waking hours to monitor its underlying pulsatile secretion for future psychobiological studies.

2.3 Materials and methods

2.3.1 Subjects and experimental design

Eighteen healthy male donors (age range 18-40, mean 28.6±7.0 yrs) were recruited from the general population. Exclusion criteria included: chronic or acute illnesses, medication within the previous two weeks and a BMI <18 or >30.

Donors who live and work close to the Clinical Investigation and Epidemiological Center were recruited to minimize the time between awakening and arrival. All donors came to the Clinical Center, several days prior to the experiment to receive detailed instruction about the study. Donors were instructed to wake up as every day, and to come to the Clinical Center as though they were going to their normal work. Care was taken that there was only minimal deviation from their daily morning routine to reduce the effect of stress on CAR as much as possible. Donors were supplied with saliva collection devices

(Salimetrics oral swabs, Salimetrics, Newmarket, UK) and they were instructed to collect salivary samples first thing after awakening while they were still in bed. This first saliva sample was used as baseline cortisol levels to calculate CAR. The mean delay between time of awakening and arrival was 71.8 ± 17.01 min. Donors arrived between 0715 and 0945 h. The procedure continued from the time of arrival every 15 min until 1600 h. EDTA blood was drawn after arrival concurrently with saliva sampling using an indwelling intravenous canula. Samples were stored at -20˚C until analysed. During the experiment the subjects were allowed normal ambulatory activity and received meals at 0900 h and 1200 h. Meals were provided immediately after saliva collection. One saliva sample was collected at 1200 h during the meal. Subjects were asked to stop eating for five minutes before the sampling. None of the participants voiced any complaints about the sampling procedure or asked to interrupt the sampling. The study protocol was approved by the Luxembourg National Research Ethics Committee (CNER) and written informed consent was obtained from all participating subjects.

2.3.2 Hormone assays

Plasma cortisol concentrations were determined by an in vitro diagnostic competitive immunoluminometric sandwich assay (Liaison Cortisol®, Diasorin, Saluggia, Italy). The assay sensitivity was 15 ng/ml. Intra-assay variability was 2.96 %, and inter-assay variability was 5.58 % (according to the manufacturer).

Salivary cortisol was measured in duplicate by commercial ELISA (Salimetrics, Newmarket, UK) with a minimal detection limit of 0.03 ng/ml and intra- and inter-assay variability of 3.5 % and 5.08 %.

2.3.3 Deconvolution analysis

For the deconvolution analysis model-free secretory profiles were generated using the pulse algorithm integrated in the Pulse_XP software (Johnson et al, 2008). Pulse_XP is an integrated software package designed for the analysis of hormone concentration time-series for both basic and clinical research. This software package provides tools for the exploration of the aperiodic fluctuations that are typical of serum concentration profiles for many neuroendocrine and peripherally secreted hormones. It is a non-commercial freeware that can be downloaded from http://mljohnson.pharm.virginia.edu/home.html. The software estimated the approximate positions and amplitudes of major secretory events and provided initial estimates of cortisol half-life and of basal secretion rates. Then, the model was refined to generate statistically significant profiles applying the Autodecon algorithm (Johnson et al, 2008) to the Akaike`s information criterion (AIC)<70 as a measure of the relative goodness of fit of the statistical model (Akaike, 1974) and using runs test for randomness to demonstrate that there is no statistical difference between modelled and observed data (i.e $p>0.05$). All experimental analyses were performed by the same person to avoid inter-operator errors. To exclude for subjective errors, models were re-generated by a second operator. Main models estimates were compared by linear regression analysis and resulted in $R^2>0.9$.

2.3.4 Concordance of secretion events

Formal statistical analyses of coincident saliva and plasma cortisol pulses were performed using the concordance module of the Pulse_XP software (Johnson et al, 2008; Johnson et al, 2009) to confirm the non-random associations ($p<0.05$) between hormone release episodes in both fluids. This module applies Monte Carlo simulations with 100 000 cycles

to evaluate the statistical significance of the observed cortisol pulse coincidence. Coincidence within a fixed time window (lag) was defined by peak maxima in samples occurring within 20 min of each other. Analyses were carried out both with a fixed time window (±20 min) irrespective of statistical significance and by varying the time window in order to achieve optimal statistical significance for each donor.

2.3.5 Statistical analysis

Comparison between plasma and saliva for the number of temporally coincident cortisol secretory peaks, their IPI and cortisol half-life were performed by student T-test and these results were presented as mean ± S.D. Mathematical relationships were calculated using the Pearson product moment correlation test. All statistical analyses were performed using SigmaStat (Systat Software, GmBH, Erkrath, Germany). Statistical significance was considered for $p<0.05$, after Bonferoni post hoc correction whenever necessary. In order to describe the CAR, the cortisol net increase as well as the area under the curve with reference to ground (AUCg) (Pruessner et al, 2003) were calculated. The cortisol net increase was defined as the difference between the individual cortisol peak value (e.g., sample 2, 3, 4, or 5) and the first cortisol measurement immediately after awakening (sample 1) (Kudielka & Kirschbaum, 2003). The cortisol zenith was defined as the highest morning cortisol peak measured for each individual.

2.4 Results

2.4.1 Plasma and saliva cortisol concentration profiles

Plasma and saliva cortisol profiles were obtained from 18 healthy donors. The sampling procedure proved acceptable to all of the donors with none dropping out or filing a complaint. All donors demonstrated a series of major fluctuations in saliva as well as in plasma cortisol throughout the observation period. These fluctuations were characterized by sharp rises in the early morning followed by a slower, generally smooth decline, following in most cases an exponential curve. Three representative donors are shown in Figure 8-10A-B. All profiles showed the typical cortisol pattern with the characteristic morning cortisol zenith, a midday meal–related peak that coincided with the subjects' lunch time (1230-1400 h) and an afternoon nadir.

Fourteen of the 18 donors showed a clear diurnal rhythm, with a characteristic CAR in salivary samples, occurring on average 42.8±16.5 min after awakening (range 15-60 min). Two subjects showed a later CAR that peaked only 75 min and 90 min after wake-up. For two other donors the cortisol zenith could not be detected due to incorrect sampling after awakening. These donors were therefore excluded from other CAR analysis. The mean saliva cortisol zenith for 14 donors was 16.6±5.9 nmol/l (range 9.4-26.4 nmol/l). CAR was calculated for each donor using the first five time points (i.e up to 60 min after awakening). The mean net cortisol increase for the 14 donors was 10.31±4.3 nmol/l, (range 4.93-20.38 nmol/l). AUCg measured on the first five morning samples averaged 714±294 nmol/l. The mean time between the salivary cortisol zenith and its drop was found to be 93.2±35.8 min (range 30-135 min). The mean saliva cortisol zenith of the midday meal-related peak was 9.38±4.3 nmol/l (range 4.1-21.9 nmol/l).

The plasma cortisol zenith was detected only for the two donors with the late CAR (i.e 75 and 90 min post awakening). For all other donors the post awakening increase and the zenith were missed. Only the post zenith CAR decrease was observed. Due to the time delay between awakening and the first blood sample it was not possible to obtain

information about CAR indices (net increase, AUCg) for any of the donors. The mean plasma cortisol zenith of the midday meal-related peak was 333.4±110 nmol/l, (range 192-505 nmol/l).

Salivary cortisol correlated positively and significantly with plasma cortisol in all donors ($r=0.48$-0.98, $p<0.05$ in all the cases, Figure 12A-B). Whilst 84 % (15/18) of the subjects showed correlations of $r>0.7$ and up to $r= 0.98$, only 16 % (3/18) of the subjects had low correlations of $r<0.7$. The lowest r-value being 0.48. This was clearly reflected in the overall correlation between salivary and plasma cortisol concentrations, that was lower than the one expected, but highly significant ($r=0.71$, $p<0.0001$, Figure 12C). When introducing a 15 min lag, the cross-correlation improved with improves with 89 % (16/18) subjects with an $r>0.7$, and only 11 % (2/18) subjects with a correlation of $r<0.7$. The area under the salivary cortisol curve was on average 3.96 %±1.12 (range 2.3 %-7 %) of the area under the plasma cortisol curve (Table 1). A significant positive correlation between total AUC values, a surrogate measure of cortisol production in plasma and saliva was detected ($r=0.66$, $p=0.002$, Figure 12D), despite the enhanced 11-β hydroxysteroid dehydrogenase (HSD) activity in saliva and CBG in the plasma preventing the bound fraction from reaching the saliva.

The mean area under the midday peak in saliva corresponded to about 2.84 %±0.85 (range 1.6-4.9 %) of AUC in plasma. Similarly, its mean amplitude in saliva was 2.80 %±0.85 (range 1.2-5.1 %) of the amplitude in plasma. A significant positive correlation between the AUC values of the midday peak in plasma and saliva was detected ($r=0.51$, $p<0.05$, Figure 12E). The same result was observed when comparing the corresponding peak amplitudes in plasma and saliva ($r=0.54$, $p<0.05$, Figure 12F). Strong correlations were also obtained between individual midday peak AUC and their corresponding peak

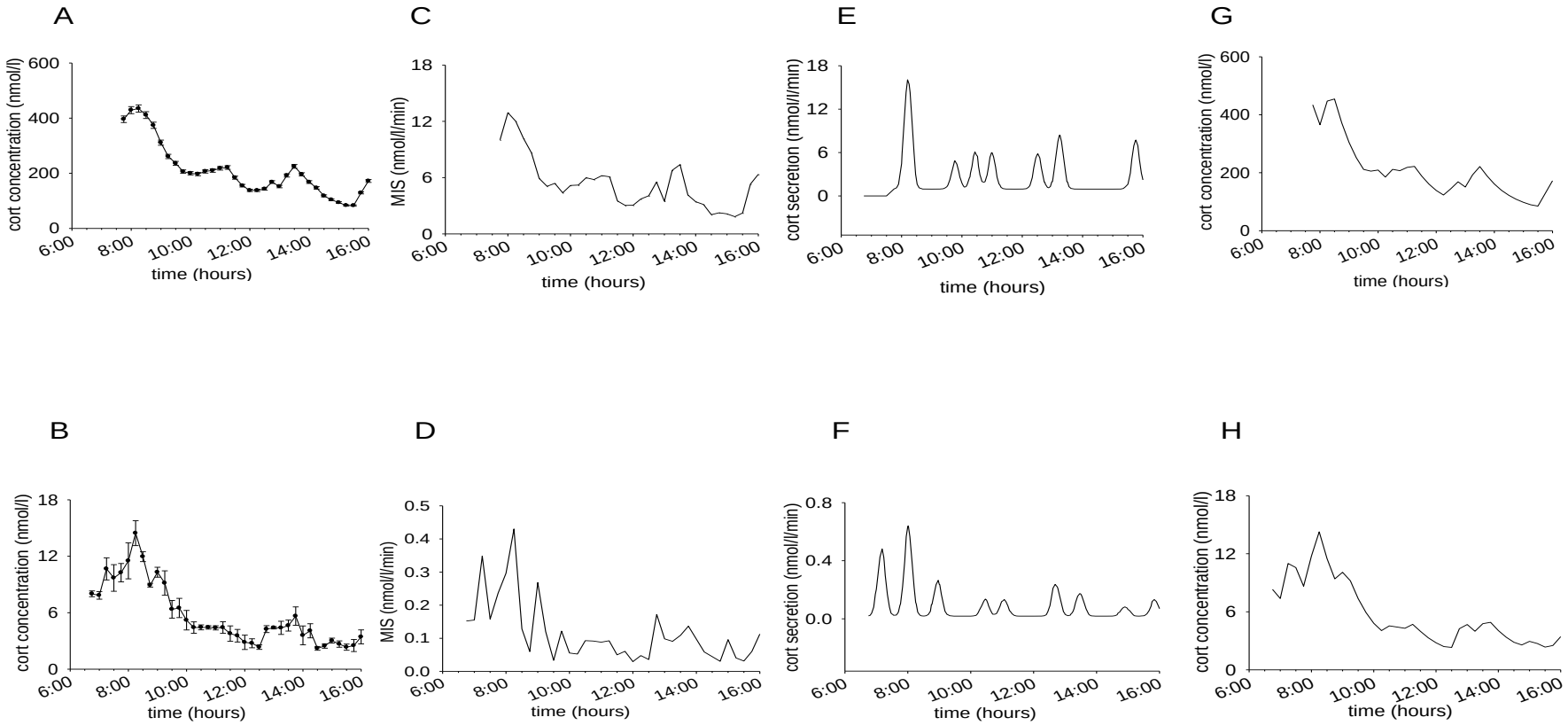

Figure 8. Plasma and saliva cortisol concentrations analysed by deconvolution analysis for one representative donor. Initial concentration profiles for plasma (A) and saliva (B) we used to generate model-independent secretory profiles (C and D), and subsequently deconvoluted using the Autodecon algorithm to give the underlying cortisol pulsatile structure (E and F). The pulsatile patterns were convoluted to give the theoretical concentration profiles (G and H) that were not statistically different from the initial concentration profiles (A and B). Concentration is expressed in nmol/l. Secretion is expressed in nmol/l/min. Error bars in plasma represent the SEM calculated based on the MDL and CV % of the assay using a standard variance model. Error bars in saliva represent the SEM from each sample assayed in duplicate.

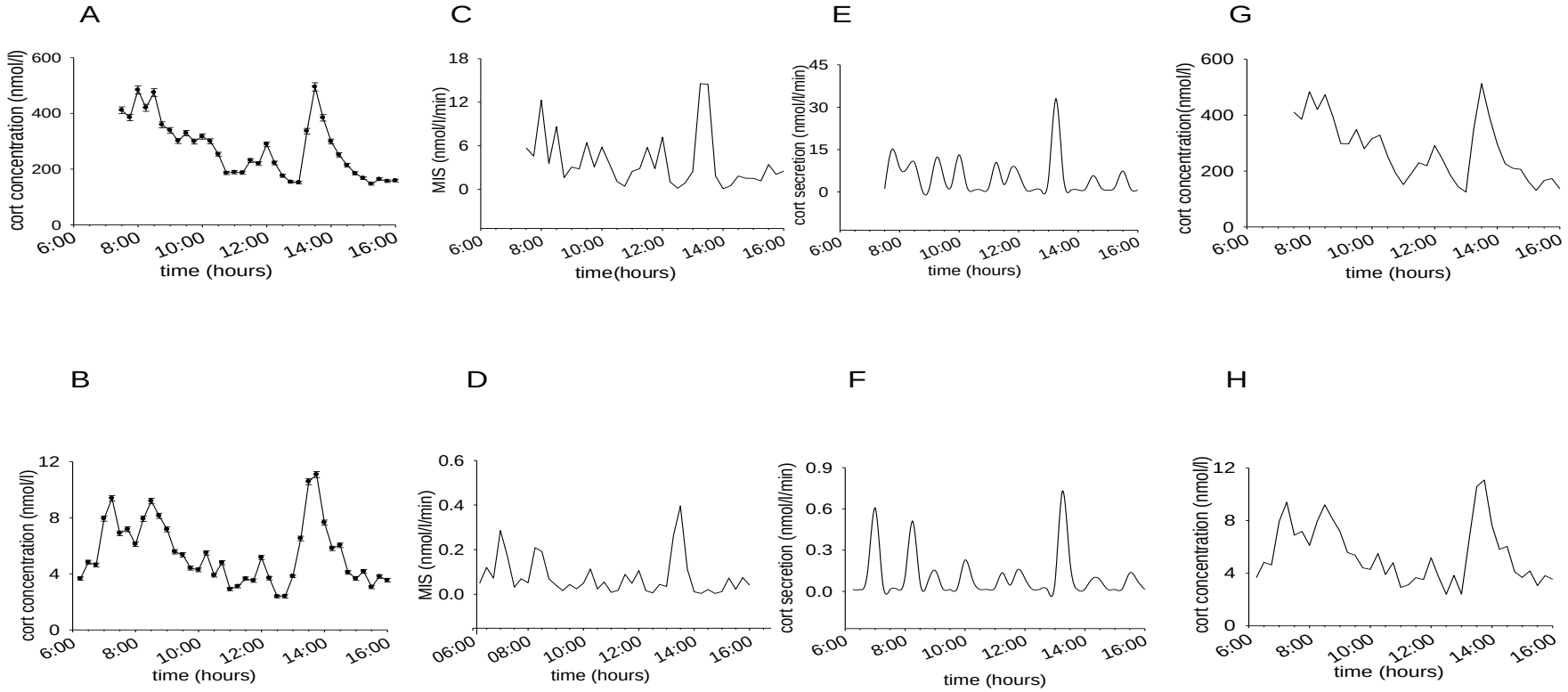

Figure 9. Plasma and saliva cortisol concentrations analysed by deconvolution analysis for a second representative donor. Initial concentration profiles for plasma (A) and saliva (B) we used to generate model-independent secretory profiles (C and D), and subsequently deconvoluted using the Autodecon algorithm to give the underlying cortisol pulsatile structure (E and F). The pulsatile patterns were convoluted to give the theoretical concentration profiles (G and H) that were not statistically different from the initial concentration profiles (A and B). Concentration is expressed in nmol/l. Secretion is expressed in nmol/l/min. Error bars in plasma represent the SEM calculated based on the MDL and CV % of the assay using a standard variance model. Error bars in saliva represent the SEM from each sample assayed in duplicate.

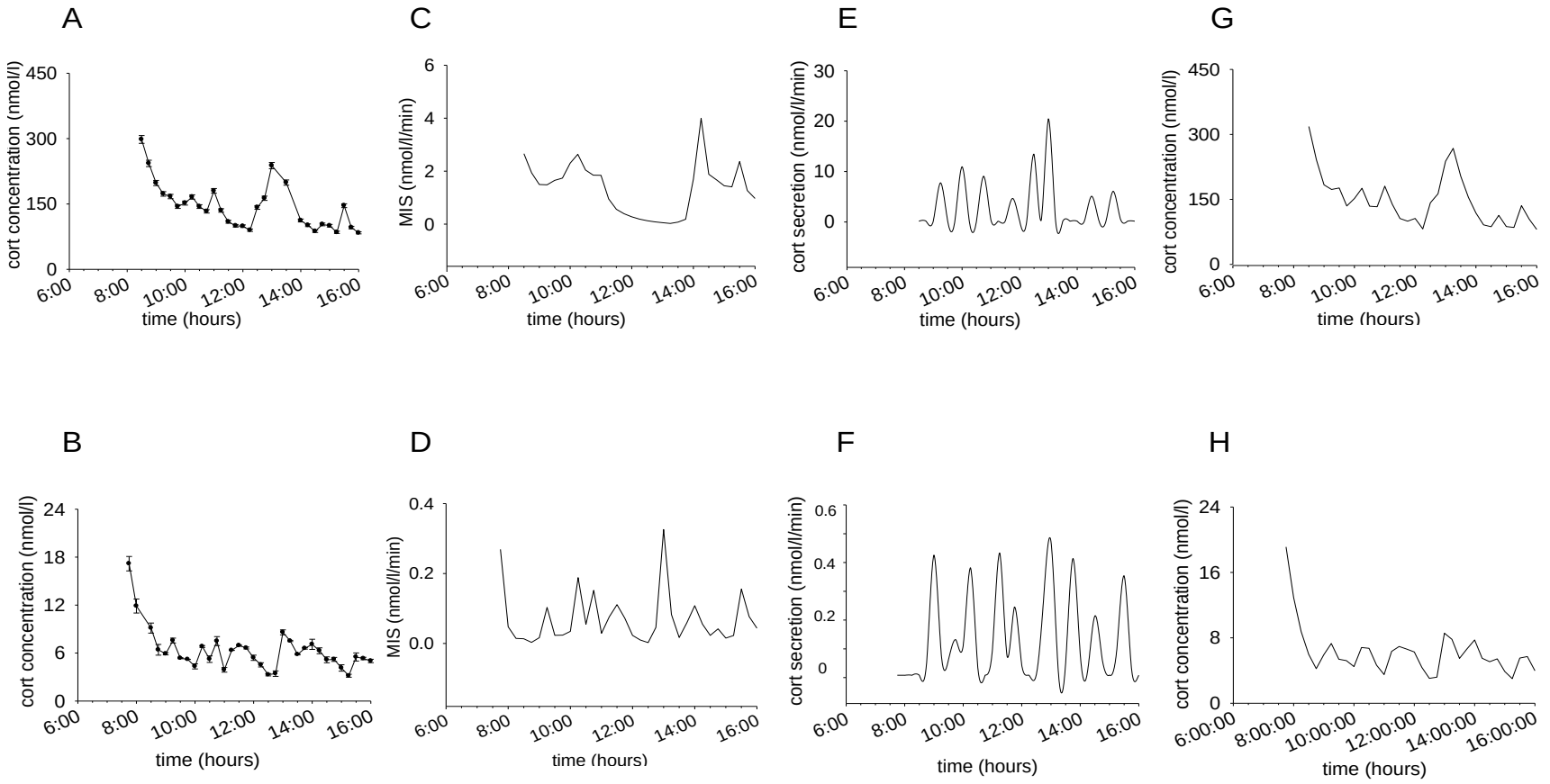

Figure 10. Plasma and saliva cortisol concentrations analysed by deconvolution analysis for a third representative donor. Initial concentration profiles for plasma (A) and saliva (B) we used to generate model-independent secretory profiles (C and D), and subsequently deconvoluted using the Autodecon algorithm to give the underlying cortisol pulsatile structure (E and F). The pulsatile patterns were convoluted to give the theoretical concentration profiles (G and H) that were not statistically different from the initial concentration profiles (A and B). Concentration is expressed in nmol/l. Secretion is expressed in nmol/l/min. Error bars in plasma represent the SEM calculated based on the MDL and CV % of the assay using a standard variance model. Error bars in saliva represent the SEM from each sample assayed in duplicate.

amplitudes in both plasma and saliva (r=0.86, p<0.0001 and r=0.81, p<0.0001, respectively, Figure 11A-B).

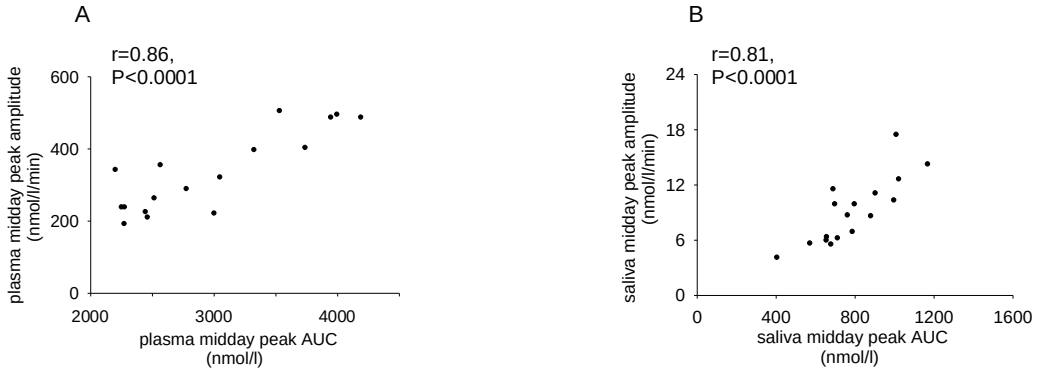

Figure 11. Pearson correlations between the midday peak AUC and the amplitudes in plasma (A) and in saliva (B). AUC is expressed in nmol/l and amplitude is expressed in nmol/l/min. Each dot represents one donor.

2.4.2 Deconvolution analysis of pulsatile cortisol secretion

Plasma and saliva concentration profiles were deconvoluted. For each donor the Pulse algorithm generated a model-independent secretory profile. This provided a preliminary estimate of the basal secretion rate of cortisol and its half-life. It also positioned the secretion pulses on the time axis and provided an estimate of their amplitude (Figure 8-10C-D). These results were further refined using Autodecon to provide a statistically valid secretory model for each donor (Figure 8-10E-F). Then theoretical concentration curves were modelled for each donor using the predicted secretion events and the calculated cortisol half-life (Figure 8-10G-H). The concentration models of all donors reached AIC<70 and a runs test significance of p>0.05 indicating that there is no statistically significant difference between the models and the observed concentrations.

Table 1 summarizes the aggregated parameters of the individual secretory models. No statistical difference (p>0.05) was found between the frequency of cortisol secretory pulses in saliva and plasma (7.0±1.4 vs. 7.8±1.5 bursts/8 h, Figure 13A).

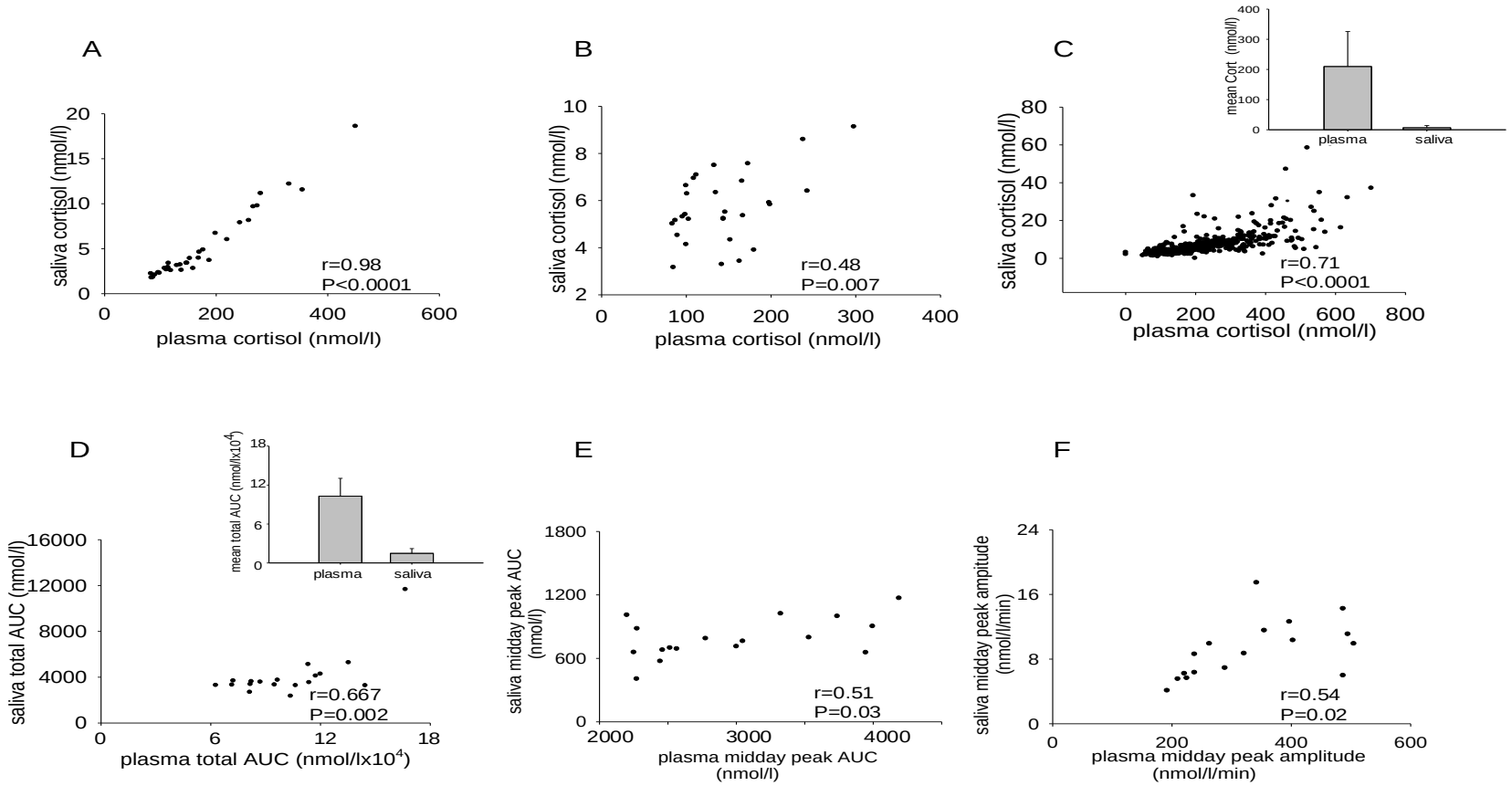

Figure 12. Pearson correlations between plasma and saliva cortisol concentrations in individual donors with the highest (A) and the lowest (B) correlation and for all donors (C) throughout the complete observation period. Insert to panel (C) represents the mean plasma and salivary cortisol concentration for all donors. Pearson correlations between the AUC of the complete observation period in plasma and saliva (D), midday peak AUC (E) and midday peaks amplitudes (F) of all donors. Insert to panel (D) is mean plasma and salivary cortisol AUC of all donors. Concentration and AUC are expressed in nmol/l and amplitude in nmol/l/min.

Moreover a strong positive correlation between the number of temporally concordant individual peaks in saliva and plasma was observed ($r=0.83$, $p<0.0001$, Figure 13A). The average amount of cortisol secreted per burst (AUC) in saliva was 4.2 %±2.1 (range 2.0-10.1 %) of the total cortisol amount secreted in plasma in the different donors (Figure 13B). Similarly, the mean amplitude of cortisol secretory bursts in saliva was 4.16 %±1.98 (range 2.0-10.1 %) of the amplitude of cortisol bursts in plasma (Figure 13C). In saliva cortisol half-life was significantly shorter than in plasma (28.9±8.5 vs. 42.1±8.5 min, $p<0.001$, Figure 13E). Cortisol half-life in plasma and saliva correlated positively with borderline significance. ($r=0.47$, $p=0.049$, Figure 13E).

Significant positive correlation was observed between the total AUC of the cortisol time profiles in plasma and the sum of the areas under the deconvoluted peaks ($r=0.67$, $p=0.002$, Figure 14A). In saliva their correlation was much stronger ($r=0.9$, $p<0.0001$, Figure 14B). Linear regression analysis demonstrated a strong positive correlation between the IPI in plasma and in saliva ($r=0.71$, $p=0.0008$, Figure 13F). No statistically significant difference was found between the IPI of saliva and plasma cortisol pulses (61.0±11.5 vs. 59.6±10.5, $p>0.05$, Figure 13F). The deconvolution revealed on average 2.5±1.1 peaks from awakening until cortisol reached baseline levels. When CAR was measured only on the first five morning samples (up to 60 min) as frequently reported (Hellhammer et al, 2007; Izawa et al, 2010; Kudielka & Kirschbaum, 2003) on average 1.4±0.5 peaks were detected.

2.4.3 Concordance

Monte Carlo concordance analysis was initially performed with a varying time window, where a significant concordance ($p<0.05$) was found for all donors. The mean concordance of

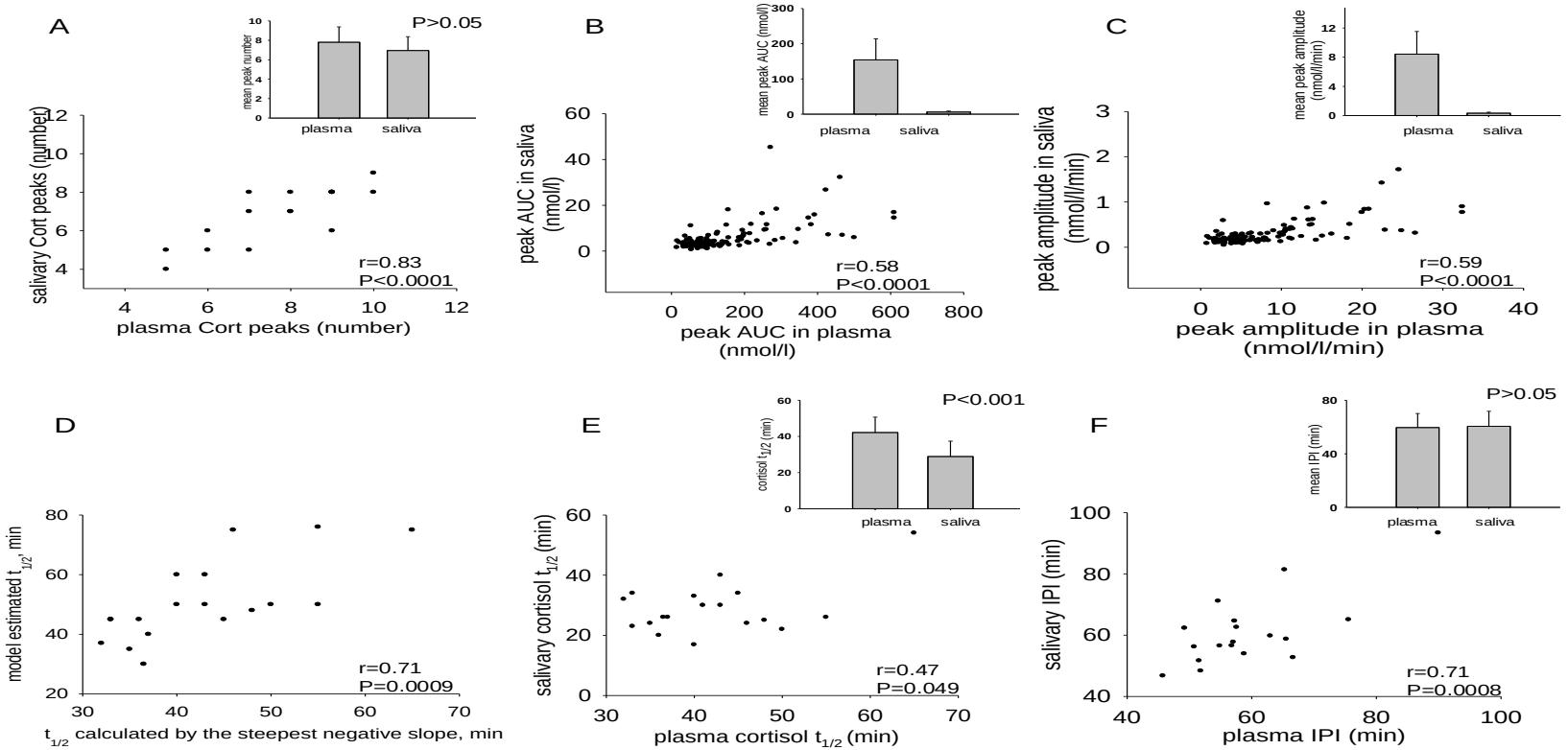

Figure 13. Pearson correlations between the corresponding number (A), AUC (B) and amplitudes amplitudes (C) of plasma and saliva peaks of all donors. Insert to panel (A) represents the mean number of corresponding peaks/8 h in plasma and saliva of all donors. Insert to panel (B) is the mean peak AUC in plasma and saliva of all donors. Insert to panel (C) is the mean peak amplitude in plasma and saliva of all donors. Pearson correlations between model estimated and cortisol half-life calculated from the steepest negative slope from the concentration curve (D), between cortisol half-life (E) and interpeak interval (F) in plasma and saliva peaks of all donors. Insert to panel (E) is the mean cortisol half-life in plasma and saliva of all donors. Insert to panel (F) is the mean interpeak interval in plasma and saliva of all donors. AUC is expressed in nmol/l, amplitude is expressed in nmol/l/min. Half-life and interpeak interval are expressed in min. Each dot represents one donor.

	Plasma Cortisol	Salivary Cortisol	P-value
Mean peak number/8h	7.8±1.5	7.0±1.4	P>0.05
Interpeak interval, min	59.6±10.5	61.0 ±11.5	P>0.05
Half life t ½, min	42.1±8.5	28.9±8.5	P<0.001
Mean AUC, nmol/l	102940.4±27425.2	4078.2±2021.6	P<0.001
Peak AUC, nmol/l	153.3±57.4	5.9±2.75	P<0.001
Amplitude of cortisol burst, nmol/l/min	8.3±2.9	0.3±0.14	P<0.001

Table 1. Quantitative features of episodic cortisol secretion resolved by multi-parameter deconvolution analysis.

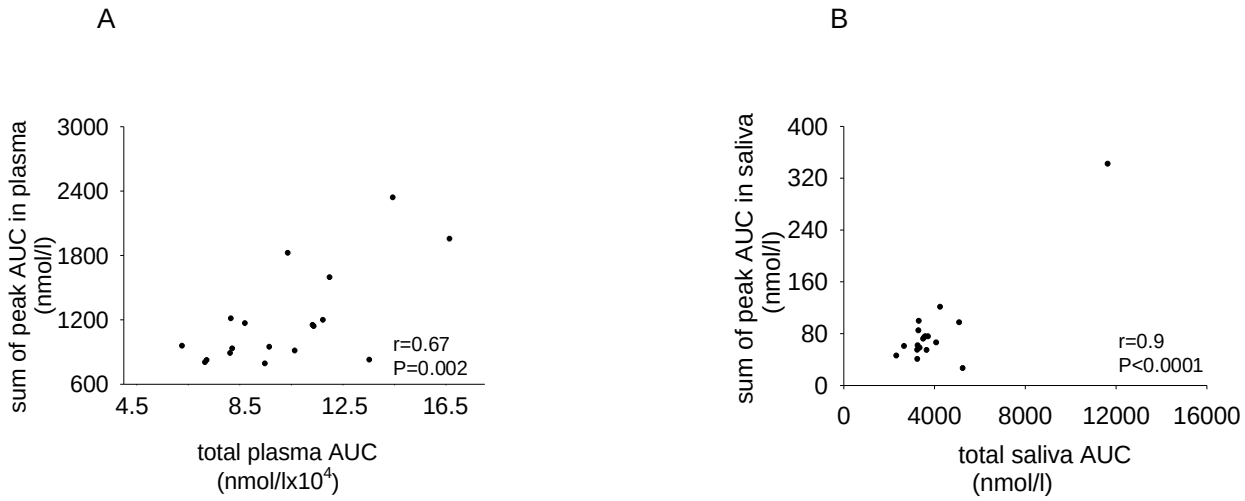

Figure 14. Correlations between total plasma AUC and sum of peak AUC (A) and between total saliva AUC and sum of peak AUC (B). AUC is expressed in nmol/l.

all plasma peaks with those in saliva was 84 % (Figure 15C), whilst 94.3 % of all salivary peaks were concorded with plasma peak. The overall correlation of the areas under the curve of the individual temporally concordant peaks was r=0.58, p<0.0001 (Figure 13B). Similarly, a strong positive overall correlation of the amplitudes of the individual peaks was r=0.59, p<0.0001 providing strong support for the validity of the models (Figure 13C). 1.3±0.8 plasma peaks of 7.8 on average were not matched with concordant peaks in saliva, whilst 0.4±0.5 peaks of a total of 7.0 salivary peaks were unmatched in plasma. 70% of the plasma peaks that remain unidentified in saliva, as well as 70 % of the saliva peaks that were not matched in plasma, occurred between 1100 to 1600 h. When comparing the concordance of the morning cortisol peaks in plasma up to 1100 h with the concordance of the eight-hour cortisol profiles the percentage of concordance increased by 6 % (90.0 %±13.7 % vs. 84 %±10.1 %, Figure 15E). Both in the morning and the complete eight-hour profiles there was a strong correlation between the total number of peaks in plasma and the number of concordant peaks in saliva (r=0.89, p<0.0001, r=0.87, p<0.0001, Figure 15D-F). Cortisol peaks were detected in saliva on average 19.4±7.4 min after their appearance in plasma. No significant correlation (r=0.25, p>0.05; r=0.06,

$p>0.05$) was found between the percentage coincidence as a function of plasma cortisol pulse frequency for all donors (Figure 16). Since a correlation would only be expected if the concordance between plasma and saliva cortisol pulses was random, this shows that plasma-saliva peak concordance is non-random and significant (Clifton et al, 1988). The concordance between plasma and saliva cortisol profiles of different, randomly selected donors was detected as non-significant ($p>0.05$).

Secondly, we performed Monte Carlo concordance analysis (Veldhuis et al, 1989a) with a fixed time window as commonly done in the literature (Backstrom et al, 1982; Johnson et al, 2009; Veldhuis et al, 1994; Veldhuis et al, 1992). Our choice for a fixed time window was based on our estimates of 19.4±7.4 min derived from the variable concordance analysis. A compromise window of ±20 min was selected to achieve an optimal balance between percentage concordance and significance. The fixed time window analysis of ±20 min showed a significant ($p<0.05$) saliva-plasma peak concordance in 61 % of the donors (11/18 donors). Under these conditions, on average 70 % of all plasma peaks concorded with a corresponding salivary peak (Figure 15A), on average 2.3±1.2 peaks of a total of 7.8 plasma peaks remained unmatched in saliva. The correlation between the total number of plasma peaks and the number of concordant peaks in saliva was $r=0.73$, $p<0.0001$ (Figure 15B). 78.4 % of all salivary peaks concorded with a corresponding plasma peak with an average of 1.4±0.8 peaks from a total of 7.0 salivary peaks remaining unmatched in plasma. However, according to our initial variable window analysis, coincidence intervals of 12 to 26.8 min would seem appropriate However, according to our initial variable window analysis, coincidence intervals of 12 to 26.8 min would seem appropriate. To allow concording salivary peaks occurring between 0 and 12 min post plasma peak, we repeated the analysis with a fixed window of 0-30 min and the concordance did not significantly improve ($p>0.05$).

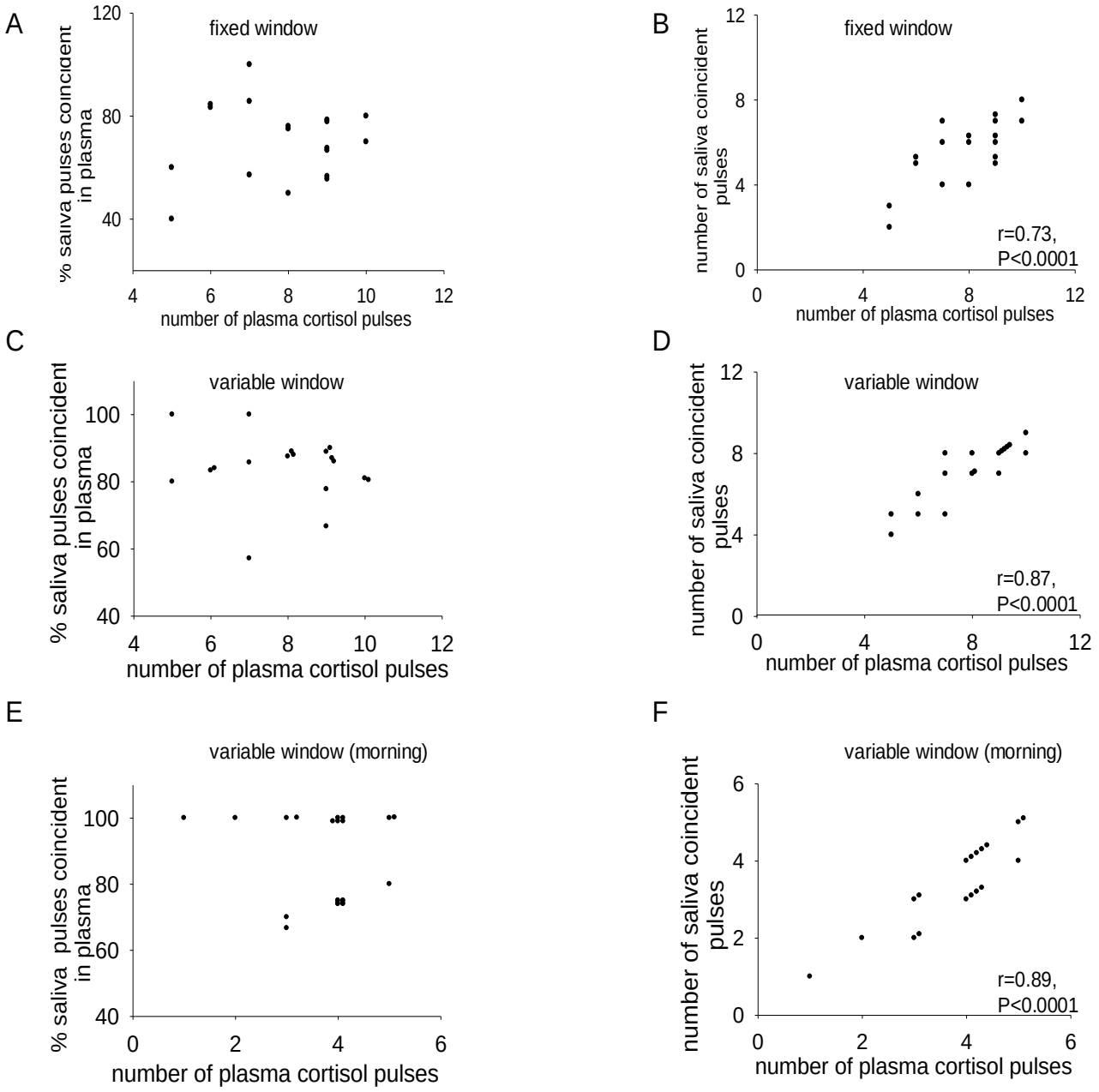

Figure 15. Concordance of saliva and plasma cortisol pulses. The percentage of salivary pulses for a total number of plasma pulses was assessed using a fixed time window (A), a donor-specific variable window (C) and during the morning hours with a variable time window (E). The number of salivary pulses for a total number of plasma pulses was assessed using a fixed time window (B), a donor-specific variable window (D) and during the morning hours with a variable time window (F). Each dot represents one donor.

A.

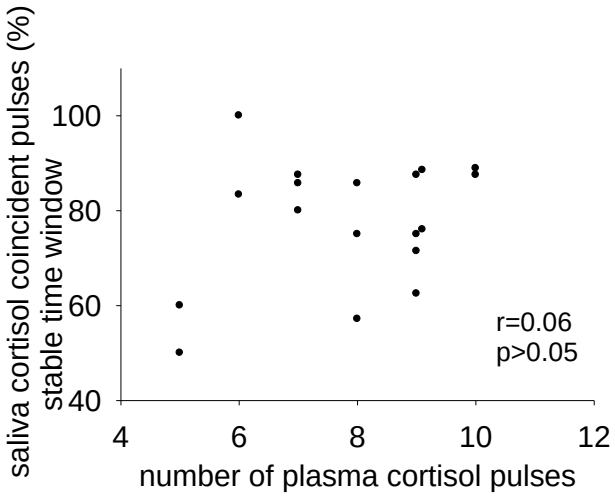

B.

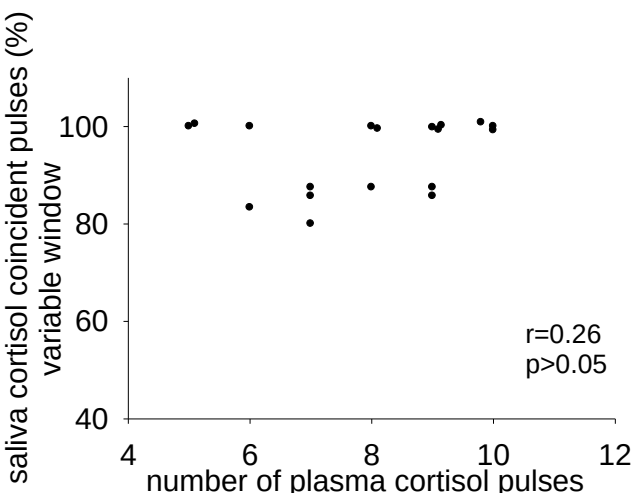

Figure 16. The relationship between the number of plasma cortisol pulses and the percentage of coincident salivary cortisol pulses using the fixed (A) and variable (B) time window. Each dot represents one donor.

2.5 Discussion

This appears to be the first study that compares ultradian cortisol pulsatility in plasma and saliva using deconvolution analysis. Deconvolution modelling successfully resolved cortisol pulses in both plasma and saliva. The pulses in saliva could be matched up with those in plasma providing highly significant estimates of numbers, amplitudes, durations and frequencies of secretory pulses as well as estimates of half-lifes for each individual. Our observation of 7.8±1.5 pulses (range 5-10 peaks/8 h) in plasma between 0800-1600 h, corresponding to a 59.6±10.5 min IPI, and a range of 45.7-89.9 min, differ than previously reported values (Henley et al, 2009; Metzger et al, 1993; Veldhuis et al, 1989b). Earlier deconvolution models reported 19±0.82 peaks/24 h, corresponding to an average IPI of 77±4.0 min (Veldhuis et al, 1989b), 17.4±0.7 peaks/24 h corresponding to an IPI of 76.1±2.0 min (Henley et al, 2009), and 5±1 peaks/6 h, with an IPI of 69±5 min (Metzger et al, 1993). Our shorter IPI is also reflected in a shorter mean cortisol half-life

of 42.1±8.5 min in plasma (range 32-65 min) and 28.9±8.5 min in saliva (range 17-54 min). Although this is lower than otherwise reported in the literature, our estimated half-lives accurately reflected the steepest negative slope of the concentration curve (r=0.71, p=0.0009, Figure 13D). When forcing the deconvolution model to use a longer cortisol half-life, the models did not reach statistical significance except for one donor. Previous deconvolution models estimated the plasma half-life to be 56±4.0 min, 67.4±3.1 and 73±5.3 min for term neonates, pubertal males and adults respectively (Kerrigan et al, 1993; Metzger et al, 1993; Veldhuis et al, 1989b). Whilst, the endogenous cortisol half-life in saliva has not been previously determined by deconvolution, after intravenous (IV) administration of 20 mg cortisol, the salivary half-life was significantly shorter than that observed in plasma (72min vs.102 min) (Tunn et al, 1992). Our data showed a similar 30 % difference, between the saliva and the plasma half-life. This shorter half-life in saliva could be explained by the accelerated metabolism of cortisol to cortisone due to elevated 11β-hydroxysteroid dehydrogenase type 2 activity in the salivary gland and saliva (Kirschbaum & Hellhammer, 1989; Vining et al, 1983). As a result saliva, unlike plasma has up to three times the level of cortisone compared to cortisol (Levine et al, 2007; Morineau et al, 1997; Stewart et al, 1995).

In contrast to our observation period, all previous studies have sampled over a 24 h period which could account for the differences in the pulse frequency, IPI and half-life. We observed higher plasma/saliva peak concordance during the morning hours, than later during afternoon hours because of a weaker resolution of the pulsatility during the second half of the day. During the late afternoon hours until post midnight the amplitude of cortisol peaks is only 20 % of those during the day, which can dramatically influence the peak detection. We speculate that this may be the reason for our higher estimates of peak frequency and the shorter IPI in comparison to previous reports (Henley et al, 2009;

Metzger et al, 1993; Veldhuis et al, 1989b). In addition, all previous studies have used a simpler algorithm which is known to have significant limitations, including the subjective identification of the secretory bursts and the lack of rigorous statistical verification (Johnson et al., 2008). Unlike all previous studies (Henley et al, 2009; Metzger et al, 1993; Veldhuis et al, 1989b), we used the latest deconvolution procedure AutoDecon developed recently by Johnson et al. (Johnson et al, 2008; Johnson et al, 2009). AutoDecon does not require hands-on interference and it has been shown that this procedure performs considerably better than the deconvolution algorithm used in all previous studies with regard to sensitivity and secretory burst detection rates for true-positive, false-positive and false-negative peaks of insulin (Johnson et al, 2010) and LH (Johnson et al, 2008). The higher sensitivity to detect peaks and the higher statistical confidence of AutoDecon led to an increase in peak detection, which was reflected in a shorter IPI and shorter cortisol half-life. Importantly, it was shown for both (LH) and GH that a better resolution of the deconvolution was obtained when the sampling frequency was higher (Evans et al, 1987). Thus it is important that the sampling intensity reflects the expected hormone pulse frequency and half-life. The sampling interval of 15 min applied in our study corresponding to roughly a quarter of the plasma cortisol half-life was as recommended by Metzger et al. (Metzger et al, 1993) and fell within the sampling intervals of 10 and 20 min used in previous studies The deconvolution profiles generated for our 18 donors reached statistically significant levels, measured by AIC and runs test. Thus differences in pulse frequency, IPI and half-life depend on the sampling period, the deconvolution model used (Evans et al, 2009; Johnson et al, 2008; Veldhuis et al, 1984) and the sampling frequency (Evans et al, 2009; Mulligan et al, 1994; Veldhuis et al, 1984).

Furthermore, biological effects may also explain differences in pulsatility. For instance serum cortisol levels have been reported to exhibit seasonal rhythmicity in goats with highest cortisol concentrations observed in winter and lowest from early spring to summer (Alila-Johansson et al, 2003). For other pituitary hormones pulsatility is also reported to be seasonal, at least for LH and FSH (Martikainen et al, 1996). A considerable increase in LH pulse frequency and a proportional decrease in pulse amplitude was observed in rams subjected to artificial changes in the day length (Almeida & Pelletier, 1988). Similarly in humans, the mean area of LH pulses was significantly higher during the winter than in the summer (Almeida & Pelletier, 1988; Elliott, 1976; Kripke et al, 2010). Irrespective of the minor differences from previous deconvolution studies, when the plasma cortisol pattern was compared to the salivary cortisol there was a remarkable agreement between the number of plasma and saliva peaks (7.8±1.5 events/8 h, 7.0±1.4 events/8 h), or between interpulse intervals (59.6±10.5 min vs. 61.00±11.5 min). The lack of statistical difference between these saliva and plasma estimates demonstrates that the ultradian cortisol pulsatility is also reflected in the saliva.

Concordance or synchrony between discrete hormone pulses has been used as an indicator of coupling between independently pulsing hormones (Backstrom et al, 1982; Veldhuis et al, 1994; Veldhuis et al, 1992). Monte Carlo simulations have been applied to evaluate the concordance between paired and triple hormonal series (Clifton et al, 1988; Guardabasso et al, 1991). Here, we applied Monte Carlo simulations to compare pulsing patterns in distinct compartments. A fixed time window analysis was performed as commonly done in the literature (Backstrom et al, 1982; Johnson et al, 2009; Veldhuis et al, 1994; Veldhuis et al, 1992), with a window width of ±20 min as an optimal balance between percentage concordance and significance. The overall peak concordance reached already 70% and left on average 2.3± 1.1 plasma peaks unidentified in saliva. It has been

shown that when two pulse generators have a higher degree of autocorrelation and are operating at approximately the same frequency it is possible, to observe a significant degree of coincidence in the absence of real coupling between the generators (Cook & Campbell, 1979). The absence of significant correlation between the plasma cortisol pulse frequency and the percent coinciding saliva cortisol pulses confirmed that the concordance that we observed was not simply due to the high operating frequencies of cortisol in both compartments.

When using a varying time window to account for differences between individuals in cortisol saliva diffusion rates, 84 % of all plasma peaks were assigned to a corresponding salivary peak. On average 1.3±0.8 peaks in plasma were not matched with a corresponding peak in saliva. The salivary cortisol pulses occurred on average 19.4±7.4 min after the correspondent plasma cortisol pulse. Our results showed large inter-individual variability in cortisol diffusion rates into the saliva. Therefore, individual time windows may be more appropriate than the same one for all donors. The minor differences between the numbers of pulses in plasma and saliva can be explained by poor resolution of pulsatility during afternoon hours. Indeed 70 % of the plasma peaks that remain unidentified in saliva occurred between 1100 to 1600 h. An additional increase in concordance was observed when only the morning cortisol peaks in plasma and saliva up to 1100 h were considered in comparison with the concordance from the complete observation period cortisol profiles (90 %±13.6 % vs. 84.0 %±10.1 %). Circadian fluctuations of CBG and lower cortisol in the afternoon hours, reduce the free cortisol fractions in plasma and in saliva and could explain the poor concordance in the afternoon hours. The differences between the deconvolution parameters of plasma and saliva cortisol profiles were minor and not statistically significant, but limiting the concordance analysis only to the morning hours eliminated plasma peaks unmatched in saliva.

Therefore, saliva would best be used for monitoring cortisol pulsatility during the morning hours.

The morning rise in cortisol is a distinct component of the diurnal pattern of cortisol and is considered to be a marker of HPA axis integrity and adrenal cortisol production (Clow et al, 2004; Hellhammer et al, 2007). It is characterised by a 50-100 % cortisol increase, peaking about 30 min after awakening (Clow et al, 2004). Although morning cortisol levels remain elevated for at least one hour after the zenith, CAR is commonly investigated within the first hour after awakening (Federenko et al, 2004; Kudielka & Kirschbaum, 2003). The deconvolution of CAR based on the individual time for cortisol to return to baseline levels revealed on average 2.5±1.1 peaks. In contrast when only the first 75 min after awakening were taken into account on average only 1.4±0.5 peaks were detected. This is the first analysis of the pulsatile structure of CAR and our results suggest that at least 120 min of observation post awakening are necessary to allow the observation of peaks in the decay phase of the CAR.

Blood sampling is an invasive, and for some donors, a stressful procedure. Plasma cortisol is largely protein-bound and usually measured as the sum of the bound and free fraction, while saliva is thought to represent the free (i.e the active) hormone (Vining et al, 1983). Importantly, saliva is obtained in a simple, non-invasive way, suitable for studying stress hormone pulsatility. During the last twenty years salivary free cortisol became an increasingly important measurement in psychobiological research. Here, we have extended the utility of saliva sampling by providing a tool for analysing the underlying secretory events. Whilst saliva is a surrogate for plasma analysis, collection does not normally induce an HPA axis response, leaving the underlying pulsatile structure unaltered by the sampling technique.

Our study was designed to investigate cortisol deconvolution in the saliva to obtain reliable data on the natural, unperturbed cortisol secretory events (except for the initial placement of the intravenous canula). The main strength of our experimental design is that we can resolve most of the underlying pulsatile events in cortisol under these baseline conditions. Further studies are required to demonstrate that our deconvolution approach is equally effective under different conditions of perturbed HPA axis and over the complete 24 h period. Another limitation is that all our results are from healthy, young male subjects only and our results may be differentially influenced throughout the menstrual cycle.

In summary, no statistical difference and a highly significant concordance was obtained between the deconvoluted 8 h plasma and salivary cortisol concentration profiles. The concordance was further improved during the morning hours, providing access to the underlying structure of CAR. The well-known advantages of salivary sampling make deconvolution of salivary cortisol levels especially in the morning a powerful technique to access the unaltered cortisol pulsatility.

Chapter 3

Diurnal redistribution of human lymphocytes and their temporal associations with salivary cortisol profiles.

Slavena T. Trifonova [a,b], Jacques Zimmer [c], Jonathan D. Turner [a,b], Claude P. Muller [a,b]

[a] Institute of Immunology, Centre de Recherche Public de la Santé/ Laboratoire national de santé, 20A rue Auguste Lumière, L-1950 Luxembourg, Grand Duchy of Luxembourg

[b] Department of Immunology, Research Institute of Psychobiology, University of Trier, D-54290 Trier, Germany

[c] Laboratory of Immunogenetics and Allergology, CRP-Santé, 84 Val Fleuri, L-1526 Luxembourg, Grand Duchy of Luxembourg.

This study has been published in *Chronobiology International (*2013) Jun;30(5):669-81

3.1 Abstract

Immune cell trafficking is crucial for surveillance and effector functions of the immune system. Circadian rhythms of the HPA axis and of cortisol have been implicated in circadian redistribution of circulating lymphocytes and granulocytes. However, information regarding the diurnal redistribution of immune cells and their temporal correlations with cortisol is scarce. In this study, we investigated the diurnal redistribution of T, B and NK cell subsets in relation to the endogenous cortisol rhythm.

Saliva and blood samples were collected every 15 min over an 8 h period. Salivary free cortisol was measured by ELISA. Surface markers (CD3, CD19, CD8, CD56, CD16, KIR) were measured in whole blood samples by 6-color flow cytometry and cell subsets quantified as a percentage of the total lymphocyte population. To study associations between the diurnal cortisol rhythm and the redistribution of T, B and NK cells we calculated cross-correlations with lag periods of 15 min.

The salivary cortisol levels showed the typical diurnal variations with a significant morning CAR peaking around 0730 h followed by an afternoon nadir. While B cells remained stable throughout the 8 h, T cells (CD3+CD8+ and CD3+CD8-) showed a significant positive cross-correlation with cortisol levels when a delay of 30-105 min was taken into account. This was followed by a negative correlation covering a period of 165-285 min after the cortisol peak. Conversely, NK cells showed an initial negative correlation at 45-105 min, followed by a positive correlation at 120-285 min. The major CD56+16+ subset and the CD56–16+ population showed similar temporal correlation profiles. The minor CD56+16– NK cell subset showed no temporal changes. The major NK subset (CD56+16+) contains cells with higher cytolytic activity (KIR+) cells, whilst the single positive subsets CD56+16– and CD56–16+ are mainly involved in cytokine

production. Significant positive correlations were observed in KIR+ subsets coincident with this of NK cells covering a period of 105-300 min after the cortisol peak.

In conclusion, increasing sampling frequency together with the inclusion of the time points immediately after the cortisol peak revealed strong lagged correlations with diurnal cortisol levels with a bimodal response for both T and NK cells. The high resolution cross-correlations applied here showed that the cellular redistribution is, much faster and more variable than previously shown with mobilization of more cytolitic innate immune cells 180 min after CAR.

Keywords: cross-correlations, cytolytic NK cells, cellular redistribution, cortisol awakening rise, immunity;

3.2 Introduction

Cortisol, the main effector molecule of the HPA axis is secreted in a well-known circadian rhythm that is produced by regular, hourly pulses varying primarily in amplitude (Lightman, 2006; Stavreva et al, 2009; Veldhuis et al, 1989b). The HPA axis is thought to play a key role in orchestrating the interplay between the neuro-endocrine and the immune system (Eismann et al, 2010; Webster et al, 2002).Thus, circadian cortisol and HPA-axis rhythmicity have been implicated in the circadian redistribution of circulating immune cells (Dimitrov et al, 2009; Levi et al, 1985; Miyawaki et al, 1984; Ritchie et al, 1983; Suzuki et al, 1997). Circadian variations in circulating human T and B cells are characterised by a nocturnal peak and a daytime nadir (Eismann et al, 2010; Kawate et al, 1981; Ritchie et al, 1983). A negative correlation was shown between absolute peak T and B cell counts and plasma cortisol throughout the 24 h period suggesting a mechanistic link (Kawate et al, 1981; Ritchie et al, 1983), but surprisingly little is known about the diurnal redistribution of important lymphocyte subsets. Reports are conflicting with respect to the circadian rhythms for B and NK cells and their correlation with cortisol rhythm (Kawate et al, 1981; Kronfol et al, 1997; Miyawaki et al, 1984; Ritchie et al, 1983). For example, Kronfol et al. reported a significant circadian rhythm for NK cells, with a lag time of approximately 2 h (Kronfol et al, 1997), whilst Ritche et al. were not able to detect such a rhythm (Ritchie et al, 1983). Also, the diurnal redistribution of the different NK cell subsets and their correlations with cortisol rhythm have not been investigated. While, the regulatory role of cortisol in the circadian redistribution is still debated, both exogenous GC (Kawate et al, 1981; Miyawaki et al, 1984; Slade & Hepburn, 1983) and stress induced GC release (Kimura et al, 2008) induced changes in absolute and relative lymphocyte counts that are comparable to circadian variations.

Exogenous GC administration in humans resulted in transient lymphopenia maximal 3-8 h after GC administration, due to cellular redistribution (Fauci & Dale, 1975; Slade & Hepburn, 1983). Less is known about NK cell subsets redistribution after GC administration, although a two-fold increase in NK counts was observed after a 7 d treatment of rats with a GC agonist (Miller et al, 1994).

The immune function also shows circadian variations that are potentially linked to GC levels (Fernandes et al, 1976; Halberg et al, 1974; Knapp et al, 1979). For instance the susceptibility of rats to reject skin and renal allografts, a measure of cell-mediated immunity, depends on the time of the day when transplantation was done (Halberg et al, 1974; Ratte et al, 1973). In humans, the majority of renal allograft rejection episodes occur during the night, when GC levels are expected to be at their lowest (Knapp et al, 1979). Similarly, specific antibody titers were higher in animals immunized during daylight when murine steroid concentrations should be lower than in those immunized during the night (Fernandes et al, 1976). A circadian rhythm of NKCA in humans with maximum activity in the morning or in the early afternoon has been documented by several studies (Gatti et al, 1987; Kronfol et al, 1997). Administration of exogenous GC resulted in an increase in NKCA of circulating human lymphocytes 4 h later (Katz et al, 1984) suggesting a direct link between circadian cortisol levels and NKCA.

However, information regarding the diurnal redistribution of immune cells and their temporal relation to the hourly ultradian cortisol rhythm are limited. This is partly because previous studies used long intervals (2 -5 h) between measurements (Kronfol et al, 1997; Miyawaki et al, 1984; Suzuki et al, 1997). To investigate the temporal relationship of psychological (Schlotz et al, 2008) and physiological (Engert et al, 2011) variables with stress-induced cortisol levels, time-lagged cross-correlations have recently been used. Such time-lagged cross-correlations allow to investigate systems that follow

their own kinetic in response to a distinct stimulus with a high temporal resolution. This approach has been used for instance to correlate, alpha-amylase (sAA) of the SAM system and, cortisol release after psychosocial stress test (TSST). Only one study has performed limited time lagged cross- correlations to study associations between circadian cortisol and lymphocyte counts (Kronfol et al, 1997), but the 2 h sampling interval was limiting.

The present study addresses limitations in the experimental design of previous studies, investigating the diurnal redistribution of lymphocyte subsets including NK cell subsets, applying an intensive 15 min sampling schedule over an 8 h observation period covering both the morning cortisol rise and the afternoon nadir. We observed a bimodal redistribution of lymphocyte subsets, and both phases correlated significantly with diurnal cortisol levels.

3.3 Materials and methods

3.3.1 Subjects and experimental design

Nineteen healthy male donors (age range 18-40, mean 28.6±7.0 yrs) volunteered to participate in the present study. Physical health status of all participants was assessed using a health questionnaire. Exclusion criteria included any chronic or acute illnesses within the prior two weeks; use of any medication in the previous week, and a BMI of <18 or >30.

To minimize the delay between awakening and arrival, as well as minimising the deviation from the normal morning routine, donors living and working close to the Clinical Investigation and Epidemiological Center were recruited as previously described (Trifonova et al., In Press). Saliva collection devices (Salimetrics oral swabs, Salimetrics,

Newmarket, UK) were supplied to all donors prior to the experiment and saliva samples were collected from immediately upon awakening whilst donors were still in bed. The mean awakening to arrival delay was 71.8 ± 17.01 min. Donors arrived between 0715 and 0945 h. EDTA blood sampled via an indwelling intravenous canula and saliva were collected concurrently from the time of arrival every 15 min until 1600 h. Blood samples were processed immediately for the determination of lymphocyte surface markers. During the experiment, subjects were allowed regular ambulatory activity and received standardized meals at 0900 and 1200 h. Participants were fully instructed about the experimental purpose and gave their written informed consent. The study protocol was approved by the Luxembourg National Research Ethics Committee (CNER).

3.3.2 Cortisol ELISA

Salivary cortisol was measured in duplicate by commercial ELISA (Salimetrics, Newmarket, UK) with a minimal detection limit of 0.03 ng/ml and intra- and inter-assay variability of 3.5 % and 5.08 % respectively.

3.3.3 Cellular immune parameters

Undiluted full EDTA blood (100 µl) was incubated with the proper combination of specific antibodies for 15 min in the dark at room temperature. The different lymphocyte subpopulations were identified by 8-parameter 6-colour flow cytometry on the basis of cell surface markers using combinations of the following fluorescent labelled monoclonal antibodies: against CD16 (FITC), CD56 (PE), CD3 (PerCP), CD19 (PE-Cy7), CD8 (APC-Cy7) (Biolegend, San Diego, USA) and KIR (APC) (R&D systems, Minneapolis,

USA). The anti-KIR antibody binds the human inhibitory KIR2DL2, KIR2DL3 and the activating KIR2DS2 and KIR2DS4 receptors.

Isotype-matched irrelevant fluorescent labelled IgG_1-FITC, IgG_{2B}-PE antibodies (Immunotools, Friesoythe, Germany) were included to test for unspecific binding. Unstained cells served as negative controls. Single stained control samples from the first time point, 1200 and 1600 h, containing each individual antibody were also used to compensate for the spectral overlap between the different fluorochromes.

Erythrocytes were lysed with 4 ml FACS lysing solution for 15 min (BD Biosciences). Cells were subsequently washed and resuspended in 1 ml FACS buffer. Analyses were performed on BD FACS Canto II (BD Biosciences, NJ, USA) within 24 h of staining. Lymphocytes, monocytes and granulocytes were identified by dual scatter and 40 000 lymphocyte events were acquired. Data analyses were performed using FACS Diva 6.0 software (BD Biosciences, NJ, USA).

3.3.4 Data analysis

Lymphocyte subsets were quantified as a percentage of the initial lymphocyte gate in the FSC/SSC plot. T and B lymphocytes were gated from a CD3/CD19 plot, (Figure 18A) and CD3/CD19 double negative lymphocytes were used for NK cell analysis. NK cell subsets were identified from CD16/CD56 plots (Figure 19A). Furthermore percentages of KIR and CD8 expressing cells in each CD56/CD16 subset were obtained based on the separate gating on KIR and CD8 expressing populations (Figure 20A-C). Data are expressed as mean ± SEM. The missing values in the time series were estimated via linear regression with SPSS 14 for Windows software (SPSS inc., Chicago, USA). Time series were analysed by one-way analysis of variance (ANOVA) with repeated measures

considered sampling time as the potential source of variance. The pairwise multiple comparisons between all data points were calculated by Tukey Test. The changes in cell numbers were considered as significant when three or more adjacent sampling time points were significantly different from others ($p<0.05$). Statistical analyses were performed using SigmaStat (Systat Software, GmBH, Erkrath, Germany). To study associations between the cortisol rhythm and the rhythm of the individual immune measures, cross-correlations with lag periods for the immune measures of every 15 min were calculated correspondingly to the 15 min collection interval. The cortisol zenith was defined as the highest morning cortisol peak measured for each individual.

3.4 Results

3.4.1 Ultradian salivary cortisol

8 h saliva cortisol concentration profiles were obtained from 19 healthy donors. Major fluctuations of cortisol were observed throughout the observation period in all participants. The most distinct secretory event was the significant ($p<0.001$) CAR occurring on average at 0730 h. CAR was visible in seventeen of the 19 donors, but was not detectable in two donors due to incorrect sampling post-awakening. The mean saliva CAR zenith for 17 donors was 19.5±10.7 nmol/l (range 9.4-51.2 nmol/l). Another distinct peak in the cortisol concentration profiles was the midday meal–related peak that coincided with the subjects' lunch (1230-1400 h). This meal-related cortisol peak averaged for 19 donors 12.9±8.7 nmol/l, (range 4.1-36.2 nmol/l). These major fluctuations in cortisol levels were followed by an afternoon nadir with lower fluctuations. Figure 17 shows ultradian saliva cortisol profiles of three representative donors (A-C) as well as the mean ± SEM of 19 healthy donors (Figure 17D).

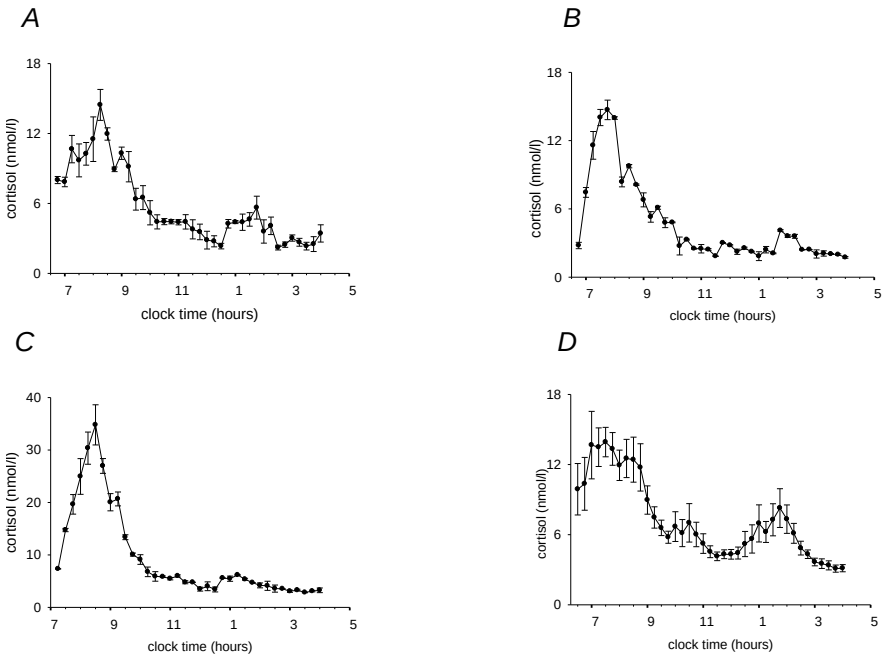

Figure 17. Ultradian salivary cortisol rhythm of three representative donors (A-C) and mean ±SEM of 19 healthy male donors (D). Clock time runs from 0700 to 1700 h.

3.4.2 Ultradian variations of T and B lymphocytes

B and T cells were identified from CD3/CD19 dot plots (Figure 18A). Figure 18C-E shows the ultradian change in the percentage of CD3 and CD19 cells throughout the day.

By one way ANOVA with repeated measures, significant percent variations ($p<0.05$) were observed for T lymphocyte population reflecting the diurnal rhythm of cortisol. Peak T cell levels occurred between 0800-0915 h, followed by a significant decrease (1115-1200 h), after which they remained unchanged at least until 1600 h (Figure 18C). CD8+ T cells were identified from CD3/CD8 dot plot (Figure 18B). CD8+ T cells accounted for 29.2 %±1.6 % on average (range 27.7-34.2%) of the total T cells. They did not show significant variations over the 8 h observation period ($p>0.05$, Figure 18D). CD3+ CD8– cells accounted for 63.4 %±2.03 % on average (range 61.5-67.2 %) of the total T cells. They showed a significant decrease between 1000-1130 h in comparison to the increase

observed in the morning at 0845-0900 h and in the afternoon between 1300 and1445 h ($p<0.05$, Figure 18E).

Relative CD19+ B cell levels did not show any significant variation ($p>0.05$) throughout the 8 h observation period. A borderline significant difference was observed between B cell counts at the first sampling time point (mean of three donors only) and 1315 h (mean of 19 donors), ($p=0.057$; Figure 18F)

3.4.3 Ultradian variation of NK lymphocytes

CD56+16–, CD56+16+ and CD56–16+ were identified from CD16/CD56 dot plot (Fig 19A), and the total number of NK was calculated as the sum of each of these subpopulations. Significant percent variations were observed for the total number of NK cells (Figure 19B). The highest total NK cell levels were detected in the first morning blood samples, immediately decreasing to the diurnal nadir at 0815-0915 h and increasing significantly ($p<0.05$) again after 1100 h. These variations were largely due to the CD56+16+ double positive NK cells which in all donors, as expected represented the largest subpopulation of NK cells (mean of 82.8 %, range 69-94 %) (Figure 19C). CD56+16+ cells peaked at 1115 h in all donors with preceding and subsequent significant nadirs at 0815-0915 h and at 1315-1345 h respectively ($p<0.05$). The remaining 17.20 % of NK cells corresponded to CD56–16+ (9.24 %) and CD56+16– (7.92 %). The second largest NK cell population (CD56–16+) cells, displayed a pattern similar to that of CD56+16+ with significant differences ($p<0.05$) between the early nadir at 0800-0945 h and a peak between 1215-1300 h, followed by a second nadir after 1315 h (Figure 19D). CD56+CD16– cells showed no significant ultradian pattern (Figure 19E).

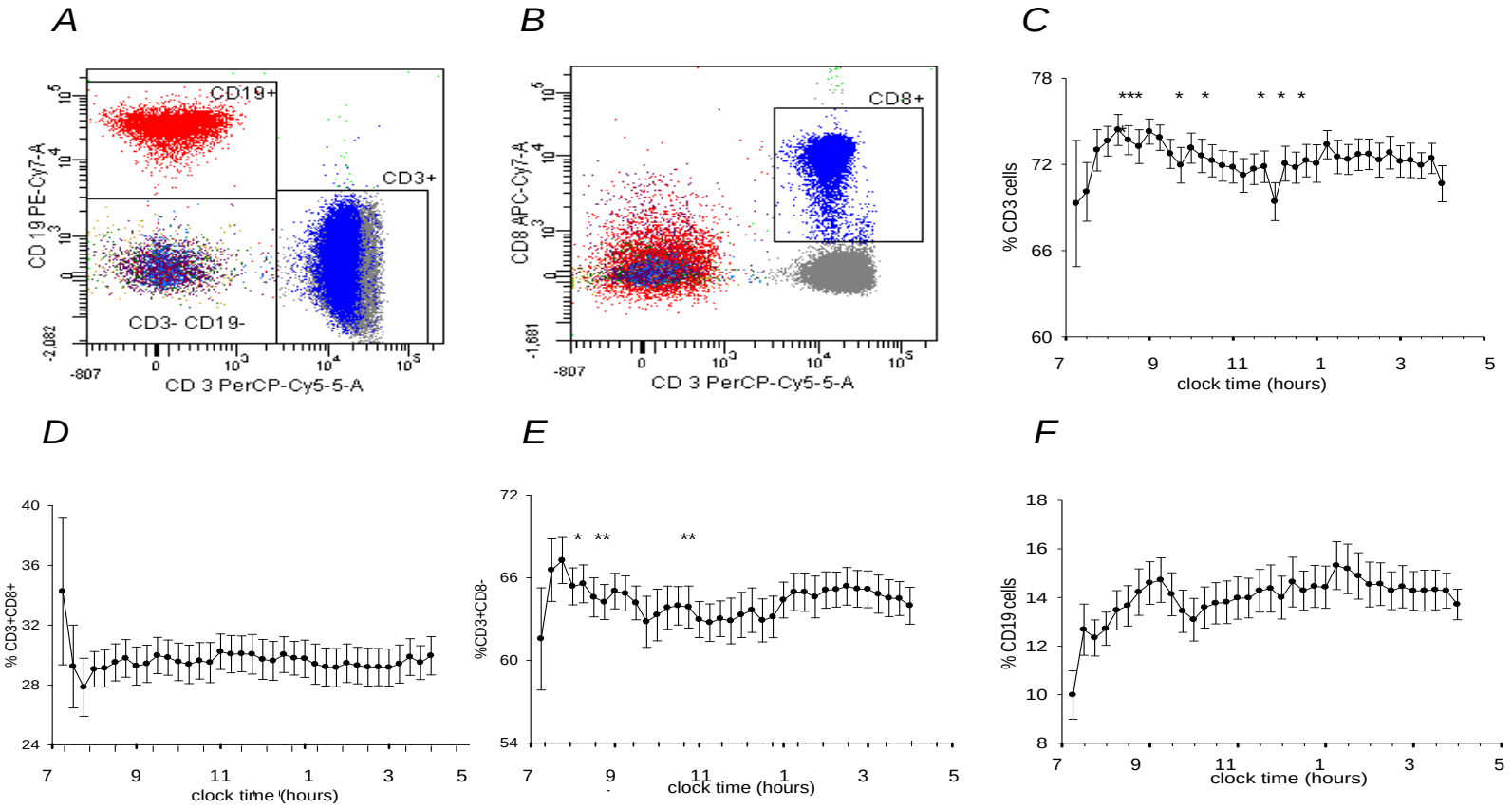

Figure 18. Dot plot from a representative donor of CD3/CD19 gating (A) and CD3/CD8 gating (B). Daily changes of total CD3+(C), CD3+CD8+ (D), CD3+CD8– (E), CD19+ (F) counts as percentage of total lymphocyte counts. Clock time runs from 0700 to 1700 h.

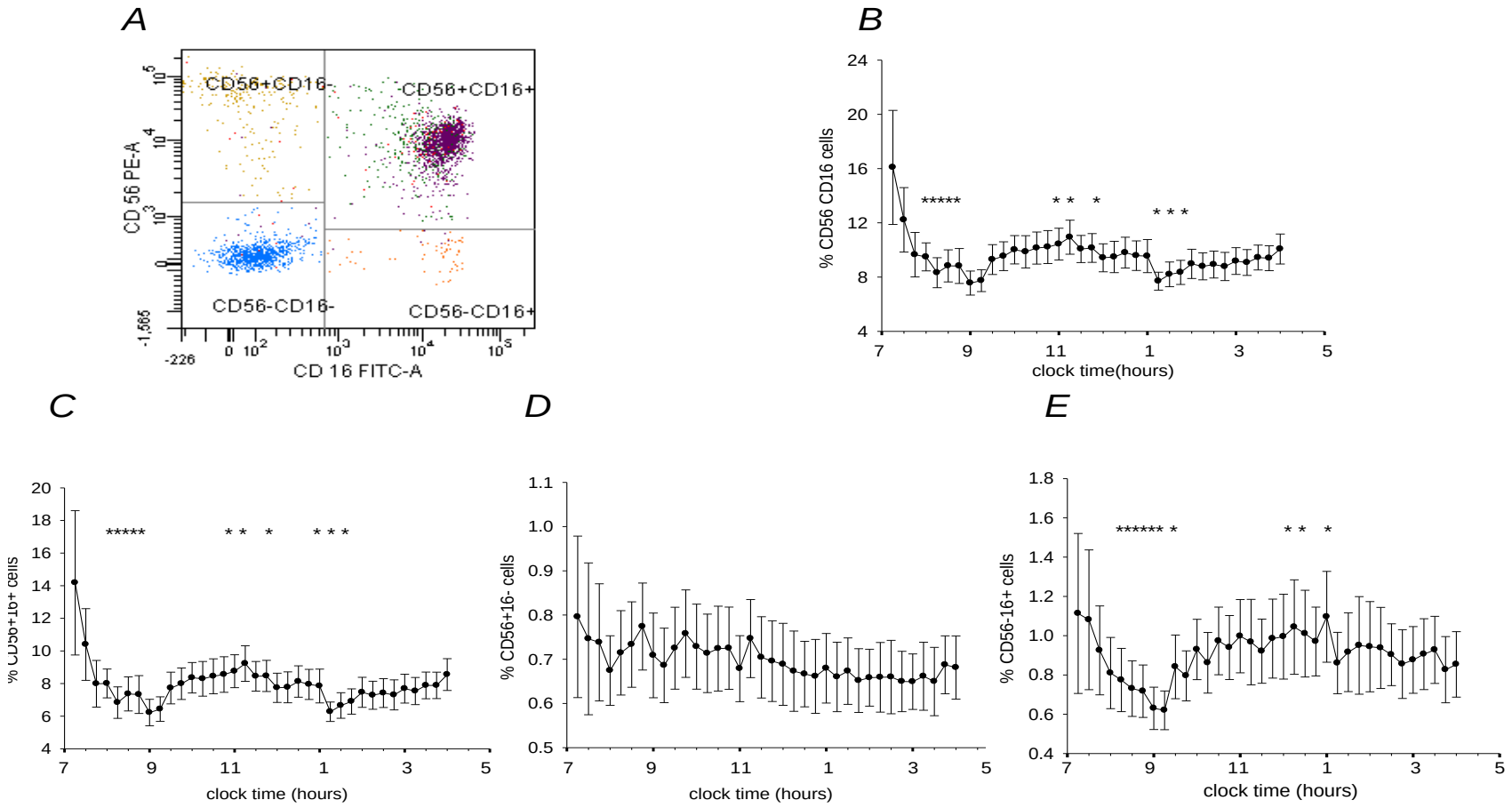

Figure 19. Dot plot from a representative subject of CD56/CD16 gating (A). Daily changes of total NK (B), CD56+16+ (C), CD56+16– (D), CD56–CD16+ cells (E) counts as percentage of total lymphocyte counts. Clock time runs from 0700 to 1700 h.

3.4.4 Redistribution of CD8 and KIR expressing NK cells

KIR–CD8+, KIR+CD8+, KIR–CD8– and KIR+CD8– within the three NK subsets were identified from KIR/CD8 dot plots after gating on each of the three NK subsets (Figure 20A). The majority of cells within the CD56+16+ population were KIR–CD8– (42.1 %). The double positive (KIR+CD8+) accounted for 12.9 %. The single positive populations KIR+CD8– and KIR–CD8+ corresponded to 27.7 % and 17.1 % respectively. The three NK subsets differed significantly ($p<0.05$) in numbers of KIR–CD8– and KIR+CD8+ cells.

Among CD56–16+ cells the relative counts of KIR–CD8– were more than twice as high as in the CD56+16+ subset, (87.5 % vs. 42.1 %). This relatively high number of KIR–CD8– cells was compensated by 6 time lower relative frequency of KIR+CD8+ in CD56–16+ than in CD56+16+ (2.0 % vs. 12.97 %). KIR+CD8– and KIR–CD8+ were approximately five times less abundant in the CD56–16+ subset (6.05 % and 4.36 %) than in CD56+16+ (27.7 % and 17.1 %).

Also in the CD56+16–, the KIR–CD8– population was twice as high as in the CD56+16+ subset (82.7 % vs. 42.1 %). This was compensated by a reduction in all other cell subtypes. The relative frequency of KIR+CD8+ was eight times lower in CD56+16– than in CD56+16+ (1.5 % vs. 12.9 %). KIR+CD8– corresponded to only 3.4% in comparison to 27.7 % in the CD56+16+ and 6.05 % in the CD56–16+ KIR–CD8+ corresponded to 12.42 % compared to 17.1 % in the CD56+16+ population and 4.36 % in the CD56–16+ (Table 2).

The single positive subsets KIR+CD8–and KIR–CD8+ within CD56+16+ showed a significant ultradian variation ($p<0.05$). KIR+CD8– showed a significantly higher count at 1100–1130 h ($p=0.02$), at the expense of a significantly lower count of KIR–CD8+

(p<0.001, Figure 20B). Within the CD56–16+ significant diurnal variations were observed only for the KIR+CD8–cells. Their percentage was significantly lower at 1315 h in comparison to values observed at 1600 h (4.2 % vs. 7.0 %, p=0.01; Figure 20C). No significant ultradian variation in the four KIR/CD8 subsets within the CD56+16- cells was detected (p>0.05; Figure 20D).

	KIR–CD8–	KIR+CD8+	KIR+CD8–	KIR–CD8+
CD56+16+	42.3%±0.5%	12.9±0.3	27.7%±0.2	17.%±0.3
CD56–16+	87.5%±0.2	2.0%±0.06	6.05%±0.21	4.36%±0.08
CD56+16–	82.7%±0.3	1.5%±0.1	3.4%± 0.1	12.4%±0.3

Table 2. Average percentages of KIR/CD8 populations within CD56+/16 NK subsets. Data is expressed by the mean percentage±SEM of all time points from 19 donors.

3.4.5 Correlations between lymphocyte ultradian fluctuations and cortisol levels

To establish the temporal influence of cortisol on the relative redistribution of lymphocytes and NK subsets, time-lagged Pearson correlations on mean cell percentage values were calculated (Figure 21 and 22). By varying the time delay between cortisol concentrations and cell numbers, the time lag with the best correlation was identified. Positive correlation between cortisol concentration and the percentage of CD3 cells was found when the time lag was increased from 0 to 150 min, reaching a maximal value after 75 min (r=0.61, p<0.0001, Figure 21A). Between 0-150 min the positive correlations (for each individual) were significant for 84 % of the donors, and for 50 % a delay of 75 min

was significant ($p<0.05$). Beyond 75 min the correlation decreased, reaching negative values between 165-285 min with the strongest negative correlation after 225 min ($r=-0.4$, $p<0.05$; Figure 21A). Between 165-285 min the negative correlations for each individual were significant in 52 % of the donors, and for 26 % at a delay of 225 min.

A significant positive correlation between cortisol concentration and the percentage of CD3+CD8– cells was found throughout the whole period with the highest correlation reached after 30 min ($r=0.79$, $p<0.1.10^{-9}$; Figure 21B). Between 0 and 300 minutes the individuals' positive correlations were significant for 79 % of the donors, and for 32 % at delay of 30 min.

A negative correlation was observed between cortisol concentration and the percentage of total NK cells with 75 min lag (45-105 min), but this result was not significant ($r=-0.26$, $p=0.1$, Figure 21C). However, between 45 to 105 min significance was detected in 68% of the donors, and for 42 % at a delay of 75 min. A positive significant correlation was detected as the lag time increased (120-285 min) with a maximum coefficient at 180 min ($r=0.7$, $p<0.0001$; Figure 21C). Between 120-285 min significance was detected in 68 % of the donors, and 42 % at a delay of 180 min. The predominance of CD56+16+ in the total NK population is reflected in time-lagged correlations that are similar to those of the total NK cells. Initially a non-significant negative correlation was observed between cortisol concentration and the percentage of CD56+16+ cells in the same period of 45-105 min with the highest although still non-significant correlation occurring after a 75 min delay, ($r=-0.24$, $p=0.1$, Figure 22A). Between 45-105 min the individuals` negative correlations were significant for 68% of the donors, and for 42 % at a delay of 75 min.

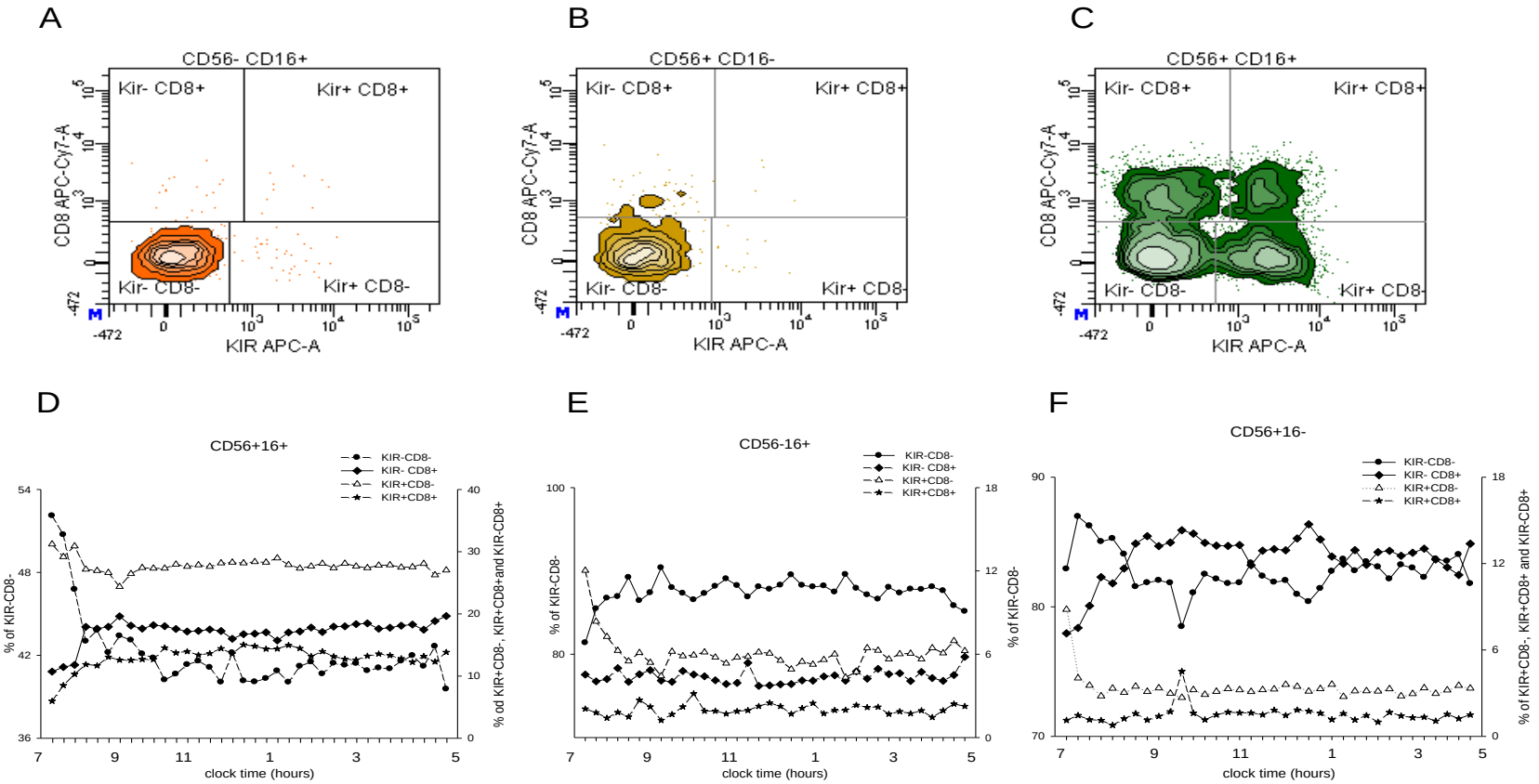

Figure 20. Dot plot from a representative donor of KIR/CD8 gating of CD56-16+ (A), CD56+16-(B), CD56+16+(C) Daily distribution of KIR/CD8 counts as percentage of the counts of CD56+16+ NK subset (D), CD56–16+ NK subset (E) and CD56+16– NK subset (F). Clock time runs from 0700 to 1700 h.

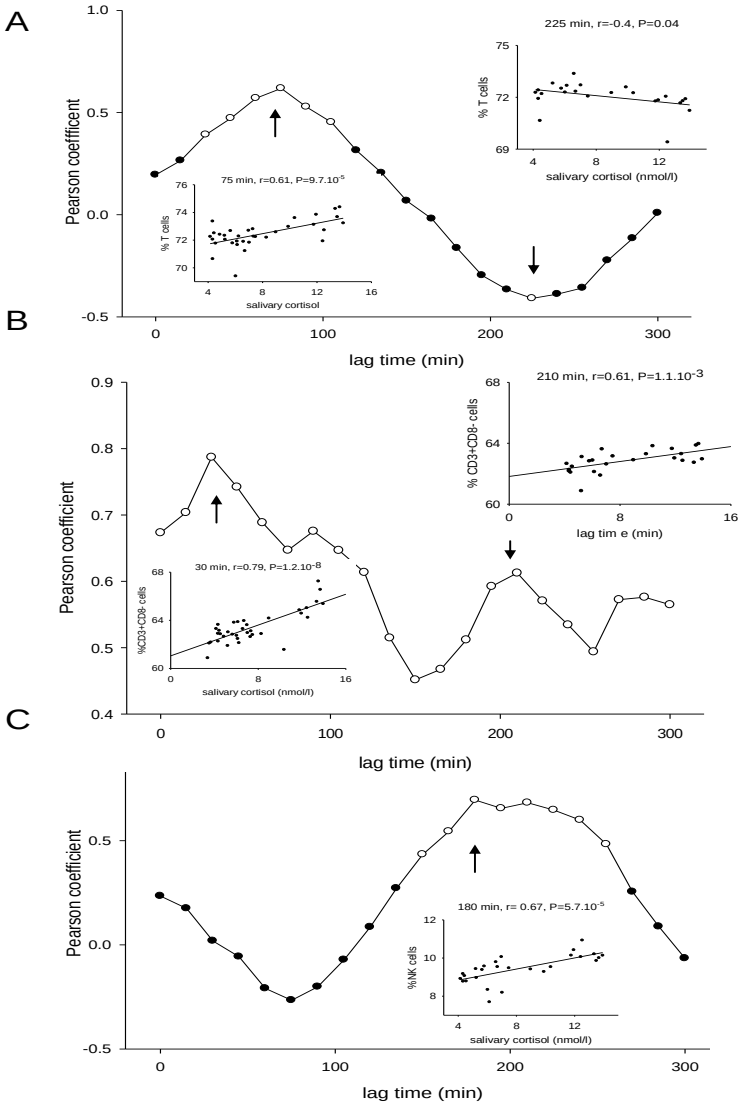

Figure 21. Average Pearson correlation profiles of CD3+ (A) CD3+CD8– (B) and total NK (C) cell counts as percentage of total lymphocyte counts with salivary cortisol concentration. Open circles indicate time points with significant correlation ($p<0.05$). Arrows correspond to the time points of maximal significant correlation and data for these points are included as inserted dot plots.

Thereafter the correlation was positive (120-285 min) reaching a significant maximal value at 180 min ($r=0.68$, $p<0.0001$; Figure 22A). Between 120-285 min the individuals' positive correlations were significant for 58 % of the donors, and for 32 % at a delay of 180 min.

Initially CD56–CD16+ cells showed a negative correlation between 0 and 165 min with a maximal negative correlation at 90 min lag (r=-0.7, p<0.0001, Figure 22B), followed by a smooth increase with positive correlation values between 180 and 300 min and the highest positive value at 255 min (r=0.68, p<0.0001; Figure 22B). Between 0-165 min the individuals' negative correlations were significant for 68 % of the donors, and for 37 % at a delay of 90 min. Between 180 and 300 min individuals` positive correlations were significant for 74 % of the donors, and for 37 % at a delay of 225 min.

The CD56+16– population was positively correlated with salivary cortisol throughout the whole period with the highest correlation reached after 150 min (r=0.87, p<0.0001; Figure 22C). Between 0 and 300 min the individuals' correlations were significant for 95 % of the donors, and for 47 % at a delay of 150 min.

Initially all KIR+ cells showed a negative correlation between 0 and 90 min with a maximal correlation at 30 min delay (r=-0.47, p=0.004, Figure 23A), followed by an increase with positive correlation values between 105 and 300 min and the highest value at 180 min (r=0.77, $p=0.10^{-6}$; Figure 23A). Between 0-90 min the individuals' negative correlations were significant for 68 % of the donors, and for 21 % at a delay of 30 min. Between 105 and 300 min individuals' positive correlations were significant for 84 % of the donors, and for 26 % at a delay of 180 min. As expected KIR– cells showed a positive correlation between 0 and 90 min with a maximal correlation at 30 min delay (r=0.47, p=0.004, Figure 23B), followed by a smooth decrease with negative correlation values between 105 and 300 min and the highest negative value at 180 min (r=-0.77, $p=0.10^{-6}$; Figure 23B). Between 0-165 min the individuals' correlations were significant for 68 % of the donors, and for 21 % at a delay of min. Between 105 and 300 min individuals' correlations were significant for 84 % of the donors, and for 26 % at a delay of 180 min.

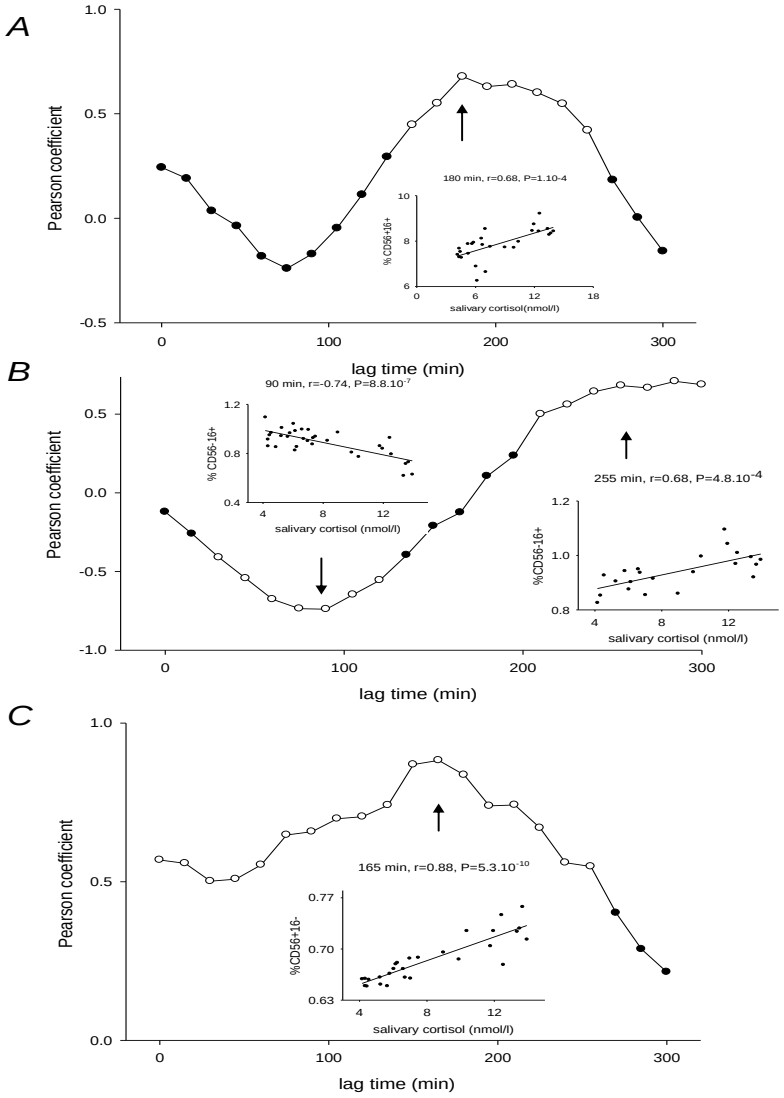

Figure 22. Average Pearson correlation profiles of CD56+16+ (A), CD56–16+ (B), CD56+16– (C) cell counts as percentage of total lymphocyte counts with salivary cortisol concentration. Open circles indicate time points with significant correlation ($p<0.05$). Arrows correspond to the time points of maximal significant correlation and data for these points are included as inserted dot plots.

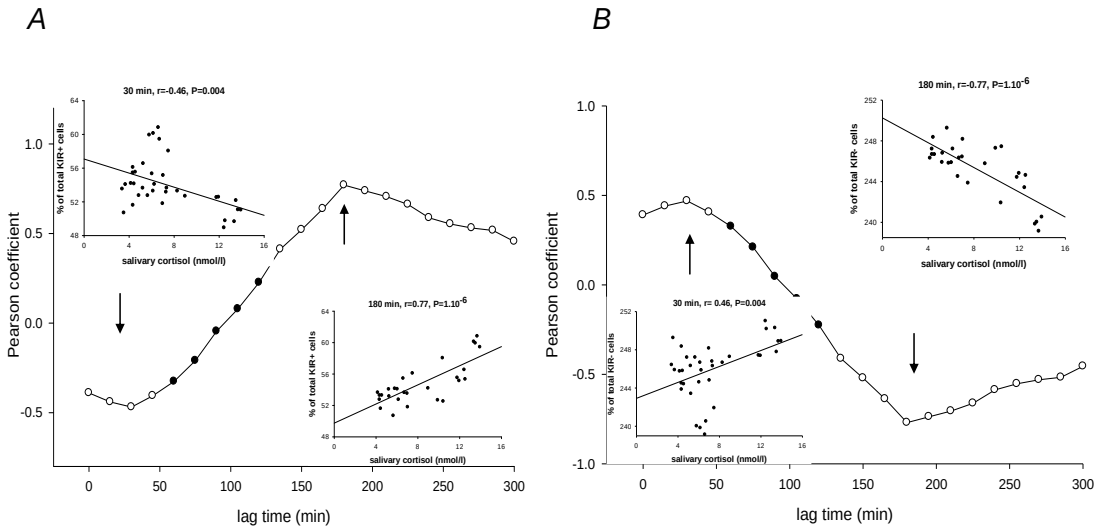

Figure 23. Average Pearson correlation profiles of total KIR+ (A), KIR– (B) cell counts as percentage of total lymphocyte counts with salivary cortisol concentration. Open circles indicate time points with significant correlation ($p<0.05$). Arrows correspond to the time points of maximal significant correlation and data for these points are included as inserted dot plots.

3.5 Discussion

In line with previous studies, we observed significant variations in the percentages of T cells throughout the observation period (Miyawaki et al, 1984; Ritchie et al, 1983). While CD3+CD8+ and CD3+CD8- (i.e primarily CD4+ cells) were highest in the first morning blood samples, the counts were lowest between 1115-1200 h. In parallel, we observed a decrease in NK cells in the early morning, followed by an increase around midday (between 1115-1300 h) which was in agreement with (Kronfol et al, 1997), but in contrast to (Fukuda et al, 1994; Ritchie et al, 1983). B cells did not show significant variations, corresponding to the stable circadian B cell counts reported by Miyawaki et al. (Miyawaki et al, 1984). Similarly, corticosteroid administration in humans also had no effect on circulating B cell levels (Fauci, 1975; Fauci & Dale, 1974). In order to examine the cross-correlations between diurnal free cortisol pattern and peripheral lymphocyte

counts with high sensitivity, we applied a high frequency sampling schedule covering the morning CAR and afternoon nadir.

Our sampling frequency included also previously ignored time points immediately after the CAR. We observed linked bimodal responses for T cells, as well as for NK cells, that seem at least temporally linked. There was a positive correlation between cortisol and total T cells that were statistically significant over a lag period of 30-105 min, with the highest correlation 75 min after the cortisol peak. Over this same lag period, NK cell numbers correlated negatively with cortisol levels, with the best correlation again 75 min after the cortisol peak. In a later, second phase 165-285 min after cortisol secretion correlations with total T cells were negative with the best correlation after 225 min, whilst those with NK cells became positive, with the best correlation 180 min after the cortisol peak. Thus, our results suggest in a first phase a delay of about 75 min until full mobilization of T cells and until NK cell depletion, and a second phase between 165-285 min post CAR with opposite diurnal profiles of T and total NK cells in healthy subjects. Kronfol et al., described, relatively weak positive and negative cross-correlations between cortisol, and NK and T cells respectively 2 h after CAR, probably corresponding to the beginning of the second phase of our bimodal redistribution. Our second phase seems to be in line with the transient lymphopenia seen after a single dose of exogenous corticosteroids, where periods of 180-360 min for maximal T cell depletion were reported (Fauci, 1976; Zweiman et al, 1984). This bimodal regulation, which affects total T cells and NK cells in an opposite way has not been previously reported.

A recent study has shown that the diurnal redistribution of T cell subsets are differentially regulated by cortisol and catecholamine rhythms. Effector CD8+ cells were recruited via β2-adrenergic receptors from the marginal pool to the circulation by reducing within minutes their adhesive properties via conformational changes of adhesion molecules

(Dimitrov et al, 2009). On the other hand, GC-induced changes in adhesion molecule expression (such as CD62L, CXCR4, ICAM-1) on either naive T cells or endothelial cells were suggested as mechanisms of selective lymphocyte migration to the bone marrow. For instance, CXCR4 was upregulated in circulating human T cells by morning cortisol levels resulting in their redistribution to bone marrow with a 180 min delay (Dimitrov et al, 2009). In vitro cortisol upregulated CXCR4 expression within one hour (Dimitrov et al, 2009). Thus, our observed second phase T cell depletion 165-225 min post CAR, may correspond to a similar up regulation of CXCR4 or other adhesion molecules such as CD62L, and CD49d.

The above adaptation towards increased numbers of circulating innate immune cells peaking 180 min post CAR was also reflected in the composition of the NK cell subsets. The anti-KIR antibody used in our study was broadly reactive with both, the inhibitory and activating KIR receptors. KIR+ cells have prominent cytolytic activity, whilst KIR− cells were mostly involved in cytokine production (Cooper et al, 2001). In our study 41 % of CD56+16+ cells, the largest NK cell population expressed KIR receptors, whilst the CD56–16+ and CD56+16− populations had five and nine times lower percentages of KIR positive cells respectively. Thus, the major NK cell subset (CD56+16+) contained cells with higher cytolytic activity, whilst the single positive subsets contained cells involved mainly in cytokine production. We observed a significant diurnal variation in the numbers of total KIR+ and KIR– cells. Interestingly, the time of KIR+ cell enrichment within both the CD56+16+ and CD56-16+ subsets coincided with the time of highest NK cell counts, corresponding to the 180 min lag period of maximal positive correlation with cortisol. Whether this corresponds to selective recruitment of cytolytic NK cells or the induction of KIR expression on KIR– cells is not clear. KIR+ cells within CD56+16- did not significantly change, as they only represent a small percentage in this subset. Higher NK

cell numbers enriched with more cytolytic KIR+ cells would protect against infections during the second phase, with a pool of circulating cells mobilized, and available to be recruited to the site of injury or infection. This increase in NK cell numbers and their bias towards a cytolytic phenotype observed here seems to be part of a generalised bias towards the increased mobilization of the innate immune cells 180 min after CAR that significantly correlates with diurnal cortisol levels and may be partially orchestrated by it.

It should be noted however that the cross-correlations observed do not prove a mechanistic link between endogenous cortisol levels and T and NK cells counts. It should be kept in mind that there are other rhythmically secreted hormones e.g cathecholamines that may also play role in the regulation of immune cell redistribution.

In conclusion, we detected significant inverse diurnal patterns for T and NK cells and strong lagged correlations with diurnal cortisol levels, in particular with CAR. Inclusion of the time points immediately after the cortisol peak, revealed a bimodal response with a first phase T cell increase and NK cell decrease peaking after 75 min. In a second phase, NK cells increased, and T cells decreased 180 and 225 min after the cortisol peak respectively. Taken together our results suggest that endogenous cortisol levels may play a role in fine-tuning the diurnal redistribution of T and NK cell populations, with a bias towards mobilising innate immune cells 180 min after CAR.

Chapter 4

Gene responses to the Trier Social Stress Test (TSST) in healthy males and females.

Slavena T. Trifonova [a,b], Anne Molitor [c], Fabian Streit [c], Stefan Wust [d], Jonathan D. Turner [a,b], Claude P. Muller [a,b]

[a] Institute of Immunology, CRP-Santé / National Public Health Laboratory, 20A rue Auguste Lumière, L-1950 Luxembourg, Grand Duchy of Luxembourg

[b] Department of Immunology, Research Institute of Psychobiology, University of Trier, D-54290 Trier, Germany

[c] Department of Psychobiology of the Graduate School of Psychobiology, University of Trier, 54290 Trier, Germany

[d]Institute for Experimental Psychology, University of Regensburg, 93040, Regensburg, Germany

Manuscript in preparation

4.1 Abstract

The endocrine stress response modulates gene expression to ensure a dynamic adaptation to stress and may represent an important factor contributing to the overall vulnerability for psychopathology. GC-induced gene expression is a functional readout that incorporates GC levels as well as receptor (GR and MR) levels and affinities. Alteration in levels and/or affinities of any of these components will change the subsequent gene response. As GC target genes have been shown to be expressed in a pulsatile manner after GC exposure, this study addressed the kinetic profile of GR target gene expression after a TSST induced pulse of endogenous GCs.

Expression of the GR target genes *GILZ, FKBP* and *SDPR* was measured by qPCR up to 120 min post-TSST in a mixed cohort of 14 male and 13 female subjects. To model the effects of TSST hormonal responses on gene expression trajectories a linear mixed effects regression model was generated.

We observed significant differences between the cortisol net increases in male and female responders, with approximately three times greater cortisol net increases in male subjects. About half of the participants, with similar gender ratio, showed a significant cortisol response 30 min before the beginning of the TSST, indicating anticipation of an upcoming stressful event. Gene expression showed a dynamic pattern with several distinct expression pulses related to anticipation, stress and meal presentation. The TSST responders who also had anticipatory and/or meal related peaks showed complex gene expression trajectories with waves of expression, complicating the modeling of corresponding hormonal and gene expression peaks. Only 40 % of all donors showed either a distinct single anticipatory or stress induced cortisol peak that could be related to a subsequent gene expression peak. On average *GILZ* was upregulated 61.3±39.2 min after peak cortisol levels, whilst for *FKBP5* this period was of 95.6 ±52.5 min.

Differences in the magnitude of the gene response were observed with a higher overall *FKBP5* response compared to *GILZ* and a trend of higher *FKBP5* response in males compared to females. Moreover, the mixed effect regression model showed that the stress induced cortisol peak did not induce a peak in expression, but rather slowed down the natural decrease in *GILZ* and *FKBP5* mRNA levels over the afternoon. The model also confirmed that anticipatory responses to stressful stimuli are significant predictors of the gene response.

In conclusion we confirmed that the GC-induced gene expression pulsing within the GR system is a common phenomenon, occurring after exogenous hormone stimulation as well as when the HPA axis is perturbed by an acute stressor. However, we suggest that stress induced cortisol levels significantly alters the transcriptional program, only if they coincide with the ascending phase of an ultradian cortisol pulse.

Keywords: stress, cortisol, glucocorticoid receptor, kinetics, gene expression, humans

4.2 Introduction

GCs are steroid hormones secreted by the adrenal gland, and they are the effector molecules of the HPA axis. They exert profound effects on a wide range of physiological and developmental processes, and they play an important role in maintaining basal and stress-related homeostasis (de Kloet et al, 2005; Stahn & Buttgereit, 2008). The steroid hormone receptors that are bound by GCs, the mineralcorticoid receptor (MR, NR3C2, OMIM# 600983) and the glucocorticoid receptor (GR, NR3C1 OMIM# 138040) play an important role in both the response to, and control of the circadian and stress induced HPA axis activity. The primary function of both receptors is to act as ligand activated transcription factors, able to detect circulating steroid levels and to activate the appropriate transcriptional responses in GC target cells. Due to its 10 fold higher affinity for cortisol, the MR is thought to be permanently activated by GCs, including during periods of low GC levels (Conway-Campbell et al, 2007; Pascual-Le Tallec & Lombes, 2005). However, the GR is activated by ultradian, circadian or stress induced peak GC levels (de Kloet et al, 2005). As such, the GR is a key component of the stress response (Zhou & Cidlowski, 2005). Induction or inhibiton of transcription, the genomic action of corticosteroids, is mediated either by direct GR-DNA binding or via protein-protein interactions with other transcription factors such as NFkB, AP-1, HNF4, C/EBP (Gross & Cidlowski, 2008; Hayashi et al, 2004). The resultant gene expression is a complex integration of GC levels as well as receptor (GR and MR) levels and affinities. Alteration in either the levels or affinities of any of these components will change the subsequent gene response.

To date genome wide and targetted gene expression studies have been performed to identify potential stress responsive genes, or potential biomarkers of stress exposure in vivo (Miller et al, 2008; Morita et al, 2005; Murata et al, 2005; Oishi et al, 2003; Pajer et

al, 2012). Morita et al. conducted a high-throughput microarray analysis to investigate the psychological stress-associated gene response in human leucocytes and revealed 70 potential stress-responsive genes whose mRNA levels significantly changed at 2 h after stress (Morita et al, 2005). Most of them were categorized into cytokines, cytokine receptors, growth- or apoptosis related molecules, and heat shock proteins, suggesting that stressful life events trigger acute responses in leucocytes. Another study analyzed genome-wide transcriptional acitvity in association with chronic isolation in humans (Cole et al, 2007). They observed an impaired transcription of GC responsive genes and increased activity of pro-inflammatory transcription control, thus explaining the elevated risk of inflammatory disease in individuals who experienced chronical social isolation. A more recent microarray study associated chronic stress with alteration in GC signal transduction which enables activation of pro-inflammatory pathways, thus contributing to stress-related morbidity and mortality (Miller et al, 2008).

By profiling gene expression after GR activation in rat hippocampal slices throughout a time window of 1-5 h, Morsink et al. reported a dynamic pattern with different waves of GR-target gene expression (Morsink et al, 2006). The resultant gene expression profiles showed a dynamic transcriptional response which shifted from a generalised downregulation of genes 1 h after GR activation, towards gene specific up- and downregulaton 3 h post stress. The GR modulated genes were mostly involved in energy metabolism, signal transduction, neurotransmitter metabolism and cell adhesion. FK506 binding protein 5 *(FKBP5*) and glucocorticoid-induced leucine zipper (*GILZ, TSC22D3*) were both shown to be GR and MR regulated, but *GILZ* is more rapidly induced (Rogerson et al., 2004; Soundararajan et al., 2005). Restraint stress in rats has showed significant *FKBP5* induction as early as 15 min after stress in thymocytes, whilst *GILZ* induction was observed after 2 h in the prefrontal cortex (Billing et al, 2012). Some of

these newly identified genes have been previously associated with stress-related disorders (Binder et al, 2004; Cole et al, 2007; Ising et al, 2008; Kato, 2007; Le-Niculescu et al; Willour et al, 2009). Decreased *GILZ* expression has been associated with some of the immune symptoms observed in FM (Macedo et al, 2008) and also in the development of delayed-type hypersensitivity reactions (Berrebi et al, 2003). Recently MDD and impaired recovery of the stress response have been associated with elevated *FKBP5* expression levels (Binder et al, 2004; Ising et al, 2008), whilst decreased *FKBP5* levels were associated with posttraumatic stress disorder (Yehuda et al, 2009). A genome wide expression analyses in genetic and chronic stress animal models, revealed a set of candidate biomarkers for depression. A panel of 11 out of 26 genes has overlapped in early-onset MDD patients, thus identifying potential peripheral biomarkers for this disease (Pajer et al, 2012).

However, these studies have measured gene expression alterations using one (Cole et al, 2007; Le-Niculescu et al; Macedo et al, 2008; Murata et al, 2005; Pajer et al, 2012; Yehuda et al, 2009) or a limited number (Morsink et al, 2006; Nater et al, 2009) of measurement points post GC exposure, thus allowing only the identification of potential stress-responsive genes. Interestingly, in vitro GC stimulation of adrenalectomized rats revealed pulsatile GR-mediated transcriptional regulation of GR target genes such as *GILZ, PER1* (Conway-Campbell et al; Stavreva et al, 2009). This phenomenon was described as a form of gene pulsing and was suggested as essential for correct transcriptional programming (Lightman et al, 2008; Stavreva et al, 2009). However, studies on the kinetics of stress induced gene expression are notably absent.

The present study was conducted to shed light on the kinetics of GR target gene expression after inducing endogenous cortisol release. For this purpose, we applied a standardized stress protocol on a mixed cohort of male and female subjects and profiled

the kinetics of gene expression at multiple time points before, during and after stress. We observed a dynamic gene expression pattern with several distinct gene expression pulses related to anticipation, stress and meal presentation. The gene expression fold changes were moderate, with difference in the magnitude of the individual gene response. Anticipation to stressful stimuli, as well as the TSST response were found to be significant predictors of the gene response.

4.3 Materials and methods

4.3.1 Subjects

A total of 27 healthy young subjects (14 males and 13 females) aged between 19 and 31 yrs old (mean age of 24.41±3.2 yrs) participated in this study. Only women who did not use ethinyl-estradiol containing oral contraceptives (OC) were included. As the menstrual cycle phase influences HPA axis stress responses (Kirschbaum et al, 1999) all females were tested within a 10 d after ovulation. Ovulation was detected with a commercial LH detection urine test ("gabControl", gabmed GmBH, Nettetal-Lobberich, Germany). No subject smoked more than five cigarettes per day, or reported a history of chronic physical or psychological diseases. All participants reported to be healthy and free of medication at the time of the experiement. The study protocol was approved by the Ethics Committee of the Medical Association of Rheinland-Pfalz and written informed consent was obtained by all participating subjects. All experiments have been conducted according to the Declaration of Helsinki.

4.3.2 Study protocol

To induce endogenous cortisol secretion, the HPA axis was stimulated by exposure to a standardized laboratory stressor, the Trier Social Stress Test (TSST) (Kirschbaum et al, 1993). The TSST consists of a three minutes preparation period, a five minute free speech and a five minute mental arithmetic task in front of an audience of two panel members. Subjects arrived at 1300 h, approximately 60 min before the initiation of the TSST, and gave the first saliva sample. They were asked to provide a written informed consent for participation and filled out a questionnaire about their health status. Subsequently, an indwelling canula was applied to the left forearm and a first blood sample was drawn about 45 min before the TSST start. The TSST was started at 1400 h (T=0 min), when donors were taken into the TSST room and were introduced to the task. Due to the long sampling period a light meal was provided 150 min post-TSST. The food was announced at 120 min post-TSST.

4.3.3 Saliva and blood sampling

Salivary samples were collected 60, 45, 30, 15, 2 min pre-TSST as well as 2, 10, 20, 30, 45, 60, 120, 150, 180, 210, 240, and 270 min post-TSST using Salivette sampling devices (Sarstedt, Nuembrecht, Germany) and stored at -20 ˚C until analysis. EDTA blood was drawn for plasma ACTH analysis 2 min pre-TSST as well as 2, 10, 20, 30, 45, 60, 120, 150, 180, 210, 240, and 270 min post-TSST. Samples were centrifuged at 4 °C, 4000 g for 10 min and 500 µl plasma aliquots were stored at -20 °C until analysis. EDTA blood was drawn for mRNA analysis at 45 and 2 min pre-TSST as well as 2, 10, 20, 30, 45, 60, 120, 150, 180, 210, 240, and 270 min post-TSST. Samples were stabilized by addition of 300 µl whole blood to 1.3 ml RNA*later*® (Ambion®, Foster City, Texas, USA) and were stored at -20 ˚C until analysis.

4.3.4 Biochemical analysis

Plasma ACTH concentrations were determined with an enzyme-linked immunosorbent assay (ELISA; Biomerica Inc., Irvine, California, USA). The assay sensitivity was 0.46 pg/ml. Intra- and inter-assay variability were 3.1 % and 5.58 %, respectively. Salivary cortisol concentrations were determined by a time resolved immunoassay with fluorescence detection as described elsewhere (Dressendorfer et al, 1992). The assay sensitivity was 0.173 nmol/l. The intra-assay coefficient of variation was between 4.0 % and 6.7 %, and the corresponding inter-assay coefficients of variation were between 7.1 - 9.0 %.

4.3.5 Gene expression analysis

Total RNA was isolated from blood samples using the RiboPure Blood Kit (Ambion, Foster City, Texas, USA), according to the manufacturer protocol. First strand synthesis of total cDNA was carried out at 55 ˚C using 200 U/µl SuperScript III reverse transcriptase, 250 ng/µl dN6 primers in a 60 µl reaction containing 250 mM Tris-HCl, 375 mM KCl, 15 mM $MgCl_2$, 10 mM dithiothreitol and 500 µM dNTPs (Invitrogen, Paisley, UK). Amplification of cDNA by PCR was performed in 25 µl reactions containing 20 mM Tris-HCl (pH 8.4), 50 mM KCl, 200 mM dNTPs, $MgCl_2$, gene specific primers, 5 U Platinum *Taq* DNA polymerase (Invitrogen) and 1 x concentrated SYBR Green (Cambrex, Verviers, Belgium). Thermal cycling was performed in an Opticon 2 (Biorad, NL). Cycling conditions were: one cycle at 95 ˚C, 2 min, followed by 40 cycles each including denaturation at 95 ˚C for 20 s; annealing, 20 s, elongation 72 ˚C, 20 s. The primers and optimised PCR conditions are shown in Table 3. All primers were synthesised by Eurogentec (Seraing, BE). The relative expression was calculated using the $2^{-(\Delta\Delta c)}$ relative

quantification method (Livak and Schmittgen, 2001). All genes were assayed in triplicates for each sample. Three reference genes *18S rRNA, GAPDH* and *β-actin*, were measured. The most stable reference gene *GAPDH* was used for data normalization, following the procedure from Schote et al. (Schote et al, 2007).

Primer pairs	Sequence	PCR product (bp)	Tm (C)	$MgCl_2$ (mM)	Primers (uM)
GAPDH	fwd: 5'-gaaggtgaaggtcggagtc-3' rev: 5'-gaagatggtgggatttc-3'	146	60	2	0.5
GILZ	fwd: 5'-gcacaatttctccatctccttctt-3' rev: 5'tcagatgattcttcaccagatcca-3'	146	60	2	0.5
FKBP5	fwd: 5'-aaaaggccaaggagcacaac-3' rev: 5'-ttgaggaggggccgagttc-3'	236	67	4	0.5
SDPR	fwd: 5'-agaacaaccacgcccagct-3' rev: 5'-tccacggtgcagggttt-3'	190	60	2	0.5

Table 3. Primers and PCR conditions

4.3.6 Statistical analysis and data reduction

To model the effects of TSST hormonal responses on gene expression trajectories linear mixed effects regression model was tested focusing on *GILZ, FKBP* and *SDPR* levels up to 120 min post-TSST. Fixed effects represent the mean changes in gene expression levels. Random effects represent variability between donors and model non-independence of repeated measures (Singer & Willet, 2003). Gene expression data were log transformed to yield a better approximation to normal distribution. For both *GILZ* and *SDPR*, one potentially influential outlying observation (more than 4 SD above/below mean) was trimmed. The first gene expression assessment 45 min pre-TSST was not used in the analysis due to the small number of participants. For this part of the analysis all observations after 120 min were cut off due to confounding meal–related gene expression peaks. As predictors of gene expression time trends, mean levels and increases were included in the model, defined as follows: mean levels were defined as the arithmetic

mean concentration of the concentrations of four consequtive time points; increases were defined as the maximal concentration at a specific time point minus the concentration at a time point where it is expected to be at basal levels.

Anticipation effects were indicated by (a) cortisol mean level (-60, -45, -30 and -15 min pre-TSST), and (b) the increase (maximum cortisol level out of the measures -30 and -15 min minus the mean of cortisol -60 and -45 min). TSST-related effects on cortisol secretion were similarly indicated by (a) cortisol mean levels (-2, +2, +10, +20 +30 min post-TSST), and (b) the increase (maximum cortisol level out of the measures +10 and +20 min minus the cortisol level -2 min). TSST-related ACTH secretion was indicated by (a) ACTH mean level (-2, +2, +10, +20 min), and (b) the increase (maximum ACTH level out of the measures at +2 and +10 min minus the ACTH level at -2 min).

Anticipation effects on gene expression levels were tested for gene expression trajectories between -2 and +120 min. TSST-related effects were tested on coefficients for gene expression trajectories between +10 and +120 min. All models included a linear time predictor reflecting exact time of assessment in minutes and an interaction with the respective cortisol or ACTH predictor. This interaction reflects differential time trends in association with cortisol or ACTH secretion. All mixed models were calculated using Stata 12.1 (StataCorp, College Station, TX, USA).

To describe the endocrine responses ACTH and cortisol anticipatory, stress-induced and meal-induced increases were calculated and compared. Anticipatory cortisol and stress-induced ACTH and cortisol increases were calculated as mentioned above. The ACTH meal induced increase was defined as the maximum ACTH level out of the measures +150 and +180 minus the ACTH level +120 min. The cortisol meal induced increase was defined as the maximum cortisol level out of the measures +150 and +180 minus the cortisol level +120 min. Group comparisons (responders vs. non-responders; males vs.

females) on the estimated increases were performed by student t-test and these results were presented as mean ± S.D. Values were log transformed to ensure normality. Statistical relationships between amplitudes of cortisol and gene expression peaks were calculated using the Pearson product moment correlation test. Time series were analysed by repeated measures analysis of variance (RM-ANOVA) considering sampling time as the potential source of variance, SPSS 20 for Windows software (SPSS inc., Chicago, USA). Greenhouse-Geisser correction (Greenhouse & Geisser, 1959) was used to adjust the degrees of freedom for the interaction effects.

Donors were considered as stress responders if their salivary cortisol response was at least 2.5 nmol/l over individual baseline levels, an elevation thought to reflect a cortisol secretory episode (Van Cauter & Refetoff, 1985).

4.4 Results

4.4.1 TSST induced hormone profiles

ACTH peaked 2 min after the cessation of the TSST with an average increase of 18.3 ± 3.6 nmol/l for all donors (Figure 24A). Although on a descriptive level males on average showed higher ACTH increases in response to the TSST than females the respective sex x time effect (RM-ANOVA) did not reach statistical significance ($F=2.14$, $p=0.14$; Figure 24C). As expected, mean cortisol peaks were observed 10 min post-TSST with an average increase of 4.56 ± 0.87 nmol/l for all donors (Figure 24B). Again, males showed higher mean responses than females on a descriptive level but the respective sex x time effect was not statistically significant (report $F=2.44$, $p=0.78$; Figure 24D). 60 % of all donors were assigned as TSST responders with similar response rate of 57 % vs. 61.5 % for males and females, respectively. The TSST induced significantly larger increases in

plasma ACTH (t=4.07, df=13, p=0.001, Figure 25A) and salivary cortisol (t=3.6, df=24, p=0.001; Figure. 25A) in the responders compared to non-responders.

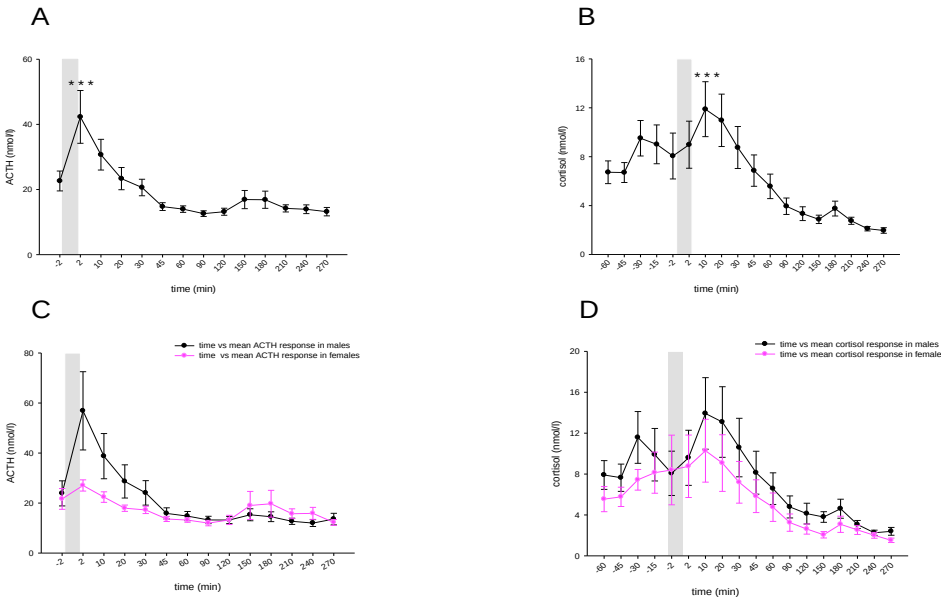

Figure 24. Mean (±SEM) ACTH (A) and cortisol (B) responses (nmol/l) for all donors. C. Mean (±SEM) ACTH (C) and cortisol (D) responses in male and female donors. The shaded area indicates the period of stress exposure. *p<0.05, **p<0.01, *** p<0.001, indicate significant differences between the time points (RM-ANOVA).

The mean ACTH increase was 31.6±7.6 nmol/l for all responders. ACTH increases were significantly higher in males than in females, (student t-test; 44.6 ± 14.1 vs.10.9 ± 3.6 nmol/l, t=2.28, df=17, p=0.04; Figure 25A). The mean cortisol increase was 8.44±2.1 nmol/l for all responders (t=3.6, df=24, p=0.001). The cortisol mean increase was also significantly higher in males than in females (12.8 ± 4.5 nmol/l vs. 4.25 ± 1.5 nmol/l, t=2.2, df=14, p=0.043; Figure 25B). A significant positive correlation was found between the increase of ACTH and cortisol in all stress responders (r=0.89, p<0.0001, Figure 25C).

Approximately 50 % (46.1 % male, 53.8 % females) of the donors showed a significant anticipatory cortisol response (t=4.76, df=15, p<0.001) occurring on average 30 min pre-

TSST. The mean increase was on average 8.83 ± 2.44 nmol/l for all anticipators. Anticipatory responses were similar in both genders with 9.19 ± 3.75 and 8.52 ± 3.22 nmol/l for males and female "anticipators", respectively (t=0.1, df=11, p=0.9, Figure 25D).

One third of the donors (43 % males and 23 % females) exhibited a small meal related peak (t=6.7, df=12, p<0.001) 180 min post-TSST. The mean increase was on average 4.85 ± 1.61 nmol/l with similar increases in males and females with 5.07 ± 2.07 nmol/l and 4.4 ± 2.54 nmol/l (t=0.22, df=10, p=0.83). This meal related peak was preceded by an increase in ACTH levels with a mean of 10.45 ± 2.9 nmol/l (t=5.3, df=17, p<0.001). The increase was similar with 9.2 ± 4.1 nmol/l for male and 11.2 ± 3.9 nmol/l for female donors. This difference was not statistically significant (student t-test: t=0.7, df=11, p=0.48), Figure 25E-F).

4.4.2 Gene expression profiles

After inducing secretion of endogenous GCs, we measured the relative expression levels of the GR-target genes *FKBP5, GILZ* and *SDPR*. The fold changes in genes expression over time were tested by RM-ANOVA. A significant doubling in *FKBP5* levels in males was detected 10 min post-TSST and the levels remained elevated up to 60 min after stress cessation. This subsequently decayed at 210-270 min post-TSST (p<0.05). The highest fold change was observed on average 30 min post-TSST with mean of 2.27±0.6 (range 0.7-6.8) fold increase (p=0.01, Figure 26A). A trend towards *FKBP5* expression trajectory change over time in females was observed (p=0.057, Figure 26B). The second GR-target gene *GILZ* showed significant high levels 2 min pre-TSST, followed by significant increase between 20 and 45 min post-TSST compared with the decay at 210-

270 min ($p<0.05$). The highest fold change was observed 30 min post-TSST with 1.65±0.44 (range 0.9-2.6) fold increase ($p=0.001$, Figure 26C). In females *GILZ* levels fluctuated around the baseline ($p=0.117$, Figure 26D). Similarly, *SDPR* levels did not show significant changes in gene expression levels in both males and females $p=0.089$, $p=0.2$) (Figure 26E-F). No significant sex or sex x time effect on *GILZ* and *SDPR* trajectories was found. A trend towards an overall higher *FKBP5* expression in males ($p=0.058$) was observed, however this was independent of the time trajectory. The average amplitude of *FKBP5* peak induced by anticipatory or stress cortisol peak was 4.04±0.68 fold (range 2.1-6.8), whilst *GILZ* peak amplitude was much lower 1.97±0.2 fold (range 1.1-2.9). Significant correlation was detected when comparing the amplitudes of anticipatory and stress induced cortisol peaks and the subsequent *FKBP5* induced peaks ($r=0.89$, $p=0.007$), whilst for *GILZ* the correlation was not significant ($r=0.1$, $p>0.05$). When comparing *FKBP5, GILZ* and *SDPR* expression levels at -2 min pre-TSST versus their levels in the corresponding time in non-stressed subjects no statistically significant difference was found ($p>0.05$).

Seven out of 27 donors, showed a clear stress induced hormonal and resultant gene expression peak (Figure 27A-B), whilst four donors showed clear anticipatory cortisol and gene expression peaks (Figure 27C-D). On average in both groups *GILZ* was upregulated 61.3±39.2 min after peak cortisol levels, whilst for *FKBP5* this period was of 95.6 ±52.5 min. In comparison the TSST responders that also showed anticipatory and/or meal related peaks showed more complex gene expression trajectories (Figure 27E-F). Assigning the corresponding individual cortisol and gene expression peaks in this case was not possible.

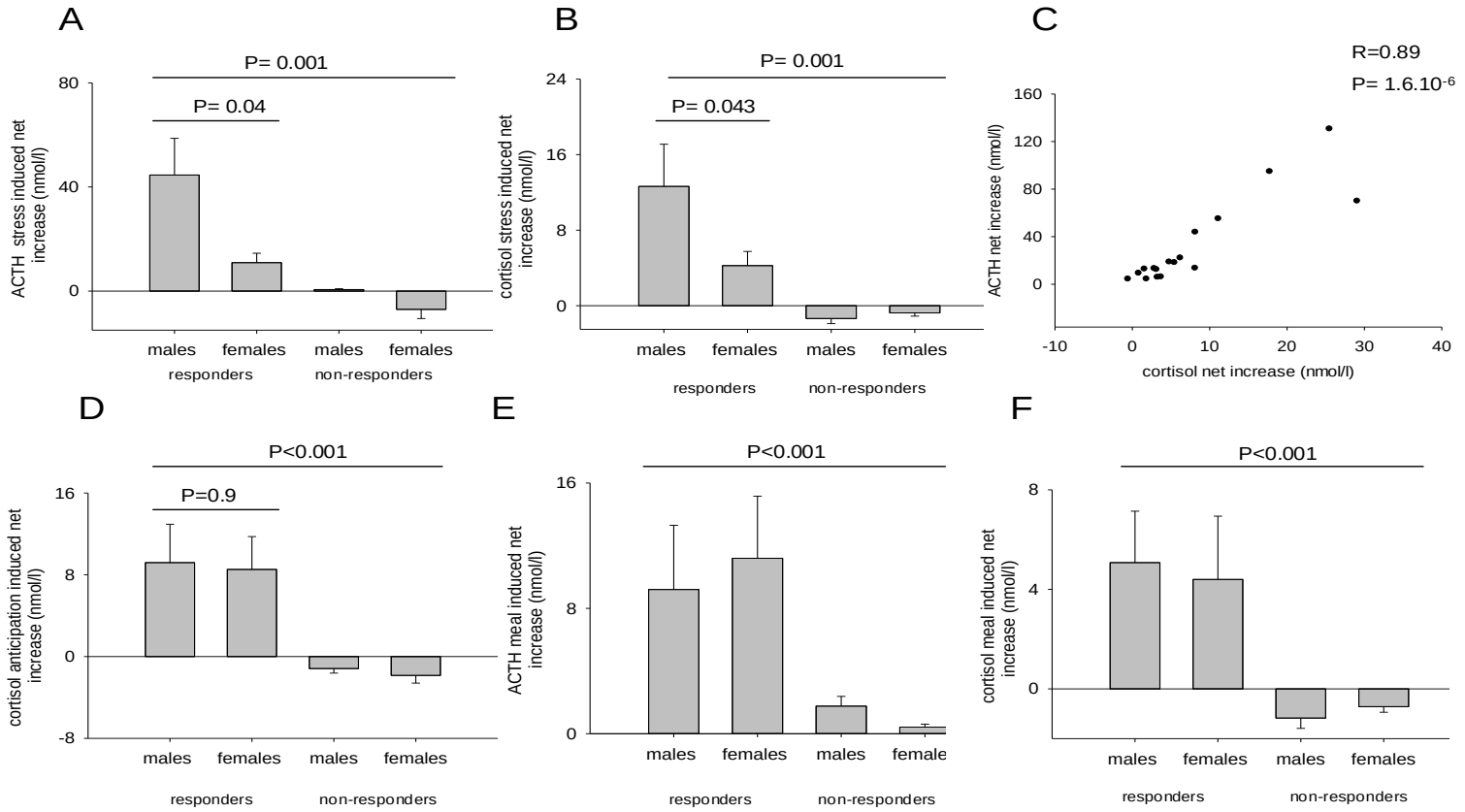

Figure 25. Mean (±SEM) ACTH (A) and cortisol (B) stress responses. Correlation between ACTH and cortisol net increases (C). Mean (±SEM) cortisol (D) anticipatory responses, ACTH (E) and cortisol (F) meal induced responses in responders and non-responders male and female donors.

4.4.3 Gene expression trajectories

4.4.3.1 Anticipation effects

There was a significant negative linear trend of *GILZ* expression from the end of the anticipation period to the last measure 135 min later (parameter=-0.002; p=0.001). A strong pre-TSST cortisol increase (i.e. between -60 and -15 min) was associated with lower *GILZ* expression immediately before the TSST (-2 min) (parameter=-0.401, p=0.044) and with a significantly less pronounced decrease of *GILZ* expression up to +120 min (parameter=0.003; p=0.001). A similar association was observed for *FKBP* expression (although no significant overall decreasing trend was observed for *FKBP*), with a positive trend after relatively high anticipatory cortisol increases (parameter=0.004; p=0.002), but starting from the same level. Figure 28A-B illustrates these trends for relatively high and low anticipatory cortisol increases. In contrast, the mean anticipatory cortisol levels showed no effect on *GILZ* or *FKBP* gene expression trajectories. No significant effect of either mean anticipatory cortisol levels or anticipatory cortisol increases was observed for *SDPR* expression. Significant random effects of time in all models demonstrated considerable individual variability in trajectories.

4.4.3.2 TSST-related effects

No significant effects of TSST-related cortisol increases on gene expression categories were observed (all ps >0.05). In contrast, mean cortisol levels during and shortly after the TSST were associated with a stronger positive time trend of *GILZ* expression

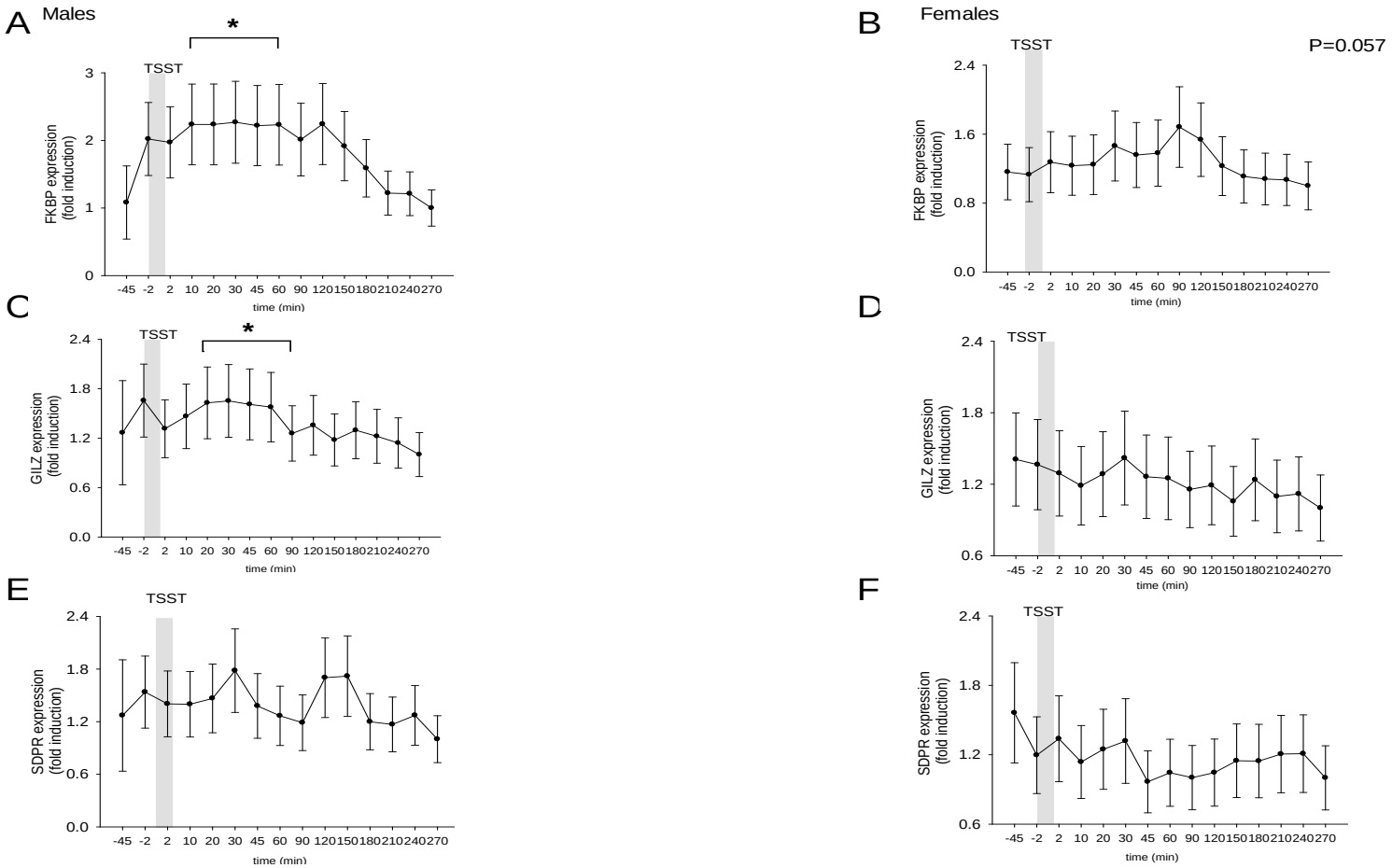

Figure 26. Mean (±SEM) fold changes for FKBP5, GILZ and SDPR in male (A, C, E) and female donors (B, D, F). *p<0.05, **p<0.01, ***p<0.001, indicate significant differences between the time points (RM-ANOVA).

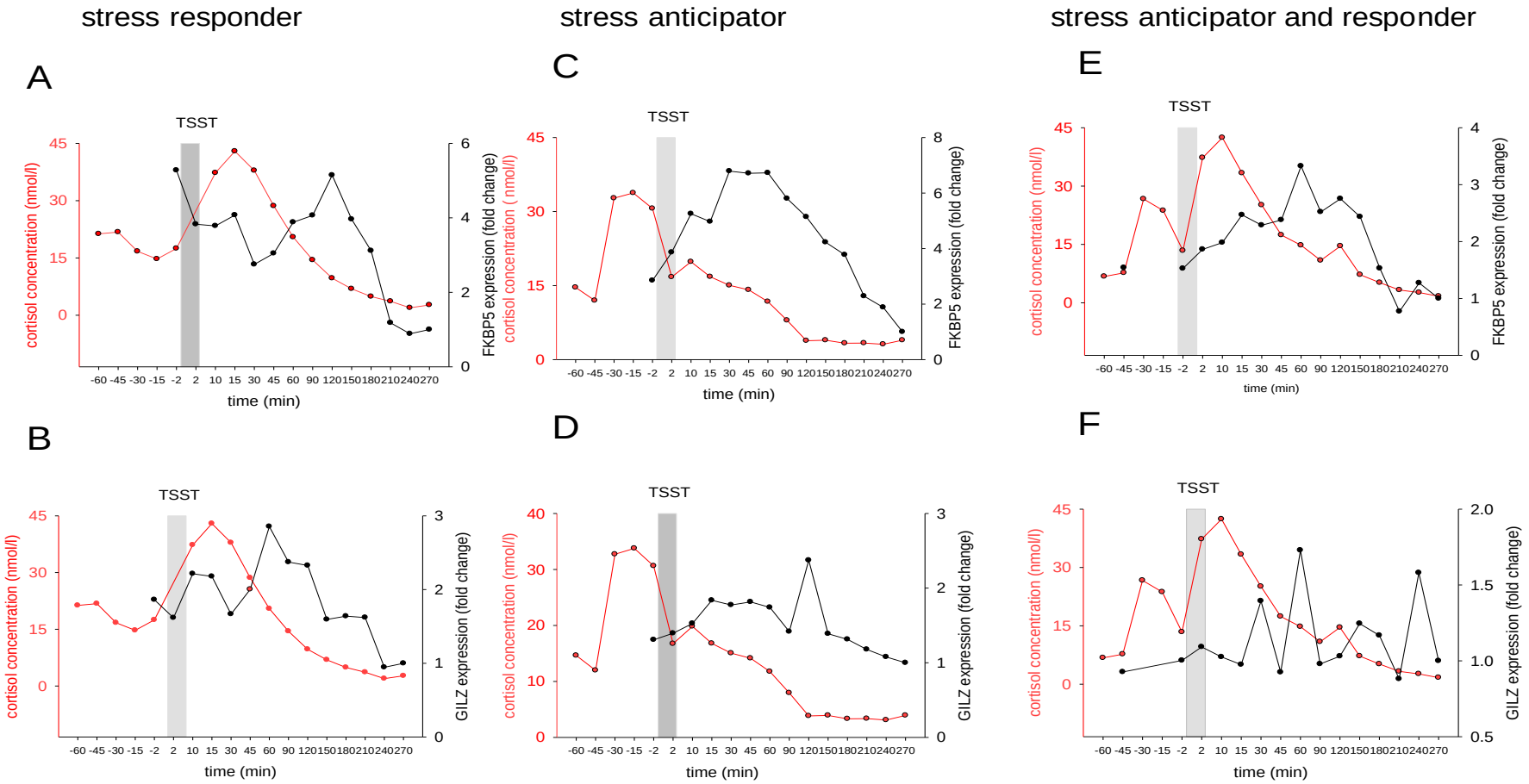

Figure 27. Cortisol responses and their respective GILZ and FKBP expression profiles from three representative donors- stress responder (A, B), stress anticipator(C, D), and stress anticipator and responder (E, F).

(parameter=0.002; p=0.047) as well as FKBP expression (parameter=0.002; p =0.013). This was qualified by a negative overall time trend (*GILZ*: parameter=-0.005; p=0.002; *FKBP*: parameter=-0.003; p=0.077), suggesting that high mean TSST-related cortisol levels attenuated the decrease of *GILZ* and *FKBP* expression from the start of the period (+30 min) to the last measure (+135 min). Figure 7 illustrates these trends for relatively high and low anticipatory cortisol increases. Again, no significant effects were observed for *SDPR* expression, and significant random time effects in all models demonstrated considerable individual variability in trajectories.

Neither ACTH mean levels nor ACTH increases showed significant associations with gene expression for any of the genes studied here, although significant random time effects again demonstrated considerable individual variability in trajectories.

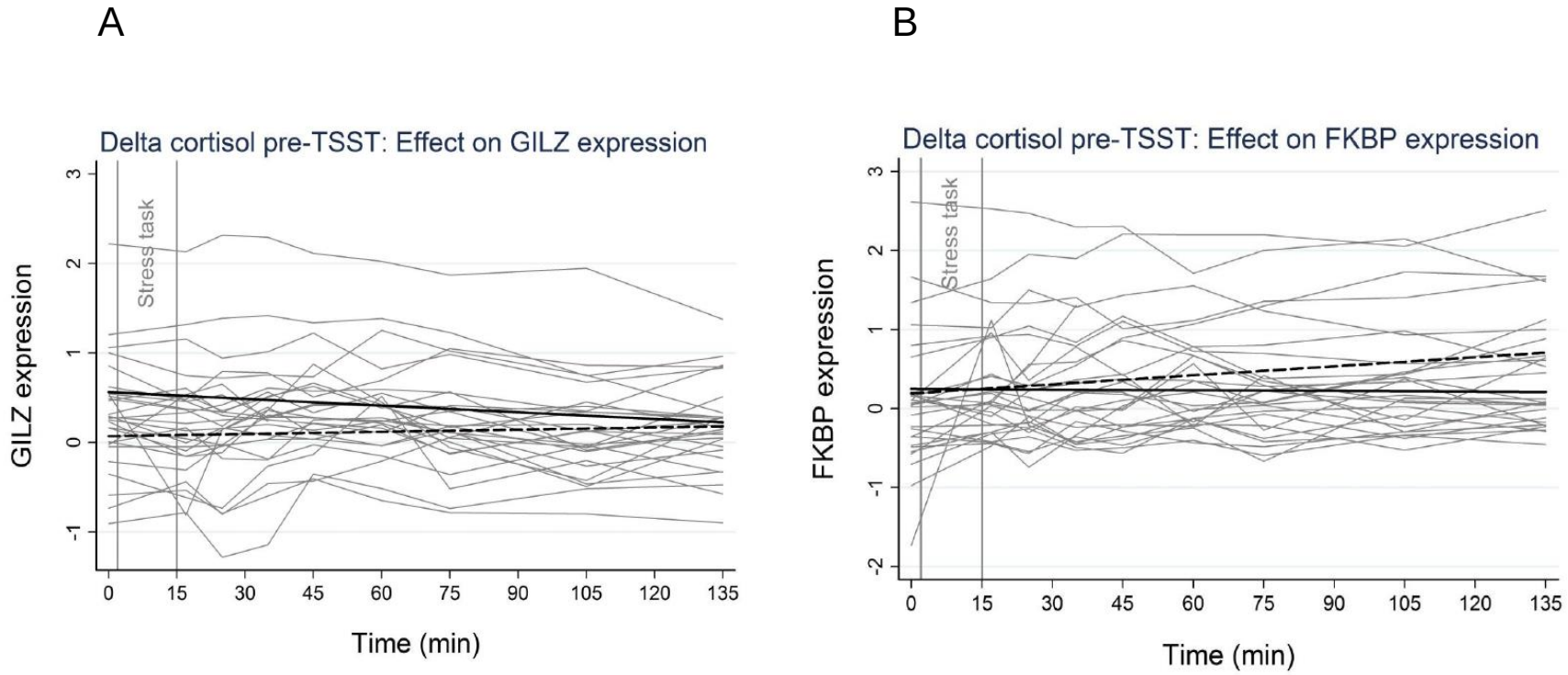

Figure 28. Log-transformed *GILZ* (A) and *FKBP5* (B) expression trajectories for high (mean +1SD; dashed line) and low (mean-1SD; solid line) increases of cortisol in anticipation of the TSST; grey lines show individual observed gene expression trajectories.

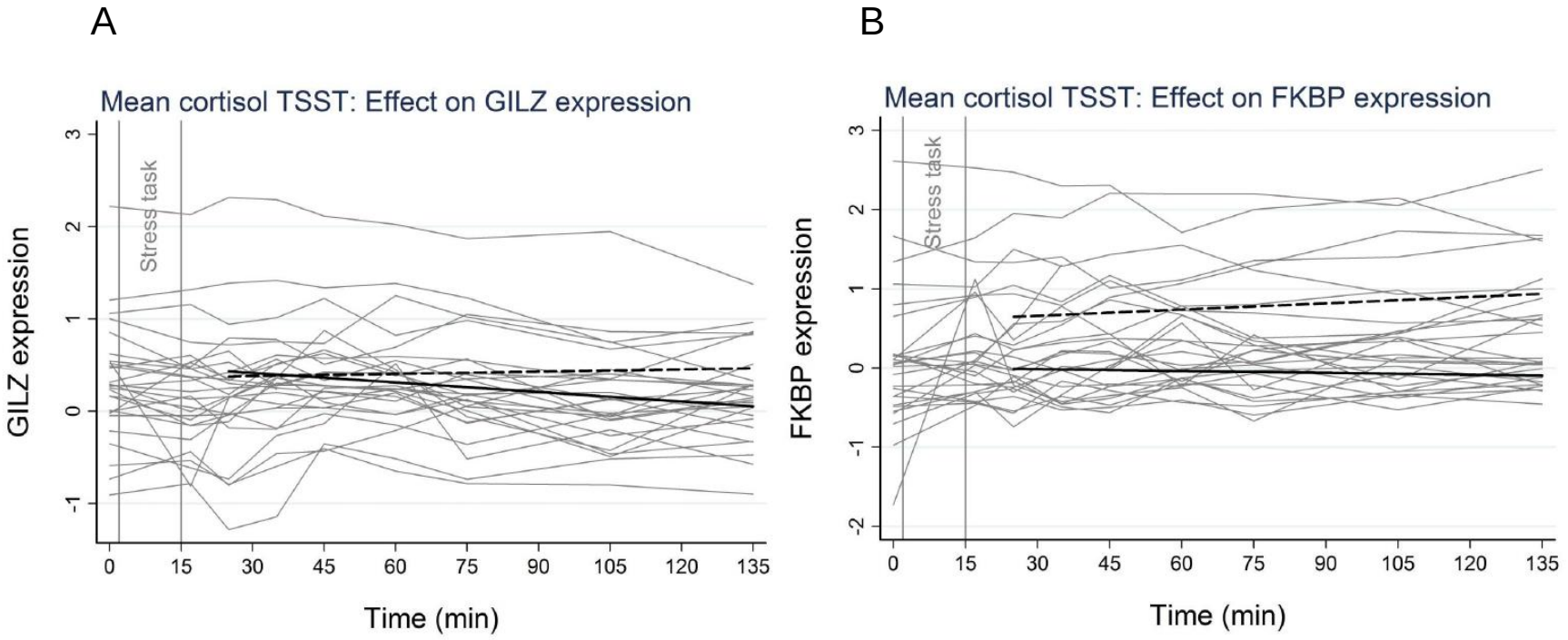

Figure 29. Log-transformed *GILZ* (A) and *FKBP5* (B) expression trajectories for high (mean +1SD; dashed line) and low (mean-1SD; solid line) increases of cortisol during the TSST; grey lines show individual observed gene expression.

4.5 Discussion

The endocrine stress response modulates gene expression, ensuring dynamic adaptation to stress and may represent an important factor contributing to the overall vulnerability for psychopathology (Ising & Holsboer, 2006; Kumsta et al, 2007). GC-induced gene expression is a functional readout that incorporates GC levels as well as receptor (GR and MR) levels, and affinities. Alteration in levels and/or affinities of any of these components will change the subsequent gene response. As GC target genes have been shown to pulse after GC exposure (Conway-Campbell et al; Stavreva et al, 2009), this study addressed the kinetic profile of gene expression after a pulse of endogenous cortisol induced by a standardised stressor.

The TSST induced a hormonal stress response in 60 % of all donors with an equal gender ratio between responders and non-responders. No significant sex x time difference was observed for ACTH responses, probably due to the modest sample size in our study. However, male responders showed significantly larger ACTH increases compared to female responders in line with an enhanced hypothalamic drive in men and sex differences in adrenal cortex sensitivity (Foley & Kirschbaum; Kirschbaum et al, 1999; Veldhuis et al, 2009). As expected, no significant sex x time differences were observed for cortisol in line with Kirschbaum et al. who reported comparable free cortisol stress responses between men and women in the luteal phase of the menstrual cycle (Kirschbaum et al, 1992). However when the absolute increase in cortisol levels were compared significant differences with approximately three times greater increases in male responders were detected. About half of the participants, with no gender difference,, showed a significant the transcriptional activity of the GC-GR complex, subjects with an ACTH or a cortisol response (anticipatory, stress or meal-induced) were compared with

the subjects who did not show these responses. The latter were an ideal internal control since they have undergone the same treatment without HPA axis activation.

The generation of GR-target gene kinetic profiles, revealed complex pulsatile patterns of expression. Our results are in line with recent studies reporting the pulsatile expression of number of genes in both cell culture and adrenalectomized rats (Conway-Campbell et al; Morsink et al, 2006; Stavreva et al, 2009). After in vitro treatment of rat hippocampal slices with $1x10^{-7}$ M corticosterone, Morsink et al. reported several similar waves of gene expression throughout time (Morsink et al, 2006). In our study the stress induced cortisol peak was followed by a distinct gene expression peak for all genes investigated. However, the TSST responders who also showed anticipatory and/or meal related peaks showed complex gene expression trajectories with waves of gene expression, complicating the modeling of the corresponding hormonal and gene expression peaks and the definition of the temporal kinetic response of the individual genes. Only 40 % of all donors showed either a distinct single anticipatory or stress induced cortisol peak that was correlated with a subsequent gene expression peak. In these donors, *GILZ* was upregulated on average 34.2 min earlier than *FKBP5* confirming previous observations where *GILZ* was shown to be the more rapidly induced gene (Rogerson et al, 2004; Soundararajan et al, 2005).

The moderate changes in gene expression that were found in the current study are in agreement with previous reports of corticosteroid-responsive genes in the hippocampus, showing fold changes of less than two for the majority of genes (Datson et al, 2001; Morsink et al, 2006; Neumaier et al, 2000). Possible explanation for these moderate fold changes might be the relatively low cortisol concentrations in human sera detected after the moderate psychosocial stress applied.

FKBP5 was more strongly induced with on average two times higher amplitude than *GILZ* peaks. This differential gene expression response may be due to differences in the

number, affinity and location of the GREs in the *FKBP5* promoter or to the different cortisol levels. This concords with our previous report of *FKBP5* as the strongest differentially expressed protein after GC exposure. The *FKBP5* promoter contained the highest number of strict GREs, among the 28-cortisol modulated proteins in THP-1 monocytes (Billing et al, 2007). Cortisol levels might also play role, as significant positive correlation was found between the amplitudes of the corresponding cortisol and *FKBP5* peaks. Although the statistical significance was borderline, an overall higher *FKBP5* gene expression was observed in males, concording with the greater hormonal responses observed in this group. GREs affinity is another factor possibly influencing the differential gene response. Recently it was found that GR can respond to different levels of corticosteroids in a gene-specific manner, with some genes (*Per1*) activated at much lower dosage of GCs. It has been speculated that the GREs affinities rather than their numbers or arrangements are responsible for the different gene response.

A mixed effect regression model allowed us to investigate the possible predictors of gene expression time trends and confirmed that anticipation responses are also predictors of the gene expression trajectories. The model identified an overall decrease over time for both *GILZ* and *FKBP5* for all donors, from the end of the anticipation period to the last measure 135 min later. Low anticipators showed more rapid decay in *GILZ* and *FKBP5* expression levels, whilst there was a sustained gene expression in the high anticipators. Correspondingly, the low TSST responders also showed a more rapid decrease compared to the high stress responders. These results suggest, that the subsequent stress induced cortisol peak did not induce a peak in expression, but slowed down the natural decrease in mRNA levels over the afternoon. As *GILZ* and *FKBP5* are well known GR target genes these effects were somewhat unexpected. *FKBP5* was previously identified as a member of the clock gene family and was shown to follow the HPA axis circadian rhythm with

rapid up- and down-regulation (Oishi et al, 2003). Strikingly, a rapid decay was observed in *FKBP5* levels in donors that did not have any HPA axis activation during the afternoon hours (1400-1800 h) when the TSST took place, probably due to the low GC levels in this time period (Weitzman et al, 1971). This study did not identify *GILZ* as a circadian clock-controlled gene, but a circadian rhythmicity is expected as *GILZ* is also directly regulated by the HPA axis. Therefore most probably the decreasing *FKBP5* and *GILZ* levels are related to the low cortisol levels during the afternoon hours when the TSST took place, masking their expected induction after anticipatory or stress induced cortisol raise.

The anticipation episode found in our study is in accordance with several studies that have shown that anticipation (negative expectancies) may reliably induce physiological responses such as heart rate (Fredrickson et al, 2000); cortisol (Kirschbaum et al, 1992) and psychological stress response by eliciting negative feelings (Feldman et al, 2004). This anticipatory episode had the same magnitude as the stress induced cortisol response and our model suggesed that gene response observed post-TSST will be biased by this anticipation. According to the pulsatility model of Walker et al. (Walker et al, 2010) after a secretory pulse, the HPA axis is in a period of hyporeactivity and the next pulse can only be triggered after a period of 60-70 min. Taking into account the time interval between the anticipatory episode (-30, -15 min) and the time for the expected stress response (+10, +20 min), we could explain the lack of stress response in most of the anticipators and in the anticipators who also exhibit the meal induced peak. This does, however, raise the possibility of using such meal related and anticipatory peaks in future experiments as a method of accurately inducing a cortisol pulse at a specified time before a laboratory stressor.

The GC pulsatile gene expression within the GR system has been shown after pulsatile hormone stimulation in both cultured cells and animal models (Conway-Campbell et al;

Stavreva et al, 2009). Here, we showed that this is a common phenomenon, occuring also when the HPA axis is challenged by an ecologically valid psychosocial stress paradigm in humans. The gene pulsing in the GR system was suggested as essential for correct transcriptional programming. Therefore, stress-induced GC pulses would lead to significant alteration of the transcriptional program set by ultradian hormonal release, resulting in dramatically altered DNA accumulation profiles. It must be taken into account that the onset of a stressor in relation to the phase of an ultradian pulse can determine the physiological response to stress. It has been shown that rats responded with rising levels of corticosterone only when the stress coincided with an ascending phase of an ultradian pulse, whilst stress during a falling phase, did not result in a significant corticosterone response (Lightman et al, 2008). Therefore, stress should significantly alter the transcriptional program only if it coincides with the ascending phase of an ultradian pulse.

Although, the absence of a control group of non-stressed donors, may appear to be a limitation of our study it was in fact a carefully evaluated alternative. The randomized selection of donors who would serve as a control non-stressed group would still exhibit at least the anticipatory hormonal and gene expression peaks. The use of non-responders allowed us to control for the anticipatory response by using donors with no anticipatory cortisol rise. Similarly, the stress and meal responses were compared with donors who showed neither ACTH nor cortisol stress or meal response, ensuring in this way the reliability of the control groups. Descriptively gender differences in hormonal and gene response were observed, but the results were not significant possibly due to the modest sample size. Based on our results a number of recommendations for future studies on the kinetics of stress induced gene response could be made. In order to be able to decipher the gene trajectories induced only by stress cortisol levels, it is necessary to include a

significantly larger delay between the arrival time and the TSST to allow the anticipation-induced gene expression to return to baseline. The meal confounding peak found on hormonal and reflected on gene expression level brings another layer of complexity and light meals post-TSST should be avoided in future. For more precise temporal data on the kinetics of stress gene response, deconvolution analysis and concordance of the resolved hormonal and gene expression peaks could be applied. For this purpose, an optimization of the sampling intensity at regular intervals of every 5 or 10 min must be applied.

In summary, by using a well-established psychosocial stress protocol we aimed to investigate the effects of psychosocial stress on the magnitude and kinetics of gene response in vivo, focusing on a small set of primary GR target genes in a cohort of healthy males and female donors. We have found a dynamic pattern of gene expression with several distinct gene expression pulses related to anticipation, stress and meal presentation. Differences in the magnitude of gene response with higher overall *FKBP5* response compared to *GILZ* and a trend for higher *FKBP5* response in males compared to females were observed. The anticipation of stressful stimuli and not only the TSST response itself was found to be a significant predictor of the gene response. Therefore further adaptation of the current TSST protocol for future research on the complex stress induced gene response in patient populations or healthy individuals is necessary.

Chapter 5

General Discussion

5.1 General Discussion

Human physiology is highly integrated with the rotation of the Earth. Cellular and systemic physiologies are synchronized with circadian cycles. Circadian coordination appears crucial for proper physicial and mental functions, while many disease states are marked by disruption of circadian endocrine rhythms (Mongrain & Cermakian, 2009). The HPA axis is one of the body's major neuroendocrine systems and pronounced ultradian and circadian rhythms of its end product cortisol were already demonstrated several decades ago (Veldhuis et al, 1989b; Weitzman et al, 1971). It is known that the hypothalamic SCN within the CLOCK system coordinates circadian events at the tissue and cellular level, partly via GCs. These hormones, secreted by the adrenals have been proven to be crucial for a plethora of body functions including cell proliferation, apoptosis, immune cell trafficking and cytotoxicity. Disturbances in their characteristic temporal secretory patterns have often been described for stress-related pathologies. However, the significance of GCs' secretory patterns for physiology, stress responsiveness and nuclear receptor signaling remains largely unexplored. This thesis investigated parameters related to the HPA axis and the immune system in cohorts of healthy subjects. Its overall objective was therefore to dissect the underlying structure of glucocorticoid pulsatility and to develop tools to investigate physiological effects of this pulsatility on immune cell trafficking and the responsiveness of the neuroendocrine system and GC target genes to stress.

The physiological and clinical importance of the circadian and the ultradian secretory rhythms is well recognized for hormones such as GH and the reproductive hormones. GCs are also secreted in pulsatile manner in all species studied (Jasper & Engeland, 1991; Loudon et al, 1994; Sarnyai et al, 1995) and changes in pulsatility pattern and/or absolute cortisol levels are reported in a number of neurological and immune diseases (Deuschle et

al, 1997; Hartmann et al, 1997; Windle et al, 2001). It is not clear if these altered pulsatile patterns are the cause or the consequence of the disease. Therefore, knowledge about the cortisol secretory pulses may help to elucidate the mechanisms underlying some of these abnormalities. Cortisol concentration profiles may be helpful for evaluating hormonal rhythmicity, but they do not provide information about the underlying pulsatility. We suggest that secretory rather than the concentration profiles are important for conditions with impaired cortisol rhythm. Moreover, cortisol pulsatile patterns have been studied so far in blood samples (Henley et al, 2009; Kerrigan et al, 1993; Metzger et al, 1993; Veldhuis et al, 1989b). Venipuncture has been considered a drawback of blood sampling because of its impact on cortisol levels and pulsatility, due to anticipatory stress or the sampling procedure itself (Mantagos et al, 1991; Stahl & Dorner, 1982). An important prerequisite of any investigation of the HPA axis requires a stress-free sampling method, especially in psychobiological research. Saliva has proved to be a popular sample for psychobiology, sports medicine, pharmacology and pediatric studies (Kirschbaum & Hellhammer, 2000). In diagnostics, salivary cortisol is used in dynamic testing of HPA axis activity at different levels and in the diagnosis of Cushing's syndrome (Groschl, 2008). An important advantage of saliva is that it represents the free (i.e the active) hormone (Vining et al, 1983), whilst plasma cortisol is largely protein-bound and usually measured as the sum of the bound and free fractions. These considerations let to our efforts to investigate saliva as an alternative sample for studing pulsatile cortisol secretion during the waking hours (Chapter 2). We analysed ultradian salivary and plasma cortisol profiles between 0800 h and 1600 h of 18 healthy male volunteers. A multiparameter deconvolution technique was used to generate a statistically significant models of cortisol secretion and elimination in both compartments. Each model consisted of estimates of the number, amplitude, duration and frequency of secretory bursts as well as the hormonal

half-life in a subject specific manner. The lower IPI and higher peak frequency in our study compared to previous literature estimates could be due to differences between the experimental designs of our and previous studies. Our 8 h observation period falls in the time range of the two most active HPA axis secretory phases, whilst previous reports studied the 24 h period, which includes phases with lower HPA axis secretory activity and lower peak amplitude. Additionally, all previous reports on cortisol pulsatility have applied longer sampling intervals and this is reflected in the quality of their pulsatile models leading to longer IPI. Importantly, the higher sensitivity, reliability and statistical validity of the algorithm used in our study are certainly reflected in an enhanced sensitivity to detect peaks. Irrespective of the minor differences from previous deconvolution studies (Henley et al, 2009; Metzger et al, 1993; Veldhuis et al, 1989b), the plasma and saliva cortisol patterns showed a remarkable agreement between the number of plasma and saliva peaks (7.8±1.5 events/8 h, 7.0±1.4 events/8 h), and between IPI (59.6±10.5 min vs. 61.00±11.5 min). The lack of statistical difference between the major saliva and plasma estimates demonstrated that the ultradian cortisol pulsatility is reflected also in saliva. The correlative validity of salivary cortisol as a surrogate of free plasma cortisol is widely accepted. However, a weaker correlation has been reported when salivary cortisol was compared with total plasma cortisol levels, because of the CBG levels, which are largely saturated in the morning hours due to the high cortisol levels. However, when introducing a 15-min lag the cross-correlation between salivary cortisol and total plasma cortisol levels significantly improved, corresponding with the expected time delay between plasma and saliva cortisol peaks. Our study showed that salivary cortisol could be also considered as a surrogate of total plasma cortisol, as minor and insignificant differences have been detected between the pulse estimates in both media. Additionally, we are the first that apply Monte Carlo simulations to determine the degree

of non-random concordance between peak positions of a single hormone secreted in different body compartments. Concordance analysis revealed on average 84 % temporal concordance between plasma and saliva peaks in all donors with mean of 1.3±0.8 unmatched plasma peaks in saliva.We hypothesized that the minor difference between the number of peaks detected in plasma and saliva could be explained by the levels of CBG and its binding capacity (Lewis et al, 2005). Coolens et al. showed that in situations where CBG levels are altered, total cortisol levels may not adequately represent the free cortisol fraction (Coolens et al, 1987). Our hypothesis was confirmed by concording only the morning cortisol peaks up to 1100 h in plasma and saliva, which resulted in an increase in concordance by 6 % (90 %±13.6 % vs. 84.0 %±10.1 %). Although the differences between the deconvoluted parameters of plasma and saliva were minor and statistically insignificant, our results suggest that saliva would be best used for monitoring cortisol pulsatility during the morning hours. Morning cortisol levels are accepted to be a useful indicator of the adrenocortical activity in basic and clinical research. The better morning concordance between pulses in both fluids suggests that cortisol pulsatility in the morning has to be evaluated on the secretory profiles rather than the concentration profiles. The concordance of individual peaks allowed us to estimate indirectly the times for cortisol diffusion from plasma to saliva. Large inter-individual variability of cortisol diffusion rates into the saliva was observed with an average rate for cortisol diffusion to saliva of 19.4 ±7.4 min.

It must be noted that we selected our study design after careful evaluation of different options. It reflects as close as possible the daily morning routine of the participants and avoids stress-induced alterations of cortisol pulsatility, which is of particular importance in psychobiological research where disturbances of the HPA axis must be kept minimal. For this purpose, the time of awakening was not standardized, but rather synchronized

with donors' daily routine and schedule. We focused on an 8 h observation period as having the subjects spend the night in a clinical/sleep research setting would have provided more disturbances of the HPA axis, and of the normal cortisol rhythm. As a result of the accepted delay in blood sampling, CAR was not directly measured in plasma and this early sampling time was not included in our saliva/plasma deconvolution comparison. As a result, our study design had several limitations, which have important consequences for the design of future experiments. We could not perform a formal comparison of plasma and saliva CAR as plasma samples were not collected immediately after awakening. Follow-up studies should also take various ways of perturbing the HPA axis into account, as well as testing our approach over the complete 24 h period, which will allow also formal comparison of CAR in plasma and saliva. Another limitation is that only healthy, young male subjects were included in our study, and our results would require comparison with a cohort of females as well as elderly subjects.

After the successful set-up of a technique that is able to provide reliable information on the individual cortisol secretory pulses, we moved forward to investigate how they affect the kinetics of cell redistribution within the immune system temporally. Increasing evidence exist that wide number of immune system parameters (enumerative (Kawate et al, 1981; Young et al, 1995) and functional (Fernandes et al, 1976; Halberg et al, 1974; Knapp et al, 1979)) exhibit fluctuations regulated by hormonal circadian rhythms. Experimental data indicate that circadian information reaches immune tissues mainly through diurnal patterns of autonomic and endocrine rhythms. There were conflicting results regarding the effects of GCs and catecholamines on circulating immune cells. It is known that the GC rhythm regulates rhythms of peripheral cellular physiology including cell proliferation, apoptosis, secretion of hormones and cytokines, immune cell trafficking and cytotoxicity (Dickmeis, 2009; Son et al, 2008). Other reports suggest that the changes

in lymphocyte migration are under regulation of the autonomic nervous system, particularly the catecholamines (Pedersen & Hoffman-Goetz, 2000; Schedlowski et al, 1996; Suzuki et al, 1997). Recently, Dimitrov et al. suggested differential regulation of the circadian variations of immune cells via cortisol and catecholamines rhythms depending on the cell type and level of maturation (Dimitrov et al, 2009). A negative correlation was shown between absolute peak T and B cell counts and plasma cortisol throughout the 24 h period, suggesting a mechanistic link (Kawate et al, 1981; Ritchie et al, 1983). However, reports are conflicting with respect to the circadian rhythms for B and NK cells and their correlation with the cortisol rhythm (Kawate et al, 1981; Kronfol et al, 1997; Miyawaki et al, 1984; Ritchie et al, 1983). Information regarding the diurnal redistribution of the immune cells, their subsets and their temporal correlations with adrenal hormones such as cortisol are limited because of the long intervals of 3 to 4 h between samples and that lagged cross-correlations were not performed in earlier studies (Kronfol et al, 1997; Miyawaki et al, 1984; Suzuki et al, 1997). It is of particular importance that the different time courses and dynamics of the neuroendocrine and the immune system are taken into account in the experimental study design. Therefore, time-lagged cross-correlations need to be tested if one wants to draw valid conclusions about the neuroendocrine-immune covariance. In Chapter 3 we addressed the limitations in the experimental design of previous studies and conducted a study that investigates the diurnal redistribution of the main effectors of the adaptive immunity-T and B cells as well as these of the innate immunity-NK cells and their subsets of KIR+ and CD8+ cells. Our sampling frequency included previously ignored time points immediately after the CAR. We observed bimodal responses for T cells, as well as for NK cells, that seem at least temporally linked. Our results suggest a first phase with a delay of about 75 min until full mobilization of T cells and until NK cell depletion, and a second phase between 165-285

min post CAR with opposite diurnal profiles of T and total NK cells in healthy subjects. It is not clear between which organ compartments the observed oscillations of the lymphocytes take place. It has been suggested that the increase in cell counts may correspond to their mobilization from lymphoid organs (Dhabar et al, 2012). Nadirs of each subpopulation would correspond to their coordinated extravasation into target organs or back to their source compartments. An attractive interpretation of our results would be that this tidal movement of immune cells may be a reflection of a circadian immune surveillance at peripheral tissues by waves of innate immune cells alternating with waves of cells of the induced immune system. Our results suggest that these movements are orchestrated by GC and the HPA axis. The sensitivity of adhesion molecules to GC (reviewed in Franchimont et al 2004) could explain the coordinated waves of lymphocyte migration to sites of potential tissue damage and inflammation. Thus, we may speculate that immune surveillance is not the result of a haphazard adventure of every cell is on its own but rather relies on diurnal or tidal waves of attack taking full advantage of the ability of immune cells to communicate and collaborate with each other. While the cross correlations observed in our study may suggest an orchestration of lymphocyte trafficking by cortisol, other rhythmically secreted hormones, e.g. catecholamines or melatonin, may also play a role in immune cell redistribution. For instance, melatonin has a number of effects, at least in-vitro, on immune cell functions such as leukocyte proliferation, cytokine production and NK cell activation (reviewed in Radogna et al 2010 and Carrillo-Vico et al 2005). Seasonal changes in the circadian melatonin rhythm have been associated with changes in immune functions (Srinivasan et al 2005), but the circadian melatonin rhythm has so far not been associated with circadian lymphocyte redistribution. Irrespective of the mechanisms, the concept of immune tides may be important for a better understanding of the immune system in health and disease. In health, alternating

waves of cells of the innate and the induced immune system would ensure a constitutive surveillance of peripheral sites of potential tissue damage or inflammation below local activation thresholds. The absence of this routine surveillance e.g. because of unresponsive adhesion molecules could lead to disease. For instance, in fibromyalgia the expected GC-induced increase in adhesion molecules such as CD11b (a β2 integrin) and CD49d (an α4 integrin) expression was abrogated (Macedo et al 2007), suggesting that impaired responsiveness of adhesion molecules may temper with "immune tides" and undermine co-operative effects in immune surveillance. The orchestration of circadian immune surveillance by cortisol also ensures an invigorated surveillance after stress that is inherently associated with a higher risk of injuries, tissue damage and inflammation. Stress-induced cortisol release would trigger a tidal wave of innate immune cells as a first line of defence followed by cells of the acquired/induced immune system. These diurnal tides should be taken into account in the design of clinical studies that evaluate the effect of immune modulating compounds (e.g. times of sampling). Knowledge about the redistribution of lymphocyte populations may also help to improve radiation strategies to protect immune cells. In the case of malignancies of the immune system, chemotherapy may be more effective during the "high tide". However, it remains unclear whether the oscillating recruitment to the circulation is a mere quantitative phenomenon or whether there are also qualitative difference in immune cell activity.

It is generally assumed that GCs are secreted either tonically, with variation only related to the circadian cycle, or as a phasic response to an acute stressor (Lightman & Conway-Campbell, 2010). Our further aim was to test the effects of induced endogenous cortisol pulses e.g via TSST on the kinetics of expression of several stress associated genes.

It has been shown that the neuroendocrine response to stress depends on circulating GCs in both a phase and amplitude dependent manner (Windle et al, 1998a). However, less is

known about the subsequent gene expression response to an acute stressor. A few studies have focused on the complete transcriptome or measurements of single genes to study the stress-induced transcriptional changes in vivo. However, they did not attempt to study gene expression alterations using more than one single measurement time points, thus identifying only potential stress-responsive genes, or potential biomarkers of stress exposure (Miller et al, 2008; Morita et al, 2005; Murata et al, 2005; Oishi et al, 2003; Pajer et al, 2012). Considering the complex chronology of biological processes that occurs due to an exposure to accute stressor, repeated measurements of gene expression is crucial. A gene pulsing pattern has been shown for a number of GR target genes (e.*g GILZ, PER1)* after an in vitro GCs stimulation both in cultured cells and in animal models (Stavreva et al, 2009), a phenomenon described as essential for correct transcriptional programming. The ultradian cortisol rhythm has been also shown to induce pulsatile expression of *GILZ* and *FKBP5* in humans (manuscript in prep). However, studies on the kinetics of gene expression after inducing endogenous cortisol release in humans are absent. Thus, we applied a standardized stress protocol (TSST) on a mixed cohort of male and female subjects to profile gene expression on a set of stress-associated genes at multiple time points before, during and after stress. Gene expression was assessed for *FKBP5* and *GILZ* known as cortisol-modulated early GR target genes. *FKBP5* is a co-chaperone of the functional GR receptor and acts as its inhibitor. It has been linked to GC resistance and negative feedback on the GC signaling (Reynolds et al, 1999). Recently, MDD and impaired recovery of the stress response have been associated with elevated *FKBP5* expression levels (Binder et al, 2004; Ising et al, 2008), whilst decreased *FKBP5* levels were associated with posttraumatic stress disorder (Yehuda et al, 2009). *GILZ* is another well known GR target gene that appears to play a key role in the anti-inflammatory and immunosuppressive effects of GCs reactions (Berrebi et al, 2003).

Some of the immune symptoms observed in FM (Macedo et al, 2008) and also the development of delayed-type hypersensitivity reactions (Berrebi et al, 2003) were linked to decreased *GILZ* expression.

Generating of GR target gene kinetic profiles revealed a complex pulsatile pattern of expression. Our results are in line with recent studies reporting the pulsatile expression of a number of genes under regulation of GCs in both cell culture and adrenalectomized rats (Stavreva et al, 2009). In our study, the stress-induced cortisol peak was followed by a distinct gene expression peak for all genes investigated. However, the TSST responders who also showed anticipatory and/or meal-related peaks showed more complex gene expression trajectories with waves of gene expression, complicating the determination of the corresponding individual hormonal and gene expression peaks and the definition of the temporal kinetic response of the individual genes.

Only eight of total of 27 donors showed either a distinct single anticipatory or stress-induced cortisol peak that was correlated with a subsequent gene expression peak. In these donors, *FKBP5* was upregulated on average 95.6 ±52.5 min, whilst for *GILZ* this period was 61.3±39.2 min after peak cortisol levels confirming previous observations where *GILZ* was shown to be the more rapidly induced gene.

A differential transcriptional response was observed with two times higher amplitudes of the *FKBP5* gene expression peaks. This could be explained by the higher number of GREs found in the *FKBP5* promoter (Billing et al, 2007). Other factors that may contribute to the differential transcriptional response are also the affinity and location of the gene's GREs as well as the cortisol levels. A positive correlation was found between the amplitudes of the corresponding cortisol and *FKBP5* peaks suggesting a mechanistic link. Additionally, an overall higher *FKBP5* gene expression was observed in males that may be due to the greater hormonal responses observed in this group. Recently, it was

found that GR can respond to different levels of corticosteroids in a gene-specific manner, with some genes (*PER1)* activated at much lower dosage of GC and speculate that the GREs affinities rather than their numbers or arrangements are responsible for the different gene responses.

Here, we showed that gene pulsing is a common phenomenon, occuring also when the HPA axis is perturbed by an acute stressor. The GR target gene pulsing was suggested as essential for correct transcriptional programming (Stavreva et al, 2009) and stress-induced GC pulses could lead to significant alterations of the DNA accumulation profiles set by ultradian hormonal release. It has been shown that rats responded with rising levels of corticosterone only when the stress coincided with an ascending phase of an ultradian pulse (Windle et al, 1998a). Therefore, alterations of the transcriptional program would occur only if the stress-induced cortisol pulse coincides with the ascending phase an ultradian pulse.

A mixed effect regression model focusing on the gene expression levels up to 120 min post TSST allowed us to investigate the possible predictors of gene expression time trends and confirmed that anticipation responses are also predictors of the gene expression trajectories. Therefore, we recommend the inclusion of a larger delay between arrival time and the TSST to allow the anticipation-induced gene expression to return to baseline. An unexpected overall decrease in GILZ and FKBP5 levels were detected over time. Stress induced cortisol rise showed stabilizing rather than increasing effect on gene expression levels. High anticipators and responders showed significantly less pronounced decreases in GILZ and FKBP5 levels compared to the greater decrease in the group of low anticipators and responders respectively. This stabilizing rather than increasing effect on gene expression levels could be possibly explained with the circadian rhythm observed for some clock genes such as *FKBP5*. We can speculate that the onset of the stressor

coincided with the circadian decay observed in the afternoon hours in FKBP5 levels (Oishi et al, 2003), thus masking its expected induction. However, no data about the circadian profile in GILZ gene expression is available to confirm our speculation.

The lack of stress response in the anticipators group could be explained with the period of hyporeactivity of the HPA axis post secretory phase (Walker et al, 2010). The anticipatory episode occurred -30, -15 min before stress, inhibiting the HPA axis for a period of 60-70 min, resulting in a lack of the expected stress response +10, +20 min post stress. This does however raise the possibility of using such meal-related and anticipatory peaks in future experiments as a method of accurately inducing a cortisol pulse at a specified time before a laboratory stressor.

In summary, the results presented in the current thesis revealed new aspects of GC endocrinology. The successful set up of the deconvolution modeling as a technique for investigation of the pulsatile secretion underlying the ultradian cortisol rhythm allowed us to further investigate the role of single endogenous cortisol pulses in the redistributional changes within the immune system. Moreover, we studied the role of induced endogenous cortisol pulses on the kinetics of expression of a set of primary GR target genes. The development of these three tools being able to induce, dissect and analyse the role of single pulses in different biological phenomena would allow us to induce and investigate the role of single endogenous as well as exogenous cortisol pulses for health and disease in future.

5.2 Future perspectives

The major findings presented in this thesis were not described previously and provide a new insight into the kinetics of GR-GC actions. So far, deconvolution of cortisol concentration profiles has been performed only in plasma samples. Moreover, the characterization of the altered cortisol pulsatility in disease has been done on concentration rather than secretion profiles. Thus, the deconvoluton of salivary cortisol concentration profiles would avoid the HPA axis activation as a result of the stressful venipuncture procedure in future studies. Additionally, it will provide more precise information about the cortisol pulse characteristics and therefore bears the potential of a valuable tool for studying the altered cortisol pulsatility observed in some psychiatric and neurological diseases. The deconvolution technique could be also used to study the pulsatile characteristics of other rhythmically secreted hormones that are passively transported to saliva. However, it should be kept in mind that the main strength of our experimental design was that we can resolve the underlying cortisol pulsatile events under baseline conditions. Further studies testing our approach under different conditions of perturbed HPA axis (e.g Cold Pressor Test, TSST) would demonstrate that it is equally effective. In future studies, the pulsatility patterns in plasma and saliva cortisol could be compared in female subjects taking into account the differential effect of CBG levels on the free cortisol fraction in plasma. A study design with subjects spending 24-h in a medical center prior the experiment would allow the analysis of the major cortisol peak-CAR in both media.

The interactions between the immune and HPA axis systems still remain largely unexplored. The bimodal response of both the adaptive and innate immune players and their significant correlations with the cortisol diurnal rhythm reported by us do not prove a mechanistic link between endogenous cortisol levels and T and NK cells counts.

Therefore, further studies investigating the effects of exogenous GCs and catecholamines on both enumerative and functional immune measures in adrenalectomized animals could help in understanding the individual contribution of both systems SAM system and HPA axis in the regulation of the immune cell rhythms. A different experimental design could be applied in humans with infusions of either GCs or catecholamines initiated at the time of the circadian nadir of these hormones. Measuring the expression of cell adhesion molecules associated with trafficking of immune cells in and out of the blood as well as functionality studies that monitor the immune response throughout different time of the day would also assist the understanding of the mechanism underlying this cell redistribution as well as will give new insights into the complex networking between the HPA axis and the immune system. The medical application of the observed tidal waves of immune cells redistribution extends to diagnostic measures, as well as treatment. The deconvolution approach applied in our first study would help us further investigate the role of the secretory cortisol pulses in the immune cells redistribution.

The GC-GR gene expression pulsing has been shown after pulsatile hormone stimulation in both cultured cells and animal models. Our translational approach in humans provided similar data after psychosocial stress. Future studies to investigate the GC-GR gene expression profiles in baseline conditions in humans need to be performed. Additionally, microarray assays to investigate the kinetics of psychological stress-associated genes at multiple time points bear the potential to detect pathological responses in stress-related disorders. Based on our findings, a number of recommendations for future studies on the kinetics of stress-induced gene response could be made. In order to avoid anticipatory cortisol peaks due to the stress of venipuncture, saliva samples could be the stress-free alternative for monitoring the hormonal and well as the gene expression stress response. In studies where venipuncture is unavoidable a significantly larger delay between the

arrival time and the TSST is necessary to be included to allow the anticipation induced gene expression to return to baseline. For more precise temporal data on the kinetics of the gene response induced by stress induced GC levels, optimized sampling intensity at 5 or 10 min intervals combined with deconvolution and concordance analysis of the resolved hormonal and gene expression peaks could be applied. Some of these directions pointed out above are already intensively studied at our institute.

In conclusion these data, combined with our observations in the first and second study, will now allow us to induce and successfully analyse cortisol pulses and to investigate more precisely their physiological and pathological effects.

References

Aardal-Eriksson E, Karlberg BE, Holm AC (1998) Salivary cortisol--an alternative to serum cortisol determinations in dynamic function tests. *Clin Chem Lab Med* **36:** 215-222

Abo T, Kawate T, Itoh K, Kumagai K (1981) Studies on the bioperiodicity of the immune response. I. Circadian rhythms of human T, B, and K cell traffic in the peripheral blood. *J Immunol* **126:** 1360-1363

Akaike H (1974) A new look at the statistical model identification. *IEEE Transactions on Automatic Control* **19:** 716-723

Alila-Johansson A, Eriksson L, Soveri T, Laakso ML (2003) Serum cortisol levels in goats exhibit seasonal but not daily rhythmicity. *Chronobiol Int* **20:** 65-79

Almeida G, Pelletier J (1988) Abolition of seasonal testis changes in the Ile-de-France ram by short light cycles: relationship to luteinizing hormone and testosterone release. *Theriogenology* **29:** 681-691

Angeli A (1992) Circadian rhythms of human NK cell activity. *Chronobiologia* **19:** 195-198

Arjona A, Boyadjieva N, Sarkar DK (2004) Circadian rhythms of granzyme B, perforin, IFN-gamma, and NK cell cytolytic activity in the spleen: effects of chronic ethanol. *J Immunol* **172:** 2811-2817

Atkinson HC, Wood SA, Kershaw YM, Bate E, Lightman SL (2006) Diurnal variation in the responsiveness of the hypothalamic-pituitary-adrenal axis of the male rat to noise stress. *Journal of neuroendocrinology* **18:** 526-533

Aziz NA, Pijl H, Frolich M, van der Graaf AW, Roelfsema F, Roos RA (2009) Increased hypothalamic-pituitary-adrenal axis activity in Huntington's disease. *J Clin Endocrinol Metab* **94:** 1223-1228

Backstrom CT, McNeilly AS, Leask RM, Baird DT (1982) Pulsatile secretion of LH, FSH, prolactin, oestradiol and progesterone during the human menstrual cycle. *Clin Endocrinol (Oxf)* **17:** 29-42

Barrett TJ, Vig E, Vedeckis WV (1996) Coordinate regulation of glucocorticoid receptor and c-jun gene expression is cell type-specific and exhibits differential hormonal sensitivity for down- and up-regulation. *Biochemistry* **35:** 9746-9753

Belchetz PE, Plant TM, Nakai Y, Keogh EJ, Knobil E (1978) Hypophysial responses to continuous and intermittent delivery of hypopthalamic gonadotropin-releasing hormone. *Science* **202:** 631-633

Berrebi D, Bruscoli S, Cohen N, Foussat A, Migliorati G, Bouchet-Delbos L, Maillot MC, Portier A, Couderc J, Galanaud P, Peuchmaur M, Riccardi C, Emilie D (2003) Synthesis of glucocorticoid-induced leucine zipper (GILZ) by macrophages: an anti-

inflammatory and immunosuppressive mechanism shared by glucocorticoids and IL-10. *Blood* **101:** 729-738

Billing AM, Fack F, Renaut J, Olinger CM, Schote AB, Turner JD, Muller CP (2007) Proteomic analysis of the cortisol-mediated stress response in THP-1 monocytes using DIGE technology. *J Mass Spectrom* **42:** 1433-1444

Billing AM, Revets D, Hoffmann C, Turner JD, Vernocchi S, Muller CP Proteomic profiling of rapid non-genomic and concomitant genomic effects of acute restraint stress on rat thymocytes. *J Proteomics* **75:** 2064-2079

Binder EB, Salyakina D, Lichtner P, Wochnik GM, Ising M, Putz B, Papiol S, Seaman S, Lucae S, Kohli MA, Nickel T, Kunzel HE, Fuchs B, Majer M, Pfennig A, Kern N, Brunner J, Modell S, Baghai T, Deiml T, Zill P, Bondy B, Rupprecht R, Messer T,

Kohnlein O, Dabitz H, Bruckl T, Muller N, Pfister H, Lieb R, Mueller JC, Lohmussaar E, Strom TM, Bettecken T, Meitinger T, Uhr M, Rein T, Holsboer F, Muller-Myhsok B (2004) Polymorphisms in FKBP5 are associated with increased recurrence of depressive episodes and rapid response to antidepressant treatment. *Nat Genet* **36:** 1319-1325

Boldizsar F, Talaber G, Szabo M, Bartis D, Palinkas L, Nemeth P, Berki T (2010) Emerging pathways of non-genomic glucocorticoid (GC) signalling in T cells. *Immunobiology* **215:** 521-526

Boyar RM, Witkin M, Carruth A, Ramsey J (1979) Circadian cortisol secretory rhythms in Cushing's disease. *J Clin Endocrinol Metab* **48:** 760-765

Breslin MB, Geng CD, Vedeckis WV (2001) Multiple promoters exist in the human GR gene, one of which is activated by glucocorticoids. *Mol Endocrinol* **15:** 1381-1395

Breslin MB, Vedeckis WV (1998) The human glucocorticoid receptor promoter upstream sequences contain binding sites for the ubiquitous transcription factor, Yin Yang 1. *The Journal of steroid biochemistry and molecular biology* **67:** 369-381

Buttgereit F, Scheffold A (2002) Rapid glucocorticoid effects on immune cells. *Steroids* **67:** 529-534

Carter-Snell C, Hegadoren K (2003) Stress disorders and gender: implications for theory and research. *Can J Nurs Res* **35:** 34-55

Chrousos GP (2009) Stress and disorders of the stress system. *Nat Rev Endocrinol* **5:** 374-381

Chrousos GP, Kino T (2007) Glucocorticoid action networks and complex psychiatric and/or somatic disorders. *Stress* **10:** 213-219

Clifton DK, Aksel S, Bremner WJ, Steiner RA, Soules MR (1988) Statistical evaluation of coincident prolactin and luteinizing hormone pulses during the normal menstrual cycle. *J Clin Endocrinol Metab* **67:** 832-838

Clifton DK, Steiner RA (1983) Cycle detection: a technique for estimating the frequency and amplitude of episodic fluctuations in blood hormone and substrate concentrations. *Endocrinology* **112:** 1057-1064

Clow A, Thorn L, Evans P, Hucklebridge F (2004) The awakening cortisol response: methodological issues and significance. *Stress* **7:** 29-37

Cole SW, Hawkley LC, Arevalo JM, Sung CY, Rose RM, Cacioppo JT (2007) Social regulation of gene expression in human leukocytes. *Genome Biol* **8:** R189

Conway-Campbell BL, McKenna MA, Wiles CC, Atkinson HC, de Kloet ER, Lightman SL (2007) Proteasome-dependent down-regulation of activated nuclear hippocampal glucocorticoid receptors determines dynamic responses to corticosterone. *Endocrinology* **148:** 5470-5477

Conway-Campbell BL, Sarabdjitsingh RA, McKenna MA, Pooley JR, Kershaw YM, Meijer OC, De Kloet ER, Lightman SL Glucocorticoid ultradian rhythmicity directs cyclical gene pulsing of the clock gene period 1 in rat hippocampus. *J Neuroendocrinol* **22:** 1093-1100

Conway-Campbell BL, Sarabdjitsingh RA, McKenna MA, Pooley JR, Kershaw YM, Meijer OC, De Kloet ER, Lightman SL (2010) Glucocorticoid ultradian rhythmicity directs cyclical gene pulsing of the clock gene period 1 in rat hippocampus. *Journal of neuroendocrinology* **22:** 1093-1100

Cook CJ (2001) Measuring of extracellular cortisol and corticotropin-releasing hormone in the amygdala using immunosensor coupled microdialysis. *J Neurosci Methods* **110:** 95-101

Cook N, Harris B, Walker R, Hailwood R, Jones E, Johns S, Riad-Fahmy D (1986) Clinical utility of the dexamethasone suppression test assessed by plasma and salivary cortisol determinations. *Psychiatry Res* **18:** 143-150

Cook TD, Campbell DT (1979) Quasi-experimentation: design & analysis issues for field settings. *Rand McNally, Chicago*

Coolens JL, Van Baelen H, Heyns W (1987) Clinical use of unbound plasma cortisol as calculated from total cortisol and corticosteroid-binding globulin. *J Steroid Biochem* **26:** 197-202

Cooper MA, Fehniger TA, Caligiuri MA (2001) The biology of human natural killer-cell subsets. *Trends Immunol* **22:** 633-640

Croxtall JD, Choudhury Q, Flower RJ (2000) Glucocorticoids act within minutes to inhibit recruitment of signalling factors to activated EGF receptors through a receptor-dependent, transcription-independent mechanism. *Br J Pharmacol* **130:** 289-298

Dallman MF, Pecoraro N, Akana SF, La Fleur SE, Gomez F, Houshyar H, Bell ME, Bhatnagar S, Laugero KD, Manalo S (2003) Chronic stress and obesity: a new view of "comfort food". *Proc Natl Acad Sci U S A* **100:** 11696-11701

Datson NA, van der Perk J, de Kloet ER, Vreugdenhil E (2001) Identification of corticosteroid-responsive genes in rat hippocampus using serial analysis of gene expression. *Eur J Neurosci* **14:** 675-689

de Kloet ER, Joels M, Holsboer F (2005) Stress and the brain: from adaptation to disease. *Nat Rev Neurosci* **6:** 463-475

De Kloet ER, Vreugdenhil E, Oitzl MS, Joels M (1998) Brain corticosteroid receptor balance in health and disease. *Endocr Rev* **19:** 269-301

DeRijk RH, Schaaf M, de Kloet ER (2002) Glucocorticoid receptor variants: clinical implications. *The Journal of steroid biochemistry and molecular biology* **81:** 103-122

Desai HD, Jann MW (2000) Major depression in women: a review of the literature. *J Am Pharm Assoc (Wash)* **40:** 525-537

Deuschle M, Schweiger U, Weber B, Gotthardt U, Korner A, Schmider J, Standhardt H, Lammers CH, Heuser I (1997) Diurnal activity and pulsatility of the hypothalamus-pituitary-adrenal system in male depressed patients and healthy controls. *J Clin Endocrinol Metab* **82:** 234-238

Di S, Malcher-Lopes R, Halmos KC, Tasker JG (2003) Nongenomic glucocorticoid inhibition via endocannabinoid release in the hypothalamus: a fast feedback mechanism. *J Neurosci* **23:** 4850-4857

Dimitrov S, Benedict C, Heutling D, Westermann J, Born J, Lange T (2009) Cortisol and epinephrine control opposing circadian rhythms in T cell subsets. *Blood* **113:** 5134-5143

Dressendorfer RA, Kirschbaum C, Rohde W, Stahl F, Strasburger CJ (1992) Synthesis of a cortisol-biotin conjugate and evaluation as a tracer in an immunoassay for salivary cortisol measurement. *J Steroid Biochem Mol Biol* **43:** 683-692

Droste SK, de Groote L, Atkinson HC, Lightman SL, Reul JM, Linthorst AC (2008) Corticosterone levels in the brain show a distinct ultradian rhythm but a delayed response to forced swim stress. *Endocrinology* **149:** 3244-3253

Eismann EA, Lush E, Sephton SE (2010) Circadian effects in cancer-relevant psychoneuroendocrine and immune pathways. *Psychoneuroendocrinology* **35:** 963-976

Elliott JA (1976) Circadian rhythms and photoperiodic time measurement in mammals. *Fed Proc* **35:** 2339-2346

Engert V, Vogel S, Efanov SI, Duchesne A, Corbo V, Ali N, Pruessner JC (2011) Investigation into the cross-correlation of salivary cortisol and alpha-amylase responses to psychological stress. *Psychoneuroendocrinology* **36:** 1294-1302

Evans SJ, Murray TF, Moore FL (2000) Partial purification and biochemical characterization of a membrane glucocorticoid receptor from an amphibian brain. *The Journal of steroid biochemistry and molecular biology* **72:** 209-221

Evans WS, Farhy LS, Johnson ML (2009) Biomathematical modeling of pulsatile hormone secretion: a historical perspective. *Methods Enzymol* **454:** 345-366

Evans WS, Faria AC, Christiansen E, Ho KY, Weiss J, Rogol AD, Johnson ML, Blizzard RM, Veldhuis JD, Thorner MO (1987) Impact of intensive venous sampling on characterization of pulsatile GH release. *Am J Physiol* **252:** E549-556

Fauci AS (1975) Mechanisms of corticosteroid action on lymphocyte subpopulations. I. Redistribution of circulating T and b lymphocytes to the bone marrow. *Immunology* **28:** 669-680

Fauci AS (1976) Mechanisms of corticosteroid action on lymphocyte subpopulations. II. Differential effects of in vivo hydrocortisone, prednisone and dexamethasone on in vitro expression of lymphocyte function. *Clin Exp Immunol* **24:** 54-62

Fauci AS, Dale DC (1974) The effect of in vivo hydrocortisone on subpopulations of human lymphocytes. *J Clin Invest* **53:** 240-246

Fauci AS, Dale DC (1975) The effect of Hydrocortisone on the kinetics of normal human lymphocytes. *Blood* **46:** 235-243

Federenko I, Wust S, Hellhammer DH, Dechoux R, Kumsta R, Kirschbaum C (2004) Free cortisol awakening responses are influenced by awakening time. *Psychoneuroendocrinology* **29:** 174-184

Feldman PJ, Cohen S, Hamrick N, Lepore SJ (2004) Psychological stress,appraisal, emotion and cardiovascular response in a public speaking task. *Psychol Health* **19:** 358-368

Fernandes G, Halberg F, Yunis EJ, Good RA (1976) Circadian rhythmic plaque-forming cell response of spleens from mice immunized with SRBC. *J Immunol* **117:** 962-966

Foley P, Kirschbaum C Human hypothalamus-pituitary-adrenal axis responses to acute psychosocial stress in laboratory settings. *Neurosci Biobehav Rev* **35:** 91-96

Follenius M, Brandenberger G (1986) Plasma free cortisol during secretory episodes. *J Clin Endocrinol Metab* **62:** 609-612

Fredrickson BL, Mancuso RA, Branigan C, Tugade MM (2000) The Undoing Effect of Positive Emotions. *Motiv Emot* **24:** 237-258

Fukuda R, Ichikawa Y, Takaya M, Ogawa Y, Masumoto A (1994) Circadian variations and prednisolone-induced alterations of circulating lymphocyte subsets in man. *Intern Med* **33:** 733-738

Galon J, Franchimont D, Hiroi N, Frey G, Boettner A, Ehrhart-Bornstein M, O'Shea JJ, Chrousos GP, Bornstein SR (2002) Gene profiling reveals unknown enhancing and suppressive actions of glucocorticoids on immune cells. *FASEB J* **16:** 61-71

Gametchu B, Chen F, Sackey F, Powell C, Watson CS (1999) Plasma membrane-resident glucocorticoid receptors in rodent lymphoma and human leukemia models. *Steroids* **64:** 107-119

Gatti G, Del Ponte D, Cavallo R, Sartori ML, Salvadori A, Carignola R, Carandente F, Angeli A (1987) Circadian changes in human natural killer-cell activity. *Prog Clin Biol Res* **227A:** 399-409

Geng CD, Vedeckis WV (2004) Steroid-responsive sequences in the human glucocorticoid receptor gene 1A promoter. *Mol Endocrinol* **18:** 912-924

Godbout JP, Glaser R (2006) Stress-induced immune dysregulation: implications for wound healing, infectious disease and cancer. *J Neuroimmune Pharmacol* **1:** 421-427

Greenhouse SW, Geisser S (1959) On methods in the analysis of profile data. *Psychometrica***:** 95-112

Greenstein S, Ghias K, Krett NL, Rosen ST (2002) Mechanisms of glucocorticoid-mediated apoptosis in hematological malignancies. *Clin Cancer Res* **8:** 1681-1694

Gross KL, Cidlowski JA (2008) Tissue-specific glucocorticoid action: a family affair. *Trends Endocrinol Metab* **19:** 331-339

Guardabasso V, Genazzani AD, Veldhuis JD, Rodbard D (1991) Objective assessment of concordance of secretory events in two endocrine time series. *Acta Endocrinol (Copenh)* **124:** 208-218

Haarman EG, Kaspers GJ, Veerman AJ (2003) Glucocorticoid resistance in childhood leukaemia: mechanisms and modulation. *Br J Haematol* **120:** 919-929

Halberg J, Halberg E, Runge W, Wicks J, Cadote L, Yunis EJ, Katinas G, Stutman O, Halberg F (1974) Transplant chronobiology. *Chronobiology***:** 320

Halbreich U, Asnis GM, Shindledecker R, Zumoff B, Nathan RS (1985) Cortisol secretion in endogenous depression. II. Time-related functions. *Arch Gen Psychiatry* **42:** 909-914

Haller J, Mikics E, Makara GB (2008) The effects of non-genomic glucocorticoid mechanisms on bodily functions and the central neural system. A critical evaluation of findings. *Front Neuroendocrinol* **29:** 273-291

Haller J, Millar S, van de Schraaf J, de Kloet RE, Kruk MR (2000) The active phase-related increase in corticosterone and aggression are linked. *Journal of neuroendocrinology* **12:** 431-436

Hartmann A, Veldhuis JD, Deuschle M, Standhardt H, Heuser I (1997) Twenty-four hour cortisol release profiles in patients with Alzheimer's and Parkinson's disease compared to normal controls: ultradian secretory pulsatility and diurnal variation. *Neurobiol Aging* **18:** 285-289

Hastings M, O'Neill JS, Maywood ES (2007) Circadian clocks: regulators of endocrine and metabolic rhythms. *J Endocrinol* **195:** 187-198

Hayashi R, Wada H, Ito K, Adcock IM (2004) Effects of glucocorticoids on gene transcription. *Eur J Pharmacol* **500:** 51-62

Hellhammer J, Fries E, Schweisthal OW, Schlotz W, Stone AA, Hagemann D (2007) Several daily measurements are necessary to reliably assess the cortisol rise after awakening: state- and trait components. *Psychoneuroendocrinology* **32:** 80-86

Henley DE, Leendertz JA, Russell GM, Wood SA, Taheri S, Woltersdorf WW, Lightman SL (2009) Development of an automated blood sampling system for use in humans. *J Med Eng Technol* **33:** 199-208

Hiramatsu R (1981) Direct assay of cortisol in human saliva by solid phase radioimmunoassay and its clinical applications. *Clin Chim Acta* **117:** 239-249

Hollenberg SM, Weinberger C, Ong ES, Cerelli G, Oro A, Lebo R, Thompson EB, Rosenfeld MG, Evans RM (1985) Primary structure and expression of a functional human glucocorticoid receptor cDNA. *Nature* **318:** 635-641

Holsboer F (2000) The corticosteroid receptor hypothesis of depression. *Neuropsychopharmacology* **23:** 477-501

Iranmanesh A, Lizarralde G, Johnson ML, Veldhuis JD (1989) Circadian, ultradian, and episodic release of beta-endorphin in men, and its temporal coupling with cortisol. *J Clin Endocrinol Metab* **68:** 1019-1026

Ising M, Depping AM, Siebertz A, Lucae S, Unschuld PG, Kloiber S, Horstmann S, Uhr M, Muller-Myhsok B, Holsboer F (2008) Polymorphisms in the FKBP5 gene region modulate recovery from psychosocial stress in healthy controls. *Eur J Neurosci* **28:** 389-398

Ising M, Holsboer F (2006) Genetics of stress response and stress-related disorders. *Dialogues Clin Neurosci* **8:** 433-444

Ismaili N, Garabedian MJ (2004) Modulation of glucocorticoid receptor function via phosphorylation. *Ann N Y Acad Sci* **1024:** 86-101

Izawa S, Sugaya N, Yamamoto R, Ogawa N, Nomura S (2010) The cortisol awakening response and autonomic nervous system activity during nocturnal and early morning periods. *Neuro Endocrinol Lett* **31:** 685-689

Jasper MS, Engeland WC (1991) Synchronous ultradian rhythms in adrenocortical secretion detected by microdialysis in awake rats. *Am J Physiol* **261:** R1257-1268

Johnson ML, Pipes L, Veldhuis PP, Farhy LS, Boyd DG, Evans WS (2008) AutoDecon, a deconvolution algorithm for identification and characterization of luteinizing hormone secretory bursts: description and validation using synthetic data. *Anal Biochem* **381:** 8-17

Johnson ML, Pipes L, Veldhuis PP, Farhy LS, Nass R, Thorner MO, Evans WS (2009) AutoDecon: a robust numerical method for the quantification of pulsatile events. *Methods Enzymol* **454:** 367-404

Johnson ML, Veldhuis PP, Grimmichova T, Farhy LS, Evans WS (2010) Validation of a deconvolution procedure (AutoDecon) for identification and characterization of fasting insulin secretory bursts. *J Diabetes Sci Technol* **4:** 1205-1213

Johnson ML, Virostko A, Veldhuis JD, Evans WS (2004) Deconvolution analysis as a hormone pulse-detection algorithm. *Methods Enzymol* **384:** 40-54

Jorm AF, Korten AE, Henderson AS (1987) The prevalence of dementia: a quantitative integration of the literature. *Acta Psychiatr Scand* **76:** 465-479

Kalinyak JE, Dorin RI, Hoffman AR, Perlman AJ (1987) Tissue-specific regulation of glucocorticoid receptor mRNA by dexamethasone. *J Biol Chem* **262:** 10441-10444

Kalsbeek A, Palm IF, La Fleur SE, Scheer FA, Perreau-Lenz S, Ruiter M, Kreier F, Cailotto C, Buijs RM (2006) SCN outputs and the hypothalamic balance of life. *J Biol Rhythms* **21:** 458-469

Karst H, Berger S, Turiault M, Tronche F, Schutz G, Joels M (2005) Mineralocorticoid receptors are indispensable for nongenomic modulation of hippocampal glutamate transmission by corticosterone. *Proc Natl Acad Sci U S A* **102:** 19204-19207

Kato T (2007) Molecular genetics of bipolar disorder and depression. *Psychiatry Clin Neurosci* **61:** 3-19

Katz P, Zaytoun AM, Lee JH, Jr. (1984) The effects of in vivo hydrocortisone on lymphocyte-mediated cytotoxicity. *Arthritis Rheum* **27:** 72-78

Kawate T, Abo T, Hinuma S, Kumagai K (1981) Studies of the bioperiodicity of the immune response. II. Co-variations of murine T and B cells and a role of corticosteroid. *J Immunol* **126:** 1364-1367

Keller M, Mazuch J, Abraham U, Eom GD, Herzog ED, Volk HD, Kramer A, Maier B (2009) A circadian clock in macrophages controls inflammatory immune responses. *Proc Natl Acad Sci U S A* **106:** 21407-21412

Kerrigan JR, Veldhuis JD, Leyo SA, Iranmanesh A, Rogol AD (1993) Estimation of daily cortisol production and clearance rates in normal pubertal males by deconvolution analysis. *J Clin Endocrinol Metab* **76:** 1505-1510

Kimura K, Isowa T, Matsunaga M, Murashima S, Ohira H (2008) The temporal redistribution pattern of NK cells under acute stress based on CD62L adhesion molecule expression. *Int J Psychophysiol* **70:** 63-69

Kirschbaum C, Hellhammer DH (1989) Salivary cortisol in psychobiological research: an overview. *Neuropsychobiology* **22:** 150-169

Kirschbaum C, Hellhammer HD (2000) Salivary Cortisol. *Encyclopedia of Stress* **3:** 379-383

Kirschbaum C, Kudielka BM, Gaab J, Schommer NC, Hellhammer DH (1999) Impact of gender, menstrual cycle phase, and oral contraceptives on the activity of the hypothalamus-pituitary-adrenal axis. *Psychosom Med* **61:** 154-162

Kirschbaum C, Pirke KM, Hellhammer DH (1993) The 'Trier Social Stress Test'--a tool for investigating psychobiological stress responses in a laboratory setting. *Neuropsychobiology* **28:** 76-81

Kirschbaum C, Wust S, Hellhammer D (1992) Consistent sex differences in cortisol responses to psychological stress. *Psychosom Med* **54:** 648-657

Knapp MS, Cove-Smith JR, Dugdale R, Mackenzie N, Pownall R (1979) Possible effect of time on renal allograft rejection. *Br Med J* **1:** 75-77

Knapp MS, Pownall R (1984) Lymphocytes are rhythmic: is this important? *Br Med J (Clin Res Ed)* **289:** 1328-1330

Knobil E, Plant TM, Wildt L, Belchetz PE, Marshall G (1980) Control of the rhesus monkey menstrual cycle: permissive role of hypothalamic gonadotropin-releasing hormone. *Science* **207:** 1371-1373

Ko CH, Takahashi JS (2006) Molecular components of the mammalian circadian clock. *Hum Mol Genet* **15 Spec No 2:** R271-277

Kripke DF, Elliott JA, Youngstedt SD, Parry BL, Hauger RL, Rex KM (2010) Weak evidence of bright light effects on human LH and FSH. *J Circadian Rhythms* **8:** 5

Kronfol Z, Nair M, Zhang Q, Hill EE, Brown MB (1997) Circadian immune measures in healthy volunteers: relationship to hypothalamic-pituitary-adrenal axis hormones and sympathetic neurotransmitters. *Psychosom Med* **59:** 42-50

Kudielka BM, Buske-Kirschbaum A, Hellhammer DH, Kirschbaum C (2004) Differential heart rate reactivity and recovery after psychosocial stress (TSST) in healthy children, younger adults, and elderly adults: the impact of age and gender. *Int J Behav Med* **11:** 116-121

Kudielka BM, Kirschbaum C (2003) Awakening cortisol responses are influenced by health status and awakening time but not by menstrual cycle phase. *Psychoneuroendocrinology* **28:** 35-47

Kudielka BM, Kirschbaum C (2005) Sex differences in HPA axis responses to stress: a review. *Biol Psychol* **69:** 113-132

Kumar R, Thompson EB (2005) Gene regulation by the glucocorticoid receptor: structure:function relationship. *The Journal of steroid biochemistry and molecular biology* **94:** 383-394

Kumsta R, Entringer S, Koper JW, van Rossum EF, Hellhammer DH, Wust S (2007) Sex specific associations between common glucocorticoid receptor gene variants and hypothalamus-pituitary-adrenal axis responses to psychosocial stress. *Biol Psychiatry* **62:** 863-869

Laudat MH, Cerdas S, Fournier C, Guiban D, Guilhaume B, Luton JP (1988) Salivary cortisol measurement: a practical approach to assess pituitary-adrenal function. *J Clin Endocrinol Metab* **66:** 343-348

Le-Niculescu H, Balaraman Y, Patel SD, Ayalew M, Gupta J, Kuczenski R, Shekhar A, Schork N, Geyer MA, Niculescu AB Convergent functional genomics of anxiety disorders: translational identification of genes, biomarkers, pathways and mechanisms. *Transl Psychiatry* **1:** e9

Le Drean Y, Mincheneau N, Le Goff P, Michel D (2002) Potentiation of glucocorticoid receptor transcriptional activity by sumoylation. *Endocrinology* **143:** 3482-3489

Levi FA, Canon C, Blum JP, Mechkouri M, Reinberg A, Mathe G (1985) Circadian and/or circahemidian rhythms in nine lymphocyte-related variables from peripheral blood of healthy subjects. *J Immunol* **134:** 217-222

Levine A, Zagoory-Sharon O, Feldman R, Lewis JG, Weller A (2007) Measuring cortisol in human psychobiological studies. *Physiology & behavior* **90:** 43-53

Lewis JG, Bagley CJ, Elder PA, Bachmann AW, Torpy DJ (2005) Plasma free cortisol fraction reflects levels of functioning corticosteroid-binding globulin. *Clin Chim Acta* **359:** 189-194

Lightman SL (1992) Alterations in hypothalamic-pituitary responsiveness during lactation. *Ann N Y Acad Sci* **652:** 340-346

Lightman SL (2006) Patterns of exposure to glucocorticoid receptor ligand. *Biochem Soc Trans* **34:** 1117-1118

Lightman SL (2008) The neuroendocrinology of stress: a never ending story. *Journal of neuroendocrinology* **20:** 880-884

Lightman SL, Conway-Campbell BL (2010) The crucial role of pulsatile activity of the HPA axis for continuous dynamic equilibration. *Nat Rev Neurosci* **11:** 710-718

Lightman SL, Wiles CC, Atkinson HC, Henley DE, Russell GM, Leendertz JA, McKenna MA, Spiga F, Wood SA, Conway-Campbell BL (2008) The significance of glucocorticoid pulsatility. *Eur J Pharmacol* **583:** 255-262

Lightman SL, Windle RJ, Julian MD, Harbuz MS, Shanks N, Wood SA, Kershaw YM, Ingram CD (2000) Significance of pulsatility in the HPA axis. *Novartis Found Symp* **227:** 244-257; discussion 257-260

Lightman SL, Windle RJ, Ma XM, Harbuz MS, Shanks NM, Julian MD, Wood SA, Kershaw YM, Ingram CD (2002) Hypothalamic-pituitary-adrenal function. *Arch Physiol Biochem* **110:** 90-93

Liu JH, Kazer RR, Rasmussen DD (1987) Characterization of the twenty-four hour secretion patterns of adrenocorticotropin and cortisol in normal women and patients with Cushing's disease. *J Clin Endocrinol Metab* **64:** 1027-1035

Lo MS, Ng ML, Azmy BS, Khalid BA (1992) Clinical applications of salivary cortisol measurements. *Singapore Med J* **33:** 170-173

Loudon AS, Wayne NL, Krieg R, Iranmanesh A, Veldhuis JD, Menaker M (1994) Ultradian endocrine rhythms are altered by a circadian mutation in the Syrian hamster. *Endocrinology* **135:** 712-718

Lowenberg M, Stahn C, Hommes DW, Buttgereit F (2008) Novel insights into mechanisms of glucocorticoid action and the development of new glucocorticoid receptor ligands. *Steroids* **73:** 1025-1029

Lowenberg M, Tuynman J, Scheffer M, Verhaar A, Vermeulen L, van Deventer S, Hommes D, Peppelenbosch M (2006) Kinome analysis reveals nongenomic glucocorticoid receptor-dependent inhibition of insulin signaling. *Endocrinology* **147:** 3555-3562

Lu NZ, Cidlowski JA (2005) Translational regulatory mechanisms generate N-terminal glucocorticoid receptor isoforms with unique transcriptional target genes. *Mol Cell* **18:** 331-342

Macedo JA, Hesse J, Turner JD, Ammerlaan W, Gierens A, Hellhammer DH, Muller CP (2007) Adhesion molecules and cytokine expression in fibromyalgia patients: Increased L-selectin on monocytes and neutrophils. *Journal of Neuroimmunology* **188**:159-166

Macedo JA, Hesse J, Turner JD, Meyer J, Hellhammer DH, Muller CP (2008) Glucocorticoid sensitivity in fibromyalgia patients: decreased expression of corticosteroid receptors and glucocorticoid-induced leucine zipper. *Psychoneuroendocrinology* **33:** 799-809

Maisel AS, Harris T, Rearden CA, Michel MC (1990) Beta-adrenergic receptors in lymphocyte subsets after exercise. Alterations in normal individuals and patients with congestive heart failure. *Circulation* **82:** 2003-2010

Mantagos S, Koulouris A, Vagenakis A (1991) A simple stress test for the evaluation of hypothalamic-pituitary-adrenal axis during the first 6 months of life. *J Clin Endocrinol Metab* **72:** 214-216

Marshall JC, Dalkin AC, Haisenleder DJ, Griffin ML, Kelch RP (1993) GnRH pulses--the regulators of human reproduction. *Trans Am Clin Climatol Assoc* **104:** 31-46

Martikainen H, Ruokonen A, Tomas C, Kauppila A (1996) Seasonal changes in pituitary function: amplification of midfollicular luteinizing hormone secretion during the dark season. *Fertil Steril* **65:** 718-720

McIntosh RP, McIntosh JE (1985) Amplitude of episodic release of LH as a measure of pituitary function analysed from the time-course of hormone levels in the blood: comparison of four menstrual cycles in an individual. *J Endocrinol* **107:** 231-239

Mendel CM (1992) The free hormone hypothesis. Distinction from the free hormone transport hypothesis. *J Androl* **13:** 107-116

Merriam GR, Wachter KW (1982) Algorithms for the study of episodic hormone secretion. *Am J Physiol* **243:** E310-318

Metzger DL, Wright NM, Veldhuis JD, Rogol AD, Kerrigan JR (1993) Characterization of pulsatile secretion and clearance of plasma cortisol in premature and term neonates using deconvolution analysis. *J Clin Endocrinol Metab* **77:** 458-463

Miller AH, Spencer RL, hassett J, Kim C, Rhee R, Ciurea D, Dhabhar F, McEwen B, Stein M (1994) Effects of selective type I and II adrenal steroid agonists on immune cell distribution. *Endocrinology* **135:** 1934-1944

Miller GE, Chen E, Sze J, Marin T, Arevalo JM, Doll R, Ma R, Cole SW (2008) A functional genomic fingerprint of chronic stress in humans: blunted glucocorticoid and increased NF-kappaB signaling. *Biol Psychiatry* **64:** 266-272

Miyawaki T, Taga K, Nagaoki T, Seki H, Suzuki Y, Taniguchi N (1984) Circadian changes of T lymphocyte subsets in human peripheral blood. *Clin Exp Immunol* **55:** 618-622

Morineau G, Boudi A, Barka A, Gourmelen M, Degeilh F, Hardy N, al-Halnak A, Soliman H, Gosling JP, Julien R, Brerault JL, Boudou P, Aubert P, Villette JM, Pruna A, Galons H, Fiet J (1997) Radioimmunoassay of cortisone in serum, urine, and saliva to assess the status of the cortisol-cortisone shuttle. *Clinical chemistry* **43:** 1397-1407

Morita K, Saito T, Ohta M, Ohmori T, Kawai K, Teshima-Kondo S, Rokutan K (2005) Expression analysis of psychological stress-associated genes in peripheral blood leukocytes. *Neurosci Lett* **381:** 57-62

Morsink MC, Steenbergen PJ, Vos JB, Karst H, Joels M, De Kloet ER, Datson NA (2006) Acute activation of hippocampal glucocorticoid receptors results in different waves of gene expression throughout time. *J Neuroendocrinol* **18:** 239-252

Mulligan T, Delemarre-van de Waal HA, Johnson ML, Veldhuis JD (1994) Validation of deconvolution analysis of LH secretion and half-life. *Am J Physiol* **267:** R202-211

Murata S, Yoshiara T, Lim CR, Sugino M, Kogure M, Ohnuki T, Komurasaki T, Matsubara K (2005) Psychophysiological stress-regulated gene expression in mice. *FEBS Lett* **579:** 2137-2142

Nater UM, Whistler T, Lonergan W, Mletzko T, Vernon SD, Heim C (2009) Impact of acute psychosocial stress on peripheral blood gene expression pathways in healthy men. *Biol Psychol* **82:** 125-132

Neumaier JF, Sexton TJ, Hamblin MW, Beck SG (2000) Corticosteroids regulate 5-HT(1A) but not 5-HT(1B) receptor mRNA in rat hippocampus. *Brain Res Mol Brain Res* **82:** 65-73

Nunez BS, Vedeckis WV (2002) Characterization of promoter 1B in the human glucocorticoid receptor gene. *Mol Cell Endocrinol* **189:** 191-199

Oerter KE, Guardabasso V, Rodbard D (1986) Detection and characterization of peaks and estimation of instantaneous secretory rate for episodic pulsatile hormone secretion. *Comput Biomed Res* **19:** 170-191

Oishi K, Miyazaki K, Kadota K, Kikuno R, Nagase T, Atsumi G, Ohkura N, Azama T, Mesaki M, Yukimasa S, Kobayashi H, Iitaka C, Umehara T, Horikoshi M, Kudo T, Shimizu Y, Yano M, Monden M, Machida K, Matsuda J, Horie S, Todo T, Ishida N (2003) Genome-wide expression analysis of mouse liver reveals CLOCK-regulated circadian output genes. *J Biol Chem* **278:** 41519-41527

Orchinik M, Murray TF, Moore FL (1991) A corticosteroid receptor in neuronal membranes. *Science* **252:** 1848-1851

Pajer K, Andrus BM, Gardner W, Lourie A, Strange B, Campo J, Bridge J, Blizinsky K, Dennis K, Vedell P, Churchill GA, Redei EE Discovery of blood transcriptomic markers for depression in animal models and pilot validation in subjects with early-onset major depression. *Transl Psychiatry* **2:** e101

Panda S, Hogenesch JB, Kay SA (2002) Circadian rhythms from flies to human. *Nature* **417:** 329-335

Pascual-Le Tallec L, Lombes M (2005) The mineralocorticoid receptor: a journey exploring its diversity and specificity of action. *Mol Endocrinol* **19:** 2211-2221

Peters JR, Walker RF, Riad-Fahmy D, Hall R (1982) Salivary cortisol assays for assessing pituitary-adrenal reserve. *Clin Endocrinol (Oxf)* **17:** 583-592

Picard D (2006) Chaperoning steroid hormone action. *Trends Endocrinol Metab* **17:** 229-235

Pickering BM, Willis AE (2005) The implications of structured 5' untranslated regions on translation and disease. *Semin Cell Dev Biol* **16:** 39-47

Presul E, Schmidt S, Kofler R, Helmberg A (2007) Identification, tissue expression, and glucocorticoid responsiveness of alternative first exons of the human glucocorticoid receptor. *J Mol Endocrinol* **38:** 79-90

Pruessner JC, Kirschbaum C, Meinlschmid G, Hellhammer DH (2003) Two formulas for computation of the area under the curve represent measures of total hormone concentration versus time-dependent change. *Psychoneuroendocrinology* **28:** 916-931

Pruessner JC, Wolf OT, Hellhammer DH, Buske-Kirschbaum A, von Auer K, Jobst S, Kaspers F, Kirschbaum C (1997) Free cortisol levels after awakening: a reliable biological marker for the assessment of adrenocortical activity. *Life Sci* **61:** 2539-2549

Pujols L, Mullol J, Perez M, Roca-Ferrer J, Juan M, Xaubet A, Cidlowski JA, Picado C (2001) Expression of the human glucocorticoid receptor alpha and beta isoforms in human respiratory epithelial cells and their regulation by dexamethasone. *Am J Respir Cell Mol Biol* **24:** 49-57

Rajkumar SV, Gertz MA, Kyle RA, Greipp PR (2002) Current therapy for multiple myeloma. *Mayo Clin Proc* **77:** 813-822

Ratte J, Halberg F, Kuhl JF, Najarian JS (1973) Circadian variation in the rejection of rat kidney allografts. *Surgery* **73:** 102-108

Reagan LP, Grillo CA, Piroli GG (2008) The As and Ds of stress: metabolic, morphological and behavioral consequences. *Eur J Pharmacol* **585:** 64-75

Rebar R, Perlman D, Naftolin F, Yen SS (1973) The estimation of pituitary luteinizing hormone secretion. *J Clin Endocrinol Metab* **37:** 917-927

Reppert SM, Weaver DR (2002) Coordination of circadian timing in mammals. *Nature* **418:** 935-941

Rhen T, Cidlowski JA (2005) Antiinflammatory action of glucocorticoids--new mechanisms for old drugs. *N Engl J Med* **353:** 1711-1723

Ritchie AW, Oswald I, Micklem HS, Boyd JE, Elton RA, Jazwinska E, James K (1983) Circadian variation of lymphocyte subpopulations: a study with monoclonal antibodies. *Br Med J (Clin Res Ed)* **286:** 1773-1775

Rogerson FM, Brennan FE, Fuller PJ (2004) Mineralocorticoid receptor binding, structure and function. *Mol Cell Endocrinol* **217:** 203-212

Santen RJ, Bardin CW (1973) Episodic luteinizing hormone secretion in man. Pulse analysis, clinical interpretation, physiologic mechanisms. *J Clin Invest* **52:** 2617-2628

Schlotz W, Kumsta R, Layes I, Entringer S, Jones A, Wust S (2008) Covariance between psychological and endocrine responses to pharmacological challenge and psychosocial stress: a question of timing. *Psychosom Med* **70:** 787-796

Schote AB, Turner JD, Schiltz J, Muller CP (2007) Nuclear receptors in human immune cells: expression and correlations. *Mol Immunol* **44:** 1436-1445

Seale JV, Wood SA, Atkinson HC, Bate E, Lightman SL, Ingram CD, Jessop DS, Harbuz MS (2004a) Gonadectomy reverses the sexually diergic patterns of circadian and stress-

induced hypothalamic-pituitary-adrenal axis activity in male and female rats. *Journal of neuroendocrinology* **16:** 516-524

Seale JV, Wood SA, Atkinson HC, Harbuz MS, Lightman SL (2004b) Gonadal steroid replacement reverses gonadectomy-induced changes in the corticosterone pulse profile and stress-induced hypothalamic-pituitary-adrenal axis activity of male and female rats. *Journal of neuroendocrinology* **16:** 989-998

Singer JD, Willet JB (2003) Applied longitudinal data anlysis: Modeling change and event occurence. *Oxford University Press, New York*

Sionov RV, Cohen O, Kfir S, Zilberman Y, Yefenof E (2006) Role of mitochondrial glucocorticoid receptor in glucocorticoid-induced apoptosis. *J Exp Med* **203:** 189-201

Slade JD, Hepburn B (1983) Prednisone-induced alterations of circulating human lymphocyte subsets. *J Lab Clin Med* **101:** 479-487

Soundararajan R, Zhang TT, Wang J, Vandewalle A, Pearce D (2005) A novel role for glucocorticoid-induced leucine zipper protein in epithelial sodium channel-mediated sodium transport. *J Biol Chem* **280:** 39970-39981

Stahl F, Dorner G (1982) Responses of salivary cortisol levels to stress-situations. *Endokrinologie* **80:** 158-162

Stahn C, Buttgereit F (2008) Genomic and nongenomic effects of glucocorticoids. *Nat Clin Pract Rheumatol* **4:** 525-533

Stahn C, Lowenberg M, Hommes DW, Buttgereit F (2007) Molecular mechanisms of glucocorticoid action and selective glucocorticoid receptor agonists. *Mol Cell Endocrinol* **275:** 71-78

Stavreva DA, Muller WG, Hager GL, Smith CL, McNally JG (2004) Rapid glucocorticoid receptor exchange at a promoter is coupled to transcription and regulated by chaperones and proteasomes. *Mol Cell Biol* **24:** 2682-2697

Stavreva DA, Wiench M, John S, Conway-Campbell BL, McKenna MA, Pooley JR, Johnson TA, Voss TC, Lightman SL, Hager GL (2009) Ultradian hormone stimulation induces glucocorticoid receptor-mediated pulses of gene transcription. *Nat Cell Biol* **11:** 1093-1102

Stewart PM, Whorwood CB, Mason JI (1995) Type 2 11 beta-hydroxysteroid dehydrogenase in foetal and adult life. *The Journal of steroid biochemistry and molecular biology* **55:** 465-471

Styczynski J, Kurylak A, Wysocki M (2005) Cytotoxicity of cortivazol in childhood acute lymphoblastic leukemia. *Anticancer Res* **25:** 2253-2258

Suzuki S, Toyabe S, Moroda T, Tada T, Tsukahara A, Iiai T, Minagawa M, Maruyama S, Hatakeyama K, Endoh K, Abo T (1997) Circadian rhythm of leucocytes and lymphocytes

subsets and its possible correlation with the function of the autonomic nervous system. *Clin Exp Immunol* **110:** 500-508

Takahashi JS, Hong HK, Ko CH, McDearmon EL (2008) The genetics of mammalian circadian order and disorder: implications for physiology and disease. *Nat Rev Genet* **9:** 764-775

Tapp WN, Holaday JW, Natelson BH (1984) Ultradian glucocorticoid rhythms in monkeys and rats continue during stress. *Am J Physiol* **247:** R866-871

Trifonova ST, Gantenbein M, Turner JD, Muller CP(In Press) The use of saliva for assessment of cortisol pulsatile secretion by deconvolution analysis. *Psychoneuroendocrinology.* DOI: 10.1016/j.psyneuen.2012.10.016

Tunn S, Mollmann H, Barth J, Derendorf H, Krieg M (1992) Simultaneous measurement of cortisol in serum and saliva after different forms of cortisol administration. *Clin Chem* **38:** 1491-1494

Turner JD, Alt SR, Cao L, Vernocchi S, Trifonova S, Battello N, Muller CP (2009) Transcriptional control of the glucocorticoid receptor: CpG islands, epigenetics and more. *Biochem Pharmacol* **80:** 1860-1868

Turner JD, Muller CP (2005) Structure of the glucocorticoid receptor (NR3C1) gene 5' untranslated region: identification, and tissue distribution of multiple new human exon 1. *J Mol Endocrinol* **35:** 283-292

Turner RC, Grayburn JA, Newman GB, Nabarro JD (1971) Measurement of the insulin delivery rate in man. *J Clin Endocrinol Metab* **33:** 279-286

Ulrich-Lai YM, Herman JP (2009) Neural regulation of endocrine and autonomic stress responses. *Nat Rev Neurosci* **10:** 397-409

Umeda T, Hiramatsu R, Iwaoka T, Shimada T, Miura F, Sato T (1981) Use of saliva for monitoring unbound free cortisol levels in serum. *Clin Chim Acta* **110:** 245-253

Van Cauter E, L'Hermite M, Copinschi G, Refetoff S, Desir D, Robyn C (1981) Quantitative analysis of spontaneous variations of plasma prolactin in normal man. *Am J Physiol* **241:** E355-363

Van Cauter E, Refetoff S (1985) Evidence for two subtypes of Cushing's disease based on the analysis of episodic cortisol secretion. *N Engl J Med* **312:** 1343-1349

Veldhuis JD, Carlson ML, Johnson ML (1987) The pituitary gland secretes in bursts: appraising the nature of glandular secretory impulses by simultaneous multiple-parameter deconvolution of plasma hormone concentrations. *Proc Natl Acad Sci U S A* **84:** 7686-7690

Veldhuis JD, Evans WS, Rogol AD, Drake CR, Thorner MO, Merriam GR, Johnson ML (1984) Intensified rates of venous sampling unmask the presence of spontaneous, high-frequency pulsations of luteinizing hormone in man. *J Clin Endocrinol Metab* **59:** 96-102

Veldhuis JD, Iranmanesh A, Clarke L, Kaiser DL, Johnson ML (1989a) Random and Non-Random Coincidence Between Luteinizing Hormone Peaks and Follicle-Stimulating Hormone, Alpha Subunit, Prolactin and Gonadotropin-Releasing Hormone ulsations. *Journal of neuroendocrinology* **1:** 185-194

Veldhuis JD, Iranmanesh A, Johnson ML, Lizarralde G (1990) Amplitude, but not frequency, modulation of adrenocorticotropin secretory bursts gives rise to the nyctohemeral rhythm of the corticotropic axis in man. *J Clin Endocrinol Metab* **71:** 452-463

Veldhuis JD, Iranmanesh A, Lizarralde G, Johnson ML (1989b) Amplitude modulation of a burstlike mode of cortisol secretion subserves the circadian glucocorticoid rhythm. *Am J Physiol* **257:** E6-14

Veldhuis JD, Johnson ML (1986) Cluster analysis: a simple, versatile, and robust algorithm for endocrine pulse detection. *Am J Physiol* **250:** E486-493

Veldhuis JD, Johnson ML, Faunt LM, Seneta E (1994) Assessing temporal coupling between two or among three or more neuroendochrine pulse trains:cross-correlation analysis, simulation methods, and conditional probability testing. *Methods in Neurosciences* **20:** 336-376

Veldhuis JD, Johnson ML, Seneta E, Iranmanesh A (1992) Temporal coupling among luteinizing hormone, follicle stimulating hormone, beta-endorphin and cortisol pulse episodes in vivo. *Acta Endocrinol (Copenh)* **126:** 193-200

Veldhuis JD, Roelfsema F, Iranmanesh A, Carroll BJ, Keenan DM, Pincus SM (2009) Basal, pulsatile, entropic (patterned), and spiky (staccato-like) properties of ACTH secretion: impact of age, gender, and body mass index. *J Clin Endocrinol Metab* **94:** 4045-4052

Vining RF, McGinley RA, Maksvytis JJ, Ho KY (1983) Salivary cortisol: a better measure of adrenal cortical function than serum cortisol. *Ann Clin Biochem* **20 (Pt 6):** 329-335

Walker JJ, Terry JR, Lightman SL Origin of ultradian pulsatility in the hypothalamic-pituitary-adrenal axis. *Proc Biol Sci* **277:** 1627-1633

Walker JJ, Terry JR, Lightman SL (2010) Origin of ultradian pulsatility in the hypothalamic-pituitary-adrenal axis. *Proc Biol Sci* **277:** 1627-1633

Walker RF, Riad-Fahmy D, Read GF (1978) Adrenal status assessed by direct radioimmunoassay of cortisol in whole saliva or parotid saliva. *Clin Chem* **24:** 1460-1463

Wallace AD, Cidlowski JA (2001) Proteasome-mediated glucocorticoid receptor degradation restricts transcriptional signaling by glucocorticoids. *J Biol Chem* **276:** 42714-42721

Webster JI, Tonelli L, Sternberg EM (2002) Neuroendocrine regulation of immunity. *Annu Rev Immunol* **20:** 125-163

Wei P, Vedeckis WV (1997) Regulation of the glucocorticoid receptor gene by the AP-1 transcription factor. *Endocrine* **7:** 303-310

Weitzman ED, Fukushima D, Nogeire C, Roffwarg H, Gallagher TF, Hellman L (1971) Twenty-four hour pattern of the episodic secretion of cortisol in normal subjects. *J Clin Endocrinol Metab* **33:** 14-22

Wildt L, Hausler A, Marshall G, Hutchison JS, Plant TM, Belchetz PE, Knobil E (1981) Frequency and amplitude of gonadotropin-releasing hormone stimulation and gonadotropin secretion in the rhesus monkey. *Endocrinology* **109:** 376-385

Willour VL, Chen H, Toolan J, Belmonte P, Cutler DJ, Goes FS, Zandi PP, Lee RS, MacKinnon DF, Mondimore FM, Schweizer B, DePaulo JR, Jr., Gershon ES, McMahon FJ, Potash JB (2009) Family-based association of FKBP5 in bipolar disorder. *Mol Psychiatry* **14:** 261-268

Windle RJ, Wood SA, Kershaw YM, Lightman SL, Ingram CD, Harbuz MS (2001) Increased corticosterone pulse frequency during adjuvant-induced arthritis and its relationship to alterations in stress responsiveness. *Journal of neuroendocrinology* **13:** 905-911

Windle RJ, Wood SA, Lightman SL, Ingram CD (1998a) The pulsatile characteristics of hypothalamo-pituitary-adrenal activity in female Lewis and Fischer 344 rats and its relationship to differential stress responses. *Endocrinology* **139:** 4044-4052

Windle RJ, Wood SA, Shanks N, Lightman SL, Ingram CD (1998b) Ultradian rhythm of basal corticosterone release in the female rat: dynamic interaction with the response to acute stress. *Endocrinology* **139:** 443-450

Wochnik GM, Ruegg J, Abel GA, Schmidt U, Holsboer F, Rein T (2005) FK506-binding proteins 51 and 52 differentially regulate dynein interaction and nuclear translocation of the glucocorticoid receptor in mammalian cells. *J Biol Chem* **280:** 4609-4616

Wood P (2009) Salivary steroid assays - research or routine? *Ann Clin Biochem* **46:** 183-196

Wust S, Wolf J, Hellhammer DH, Federenko I, Schommer N, Kirschbaum C (2000) The cortisol awakening response - normal values and confounds. *Noise Health* **2:** 79-88

Yehuda R, Cai G, Golier JA, Sarapas C, Galea S, Ising M, Rein T, Schmeidler J, Muller-Myhsok B, Holsboer F, Buxbaum JD (2009) Gene expression patterns associated with posttraumatic stress disorder following exposure to the World Trade Center attacks. *Biol Psychiatry* **66:** 708-711

Yen SS, Tsai CC, Naftolin F, Vandenberg G, Ajabor L (1972) Pulsatile patterns of gonadotropin release in subjects with and without ovarian function. *J Clin Endocrinol Metab* **34:** 671-675

Young EA, Abelson J, Lightman SL (2004) Cortisol pulsatility and its role in stress regulation and health. *Front Neuroendocrinol* **25:** 69-76

Yudt MR, Cidlowski JA (2002) The glucocorticoid receptor: coding a diversity of proteins and responses through a single gene. *Mol Endocrinol* **16:** 1719-1726

Zhou J, Cidlowski JA (2005) The human glucocorticoid receptor: one gene, multiple proteins and diverse responses. *Steroids* **70:** 407-417

Zweiman B, Atkins PC, Bedard PM, Flaschen SL, Lisak RP (1984) Corticosteroid effects on circulating lymphocyte subset levels in normal humans. *J Clin Immunol* **4:** 151-155

Annexes

Meetings and workshops attended

2008

12/09/08 Sar-Lor-Lux meeting of Virology, Luxembourg 20081-3/12/08 Eitorf, Germany IRTG-Workshop Introduction into pharmacokinetic-pharmacodynamic modeling

2009

15/05/09 Symposium "50th Doctoral Student at the Department of Immunology", Luxembourg.
14/07/09 IRTG (International-research training group) monthly organized meeting, Trier, Germany
Talk: Transcriptional control of hGR and its interaction partners: target genes and their expression kinetics
09/09/09 Sar-Lor-Lux meeting of Virology, Nancy, France,
22/09/09 Centre Hospitalier de Luxembourg (CHL) Course 1st Cytometry Summer Course.
09/10/09 LuciLinX symposium Workshop Introduction to R, Luxembourg.
08-11/11/09 IRTG Autumn school " Stress to pathology, Mechanisms to Action", Remich, Luxembourg
Talk: Transcriptional control of hGR and its interaction partners: target genes and their expression kinetics

2010

16/09/10 Ph.D student day, Luxembourg
Poster: Ultradian and stress induced genomic and non genomic cortisol actions
17/09/10 LuciLinX symposiumWorkshop Image processing in microscopy and Biomedical imaging using ImageJ, Luxembourg
27/09/10 Sar-Lor-Lux meeting of Virology, Homburg ,Germany
9-10/07/10 IRTG Summer Symposium, Trier, Germany
Talk: Ultradian and stress induced genomic and non genomic cortisol actions

16/12/10 4th Biolux Network Meeting

2011

01/07/11 The annual Meeting of the Workgroup VACCINES, Luxembourg.
04-06/08/11 ISPNE Annual Conference, Berlin, Germany

Poster: The use of saliva for assessment of cortisol pulsatile secretion by deconvolution analysis
13/09/11 SaarLorLux Meeting of Virology, Remich, Luxembourg
10-13/11/11 Science festival, Luxembourg

2008-2012 Immunology lectures, journal clubs, writing schools and department seminars, Institute of Immunology, Laboratoire National de Santé, Luxembourg.

Publications

Turner JD, Alt SR, Cao L, Vernocchi S, **Trifonova ST**, Battello N, Muller CP (2010)
Transcriptional control of the glucocorticoid receptor: CpG islands, epigenetics and more.
Biochem Pharmacol (2010) 80: 1860-1868.

Trifonova ST, Gantenbein M, Turner JD, Muller CP
The use of saliva for assessment of cortisol pulsatile secretion by deconvolution analysis
Psychoneuroendocrinology (2013) 38: 1090-101

Trifonova ST, Zimmer J, Turner JD, Muller CP
Diurnal redistribution of human lymphocytes and their temporal associations with salivary cortisol profiles
*Chronobiology International (*2013) 30: 669-81

Trifonova ST, Molitor A, Streit F, Wust S, Turner JD, Muller CP
Gene responses to the Trier Social Stress Test (TSST) in healthy males and females
In preparation

Trifonova ST, Turner JD, Muller CP
The concordance of pulsatile ultradian release of hypothalamo pituitary adrenal (HPA)/gonadal (HPG) axises with GR target genes expression levels
In preparation

Erklärung

Hiermit versichere ich, dass ich die vorliegende Dissertationsschrift selbständig verfasst und keine anderen als die angegebenen Hilfsquellen verwendet habe. Die Arbeit wurde bisher weder im Inland noch im Ausland in gleicher oder ähnlicher Form einer anderen Prüfungsbehörde vorgelegt.

Luxemburg, 12 December 2012

Slavena T. Trifonova